



Centre for
Organismal
Studies
Heidelberg

Assembly and quality control of the V- ATPase in Arabidopsis

Christoph Neubert

Ruprecht-Karls-University Heidelberg

INAUGURAL – DISSERTATION

Zur Erlangung der Doktorwürde
der Naturwissenschaftlich-Mathematischen Gesamtfakultät
der Ruprecht-Karls-Universität Heidelberg

vorgelegt von
Diplom-Biologe Christoph Neubert
aus Leverkusen

Tag der mündlichen Prüfung:.....

Assembly and quality control of the V- ATPase in Arabidopsis

Referees: Prof. Dr. Karin Schumacher
Prof. Dr. Jan Lohmann

Eidesstattliche Erklärung

Hiermit erkläre ich, dass ich die vorgelegte Dissertation selbst verfasst und mich dabei keiner anderen als der von mir bezeichneten Quellen und Hilfen bedient habe.

Ich erkläre hiermit, dass ich an keiner anderen Stelle ein Prüfungsverfahren beantragt bzw. die Dissertation in dieser oder anderer Form bereits anderweitig als Prüfungsarbeit verwendet oder einer anderen Fakultät als Dissertation vorgelegt habe.

Heidelberg, 24.4.2012

(Christoph Neubert)

Zusammenfassung

Das Proteom der Modellpflanze *Arabidopsis thaliana* wird auf ~ 13.000 nicht-redundante Proteine geschätzt (Baerenfaller et al., 2008). Die meisten dieser Proteine interagieren miteinander entweder über transiente Assoziationen oder durch den Aufbau von stabilen Protein-Komplexen. Diese Interaktionen werden von Chaperonen katalysiert und von verschiedenen Qualitätskontrollen überwacht. Anhand des hier verwendeten Modell-Protein-Komplex, der vakuolären H⁺-ATPase (V-ATPase), widmet sich diese Arbeit sowohl der Qualitätskontrolle, als auch der Interaktion von Chaperonen.

In Kapitel 1 dieser Arbeit wird die Rolle der ER lokalisierten Proteine AtVMA12 und AtVMA22 im Detail charakterisiert. Lokalisationstudien zeigen, dass AtVMA22 von AtVMA12 zur ER-Membran rekrutiert wird. Expression von microRNAs gegen beide putative Assembly Faktoren verursacht Phänotypen die charakteristisch für Pflanzen mit fehlender V-ATPase-Aktivität sind. Dies weist darauf hin, dass beide Proteine eine entscheidende Rolle bei dem Zusammenbau der V-ATPase haben. Eine eingehendere biochemische Charakterisierung zeigte dass AtVMA12 direkt mit einer integralen Untereinheit VHA-a3 und AtVMA22 mit der peripheren Untereinheit VHA-C der V-ATPase interagiert. Zusammenfassend zeigen die Ergebnisse, dass AtVMA12 und AtVMA22 spezifische Chaperone darstellen, die für den Zusammenbau der V-ATPase erforderlich sind. Im zweiten Teil dieser Arbeit wird ein Mechanismus vorgestellt, der nicht-funktionellen V-ATPase-Komplexe im ER zurückhält. Unter Verwendung von pharmakologischen und genetischen Ansätzen konnte nachgewiesen werden, dass aktive V-ATPase Komplexe und das membran-assoziierte Chaperon Calnexin erforderlich sind, um nicht-funktionellen Protein-Komplexe im ER zurückzuhalten.

Schlägt die Qualitätskontrolle von nicht-funktionalen Komplexen fehl, wird die Fitness der Pflanze negativ beeinflusst, was die Bedeutung einer funktions-abhängigen Qualitätskontrolle unterstreicht.

Summary

The proteome of the model plant *Arabidopsis thaliana* is estimated to contain ~13000 non-redundant proteins (Baerenfaller et al., 2008). During their lifetime most of these proteins interact with each other, either via transient association or by assembling into stable protein complexes. These interactions are facilitated by chaperones and monitored by various quality control systems. This thesis presents data on both topics, using the plant vacuolar H⁺-ATPase (V-ATPase) as a model protein complex.

In chapter 1 of this thesis the role of the ER localized proteins AtVMA12 and AtVMA22 are characterized in detail. Localization studies demonstrate that AtVMA22 is recruited to the ER membrane by AtVMA12. Artificial microRNAs directed against both assembly factors cause phenotypes characteristic for plants lacking V-ATPase activity, suggesting a pivotal role in V-ATPase assembly. Further biochemical characterization revealed a direct interaction between AtVMA12 and the integral membrane subunit VHA-a3 and an association of AtVMA22 with the peripheral subunit VHA-C of the V-ATPase. Taken together the results lead the author to postulate that AtVMA12 and AtVMA22 represent true assembly factors of the plant V-ATPase.

In the second part of this work, the mechanism is characterized by which non-functional V-ATPase complexes are retained in the ER. Using a combination of pharmacological and genetic approaches it is demonstrated that V-ATPase activity and the membrane associated chaperone calnexin are required to retain non-functional protein complexes.

However, non-functional complexes escaping the quality control negatively affect the fitness of the plant, underpinning the importance of a QC that retains non-functional proteins.

Contents

General Introduction	1
Structure of the V-ATPase	1
Proton translocation.....	3
Assembly of the V-ATPase.....	5
ER quality control (ERQC)	6
Contribution to the manuscripts.....	9
I – Assembly of the V-ATPase	10
Abstract.....	10
Introduction	11
Results.....	13
Identification of Vma12p and Vma22p orthologues	13
Localization and interaction of AtVMA12 and AtVMA22	14
Do AtVMA12 and AtVMA22 function in V-ATPase assembly in yeast?.....	16
AtVMA22 and AtVMA12 are essential for the plant.....	18
Are AtVMA12 and AtVMA22 functional assembly factors of the V-ATPase?.....	20
Knockdown of AtVMA22 or AtVMA12 does not affect vacuolar V-ATPase stability....	24
AtVMA12 interacts with the V ₀ subcomplex	24
AtVMA22 interacts with the V ₁ subcomplex	26
Appendix.....	27
Appendix A.....	27
Appendix B.....	28
Appendix C.....	29
Discussion	30
Model for V-ATPase assembly	32
Material and Methods.....	34

Plant Materials and Growth Conditions	34
Staining of Seedlings with FM4-64 and Microscopy.....	34
Constructs generated for this study	34
Molecular complementation	38
Protein Extraction	39
Co-Immunoprecipitation	39
Fluorescence Microscopy	40
Primer used.....	40
II – Quality control of the plant V-ATPase.....	42
Abstract	42
Introduction.....	43
Results	45
The VHA-a3R729N-GFP containing V-ATPase complexes are retained in the ER and degraded by the 26S Proteasome in wild type plants.....	45
V-ATPase activity is required to retain VHA-a3R729N-GFP in the ER	47
VHA-a3E780Q-GFP is transported to the vacuole	49
VHA-a3R790K-GFP localized to the trans-Golgi network and the vacuole	49
What molecular components are required to retain non-functional V-ATPase complexes?	51
If the V-ATPase is already assembled in the ER, is it active?.....	54
Is the V-ATPase part of the ERQC system?	55
Appendix.....	57
Discussion	58
V-ATPase activity determines the fate of non-functional complexes	58
Calnexin is required for a function dependent ER quality control (FERQCL)	60
VHA-a3-GFP is not transported to the tonoplast via the secretory pathway	61
The V-ATPase is assembled in the ER	62

Model of the FERQCL system.....	64
Material and Methods.....	65
Plant Materials and Growth Conditions	65
Constructs generated for this study	65
Protein Extraction	67
Co-Immunoprecipitation	68
Fluorescence Microscopy	68
Primer used.....	68
Concluding remarks and outlook	70
References.....	71
List of Abbreviations	83
Acknowledgement.....	86

General Introduction

Structure of the V-ATPase

The eukaryotic cell contains membrane-bound organelles, which provide optimal conditions for a variety of biochemical reactions. Transport proteins control the internal milieu of these compartments by regulating the ion and solute composition. One important factor is the pH, which is controlled by three proton pumps in plants. The plasma membrane H^+ -ATPase (PM H^+ -ATPase) acidifies the extracellular space, whereas the vacuolar pyrophosphatase (V-PPase) and the vacuolar H^+ -ATPase (V-ATPase) translocate protons into the lumen of compartments. Among these pumps, the V-ATPase is the most ubiquitous pump found in endomembranes of all eukaryotic cells.

V-ATPases are a multi-subunit, membrane-bound protein complexes which are structurally and mechanistically related to the F_1F_0 -ATP synthases (F-ATPase) (Fillingame et al., 2000b), but in contrast to the F-ATPases, V-ATPases can only hydrolyze ATP under physiological conditions (Saroussi and Nelson, 2009). Similar to the F-ATPase, the V-ATPase operates by a rotational mechanism (Cipriano et al., 2008). The peripheral V_1 subcomplex serves as an ATP hydrolysis engine (Watanabe et al., 1999), driving the rotation of the proteolipid ring of the V_0 subcomplex (Kawasaki-Nishi et al., 2003). V_1 and the V_0 subcomplex are connected by a central and a peripheral stalk. In terms of composition the peripheral 650 kDa V_1 subcomplex consists of eight subunits (A, B, C, D, E, F, G and H) (Forgac, 2007). Subunits A and B are arranged in alternating positions forming a hexamer. At the interface of subunit A and B ATP is hydrolysed. ATP is bound by subunit B (Nelson et al., 1989), while subunit A hydrolyses ATP (Hirata et al., 1990). Subunit B has also been implicated in regulating V-ATPase activity. The remaining V_1 subunits are part of the peripheral or the central stalk. The peripheral stalk, also referred to as stator, composed of subunits C, E, H and G prevents the AB hexamer from rotating (Tomashek et al., 1997). Subunit H is the only subunit of the V_1 subcomplex that is not required for correct assembly, but is still needed for proper function (Hirata et al., 1993). The central stalk, which is composed of subunit D and F serves as a rotor that couples the energy that is released from the hydrolysis of ATP to the proton translocation through the V_0 subcomplex. It is assumed that subunit H may play a role in inhibiting the ATPase activity of dissociated V_1 subcomplexes found in the cytosol (Parra and Kane, 1998).

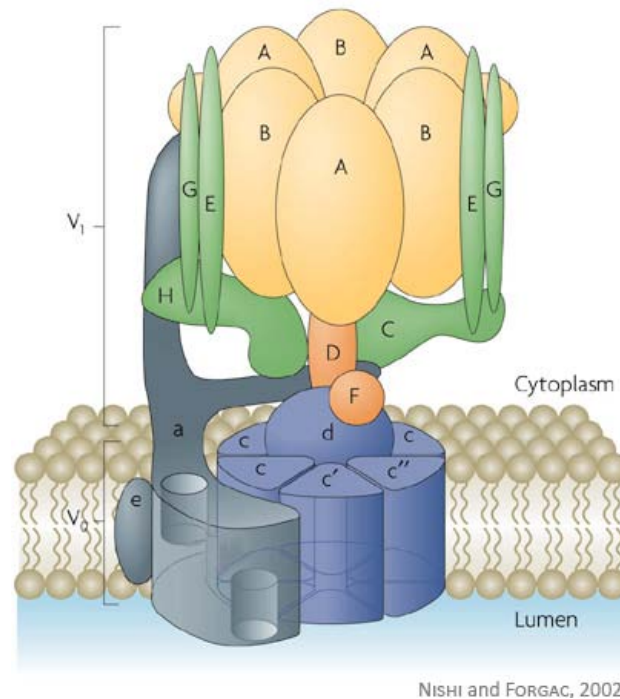


Fig. 1 Structure of the V-ATPase The vacuolar H^+ -ATPase (V-ATPase) complex is composed of a peripheral V_1 domain, which is responsible for ATP hydrolysis, and an integral V_0 domain which is involved in proton translocation across the membrane. The core of the V_1 domain is composed of a hexameric arrangement of alternating A and B subunits, which participate in ATP binding and hydrolysis. The V_0 domain includes a ring of proteolipid subunits (c, c' and c'') that are adjacent to subunits a and e. The V_1 and V_0 domains are connected by a central stalk, composed of subunits D and F of V_1 and subunit d of V_0 , and multiple peripheral stalks, composed of subunits C, E, G, H and the N-terminal domain of subunit a (Ondzighi et al., 2008).

The integral 260 kDa V_0 subcomplex is composed of six different subunits (a, d, e, c, c' and c''). Within the V_0 subcomplex the 100 kDa subunit a works similar to the subunit a of the F-ATPase (Fillingame et al., 2000a). It contains two hemi-channels, which transfer protons from the cytosol, via the proteolipid ring (c, c' and c'') into the lumen of endomembrane compartments. The exact stoichiometry of the proteolipid ring proteins is not clear. It is assumed that at least 5 of those proteins need to be present (Powell et al., 2000). Subunit d is positioned on top of the proteolipid ring, serving as a link between the V_0 and V_1 complex. The small hydrophobic subunit e was first identified in bovine brain ATPase (Ludwig et al., 1998) and recently the homologue has been also identified in yeast (Sambade and Kane, 2004). Its exact position within the V_0 subcomplex is not entirely clear, but it is believed to be associated with subunit a (Fig. 1) (Compton et al., 2006).

Proton translocation

The V-ATPase carefully controls the pH of intracellular compartments in a eukaryotic cell by acidifying organelles relative to the cytosol and by establishing a negative potential difference. The proton gradient and the proton motive force (pmf) generated by the V-ATPase are used in a number of cellular processes (Forgac, 1989) like receptor-mediated endocytosis (Nishi and Forgac, 2002), intracellular membrane trafficking (Stevens and Forgac, 1997) and coupled transport of small molecules. Previous studies on the yeast vacuolar H^+ -ATPase (V-ATPase) have elucidated the importance of the 100 kDa subunit a for proton translocation (Leng et al., 1996; Kawasaki-Nishi et al., 2001a; Finnigan et al., 2011). Topological studies have revealed a two-domain structure with a hydrophilic, cytoplasmic N-terminus and a membrane integral C-terminal region with nine putative transmembrane helices (Leng et al., 1999). In *Arabidopsis* and in yeast the N-terminus is required for the targeting of V-ATPase complexes (Kawasaki-Nishi et al., 2001c; Dettmer et al., 2006). In yeast two isoforms target the V-ATPase either to the Golgi (Stv1p) or to the vacuole (Vph1p) (Manolson et al., 1994; Kawasaki-Nishi et al., 2001c). *Arabidopsis* has three different isoforms, designated as VHA-a1, VHA-a2 and VHA-a3 (Sze et al., 2002). V-ATPase complexes containing VHA-a1 will localize to the *trans*-Golgi network/early endosome (TGN/EE), whereas complexes containing the VHA-a2 or VHA-a3 isoform are targeted to the tonoplast (Dettmer et al., 2006). The C-terminus of subunit a marks the entry and exit point for protons (Powell et al., 2000). Similar to the F-ATPase, the C-terminus of the subunit a of the V-ATPase has two hemi-channels, through which protons enter and exit the V-ATPase (Fig. 2A). Access of the cytosolic hemi-channel is facilitated by the several amino acid (aa) residues, i.e. glutamic acid at position 789 (Glu-789) and the arginine at position 799 (Arg-799) (Fig. 2B, shaded area). The exchange of a Glu-789 to a glutamine has been shown to reduce V-ATPase activity to less than ~20 % (Leng et al., 1996), while exchanging the Arg-799 to a lysine retains ~10% of V-ATPase activity (Kawasaki-Nishi et al., 2001a). Interestingly none of these mutations had any effect on V-ATPase assembly. Protons are transferred from the cytosolic hemi-channel to carboxy groups of glutamic acid residues within the proteolipid ring. The energy transferred from the V_1 subcomplex results in clockwise rotation of the proteolipid ring, allowing protons to pass through the hydrophobic lipid milieu, eventually returning back to subunit a. The deprotonation of the carboxy groups is promoted by an essential arginine at position 735 (Arg-735) in the luminal hemi-channel (Kawasaki-Nishi et al., 2001a). Exchanging the Arg-

735 to an asparagine (Vph1pR735N) renders the V-ATPase completely inactive, while V-ATPase assembly was again not affected (Kawasaki-Nishi et al., 2001a).

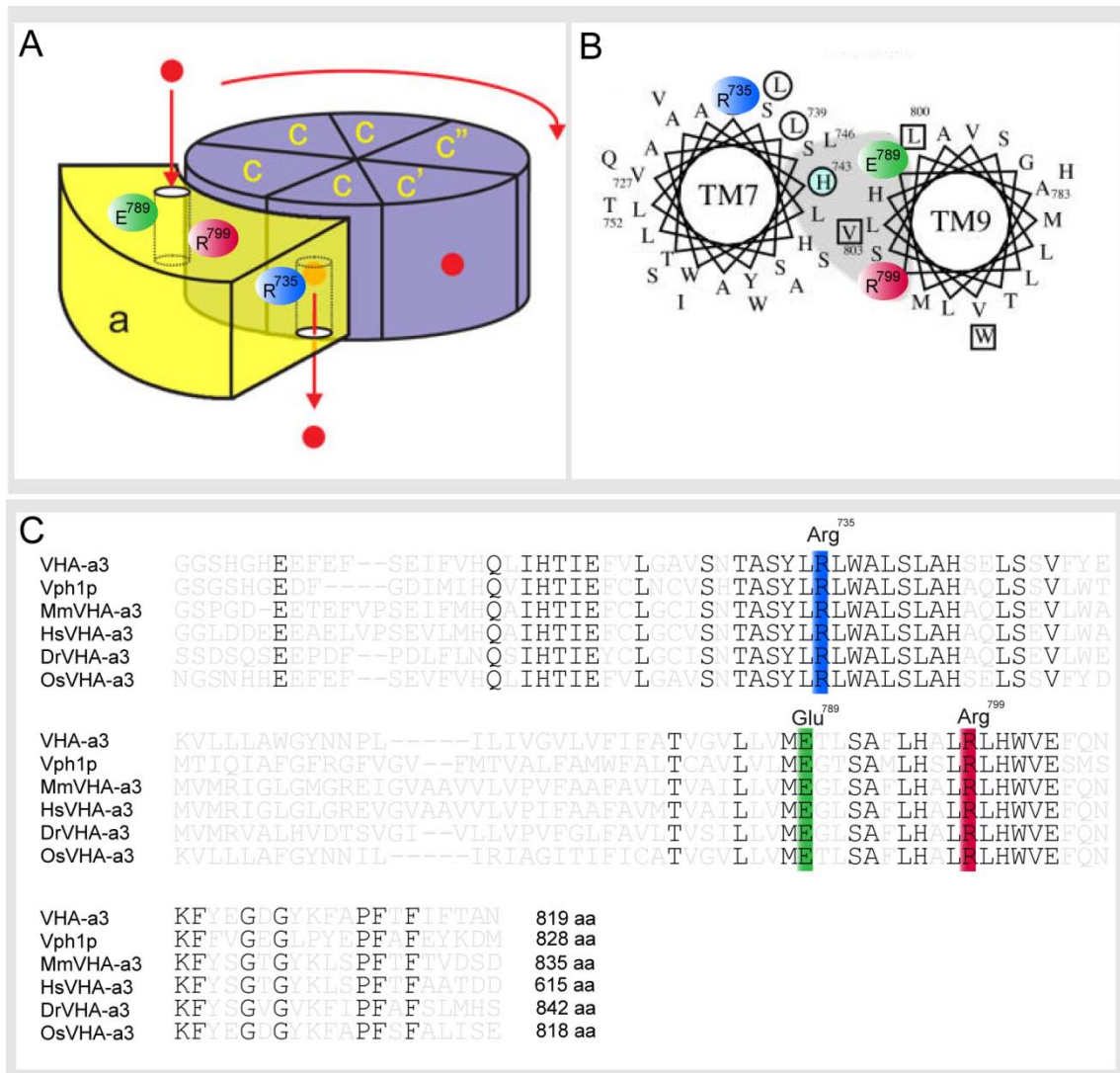


Fig. 2: Three amino acid residues within subunit a are essential for proton translocation. (A) Model of rotary mechanism in the V_0 subcomplex. Shown are: C-terminus of subunit a (yellow) and proteolipid ring (blue). Exposed glutamic acid residue (E-789, green) accepts proton (red circle) from the cytosol. As the proteolipid ring rotates a neutral glutamic acid residue is exposed to the cytosolic hemi-channel, accepting the proton. Further rotation transports the proton towards the luminal hemi-channel. A critical arginine residue (R-735, blue) interacts with the glutamic acid, promoting deprotonation and release of the proton into the luminal hemi-channel. Model adopted from Jeffries et al., 2008 (Jeffries et al., 2008). (B) Model of proton hemi-channel within subunit a. Putative transmembrane regions are shown as circles (TM7 and TM9). Aa residues important for proton translocation are indicated by colored circles with numbers indicated. Putative access channel is indicated as shaded area. Model adopted from Kawasaki-Nishi et al., 2001a (C) Alignment of the subunit a from *Arabidopsis thaliana* (AtVHA-a3), *Saccharomyces cerevisiae* (Vph1p), *Oryza sativa* (OsVHA-a3), *Danio rerio* (DrVHA-a3), *Mus musculus* (MmVHA-a3) and *Homo sapiens* (HsVHA-a3). Identical residues are indicated with black letters. Conserved aa residues, which reduce V-ATPase activity without affecting assembly are highlighted and the yeast amino acid position is mentioned (For VHA-a3 these aa residues correspond to: Arg-729, Glu-780, Arg-790).

Assembly of the V-ATPase

In *Arabidopsis* all subunits of the V_0 subcomplex and the subunit B, E and G of the V_1 subcomplex have different subunit isoforms. In total, 28 *Vacuolar H⁺-ATPase (VHA)* genes are present in the genome of *Arabidopsis* encoding for the different V-ATPase subunits and their corresponding isoforms (Frydman et al., 1994). To orchestrate the V-ATPase assembly process, a highly specific assembly machinery has evolved.

In yeast, three assembly factors (*VMA12*, *VMA22*, *VMA21*) coordinate the assembly and the biogenesis of the V-ATPase (Hill and Stevens, 1994, 1995; Jackson and Stevens, 1997; Dixon et al., 2003). All assembly factors have been located to the ER, and they are not part of the final V-ATPase holo-complex. Loss of any of the three essential assembly factors *VMA12*, *VMA22* and *VMA21* results in a phenotype identical to those observed for mutant cells lacking any V-ATPase subunit (Graham et al., 1998). This phenotype includes the inability to grow on high concentrations of calcium and zinc as well as the inability to grow on neutral and alkaline media buffered to pH 7 (Kane, 2006). Vma12p, Vma22p and Vma21p stabilize Vph1p of the V_0 subcomplex (Hill and Stevens, 1994; Graham et al., 1998). Yeast knock-out strains lacking *VMA12*, *VMA22* and *VMA21* do not display defects in targeting, assembly and processing of other vacuolar membrane or plasma membrane proteins (Hill and Stevens, 1994). *VMA12* encodes for a 25 kDa protein (Vma12p), with two predicted transmembrane domains, both N- and C-termini are orientated towards the cytosol (Tamura et al., 2004). *VMA22* encodes for a 21 kDa protein (Vma22p), located in the cytosol that is recruited to the ER by Vma12p forming a heterocomplex that transiently interacts with the V_0 subcomplex in the ER during V-ATPase assembly (Graham et al., 1998). *VMA21* codes for an 8.5 kDa protein (Vma21p) with two predicted transmembrane domains that interacts with the proteolipid ring of the V_0 subcomplex made up of subunits c, c' and c'' (Malkus et al., 2004). Recently two additional assembly factors have been identified as part of the V-ATPase assembly machinery, however they are not essential. *VOA1* encodes for a 35 kDa glycoprotein (Voa1p) with two transmembrane domains that works in the ER in conjunction with Vma21p (Ryan et al., 2008). *voa1Δ* cells do not display a growth phenotype due to a modest decrease in V-ATPase activity; however in combination with a mutant allele of *vma21*, V-ATPase assembly is significantly reduced (Ryan et al., 2008). *PKR1* encodes for a 14 kDa ER membrane protein (Pkr1p) that has been proposed to increase the efficiency of the V_0 subcomplex assembly (Davis-Kaplan et al., 2006). *pkr1Δ* mutant cells can assemble V-ATPases, though at decreased efficiency. After

completion of V_0 assembly, the V_0 -Vma21p complex is transported to the Golgi (Malkus et al., 2004). Vma21p dissociates from the V_0 subcomplex in the cis-Golgi and is recycled to the ER via a di-lysine ER retention signal at the C-terminus of Vma21p. The exact point, where the V_1 sector associates with the V_0 sector is still elusive.

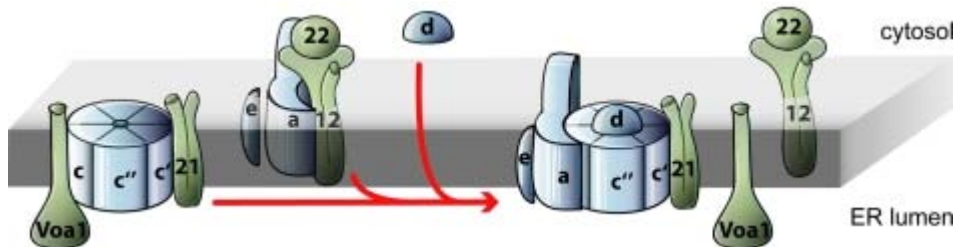


Fig. 3 Assembly of the V_0 subcomplex. Vma21p associates with the subunits c, c' and c'' of the proteolipid ring of the V_0 subcomplex. Voa1 associates with the assembled complex, consisting of Vma21p and the proteolipid ring. Simultaneously the hetercomplex of Vma12p and Vma22p with subunit a. After the disassociation of Voa1, subunit a, d and e assemble with the proteolipid ring, forming a V_0 -Vma21p complex. The assembled V_0 -Vma21p complex is now competent to exit the ER.

In *Arabidopsis thaliana*, AtVMA21a and AtVMA21b have been identified as first Vma21p orthologues. The two orthologues share only 25% sequence identity with Vma21p, and they both can functionally replace the endogenous Vma21p in yeast V-ATPase assembly (Neubert et al., 2008). The phenotype of RNA interference knockdown of AtVMA21a resembles plants with impaired V-ATPase function (Neubert et al., 2008). As a consequence of the reduced V-ATPase activity plants exhibit a significant reduction in hypocotyl length and bending and swelling of Golgi cisternae as it has been previously described for *VHA* null alleles (Dettmer et al., 2005; Strompen et al., 2005). Despite these findings the molecular mechanism of V-ATPase assembly in *Arabidopsis* remains unclear.

ER quality control (ERQC)

Almost one-third of all eukaryotic proteins are destined for the secretory pathway and the endoplasmic reticulum (ER) is the first organelle they encounter (Ghaemmaghami et al., 2003; Kanapin et al., 2003). In contrast to the cytosol, the ER provides an optimal environment for protein folding and maturation. Here, favorable redox conditions and the presence of molecular chaperones allow the formation of disulphide-bonds, N-linked glycosylation, signal-peptide cleavage and glycosphatidylinositol (GPI)-anchor addition (Coleman et al., 1995; Vitale and Denecke, 1999). In plant cells, proteins usually enter the ER cotranslationally in three phases. First, nascent proteins are channeled cotranslational

and cotranslocational through the ER translocon complex, entering the lumen of the ER. After the completed protein chain is released from the translocon complex, post-translational modifications take place. And finally, single subunit proteins assemble into higher oligomeric structures. Several molecular chaperones in the ER participate folding process. These folding enzymes and chaperones ensure that only correctly folded proteins exit the ER and that aberrantly and incompletely assembled proteins are eliminated from the ER (Hartl, 1996; Ellgaard and Helenius, 2003). The presence of a strict ER quality control (ERQC) is crucial to prevent incorrectly folded and thus non-functional proteins from reaching other compartments, where they could have toxic effects (Zerangue et al., 1999).

In general ERQC can be distinguished into a primary and a secondary quality control (Ellgaard et al., 1999; Ellgaard and Helenius, 2003). The primary quality control applies to all proteins encountering the ER, while secondary quality control is reserved for special classes of proteins (Ellgaard et al., 1999). One well studied primary QC system is the so-called calnexin/calreticulin (CNX/CRT) cycle (Denecke et al., 1995; Hebert et al., 1995). Especially under stress conditions, glycoproteins repeatedly fold and refold, constituting the CNX/CRT cycle (Hammond et al., 1994). This cycle promotes the folding of glycoproteins and retains immature proteins either until they reach their mature conformation or if maturation fails, targets misfolded proteins for degradation (Ou et al., 1993; Ware et al., 1995). The CNX/CRT cycle is driven by opposing actions of glucosidase II that removes the glucose and UDP-glucose:glycoprotein glucosyltransferase (UGGT) that reattaches it (Caramelo et al., 2003). Prolonged stay of an immature glycoprotein within this cycle retards their export from the ER, and proper folding may be promoted by the thiol oxidoreductase ERp57, which associates with both CNX and CRT (Elliott et al., 1997; Jessop et al., 2009). In *Arabidopsis* the ERp57 proteins belong to the PDI family, but it is yet not known whether a member of the PDI can function as ERp57 in *Arabidopsis* (Lu and Christopher, 2008). *Arabidopsis thaliana* has two isoforms of CNX and three of CRT. Both, CNX and CRT have a similar structure: An extended hairpin structure called the P domain and a C domain. In yeast Ca^{2+} has been shown to bind within the P domain of CRT (Parlati et al., 1995), while a similar interaction for CNX has so far only been reported in mammals (Wada et al., 1991). Recently, the hairpin domain and the transmembrane domain of CNX have been suggested to play a role in glycosylation independent protein quality control (Ihara et al., 1999; Swanton et al., 2003). *In vitro* showed that the purified hairpin domain

of CNX can suppress protein aggregation of non-glycosylated cytosolic substrate under physiological conditions (Ihara et al., 1999; Brockmeier and Williams, 2006). *In vivo* experiments done in human cell lines demonstrated that the transmembrane domain of CNX is required to specifically recognize non-glycosylated transmembrane proteins (Swanton et al., 2003). How the recognition specificity is achieved is still unclear, however the exchange of a single amino acid within the transmembrane domain of CNX substrates is sufficient for the retention of these proteins to the ER membrane (Swanton et al., 2003). Until today the role of the transmembrane domain of CNX in quality control of non-glycosylated polytopic membrane proteins has so far only been shown in human cell lines. If the maturation process fails, misfolded or aberrant proteins are recognized, retrotranslocated, poly-ubiquitylated and then eventually degraded by the 26S proteasome by a process termed ER-associated degradation (ERAD) (McCracken and Brodsky, 1996). Retrotranslocation of target proteins into the cytosol requires the ubiquitin-proteasome system and the AAA-ATPase Cdc48 complex (Brodsky et al., 1999). Until today it remains unclear if and to what extent the QC machinery recognizes V-ATPase complexes in plants. Only for Vph1p it has been shown to be a substrate for ERQC in yeast cells (Hill and Cooper, 2000).

Contribution to the manuscripts

The author of this thesis wrote all the manuscripts presented in the current work. Apart from the author and the supervisor, persons listed below contributed to this work as indicated.

Assembly of the plant V-ATPase

- Immunogold electron microscopy and quantification of Golgi morphology Corrado Viotti
- Technical assistance for plant work Beate Schöfer

Quality control of the plant V-ATPase

- Construct design, cloning and transformation of *U:VHA- α 3R729N-GFP* Melanie Krebs
- Cloning and transformation of *p16:SP-pHluorin-HDEL* Fabian Fink
- Generation of yeast constructs Upendo Lupanga
- Technical assistance for plant work Beate Schöfer

I – Assembly of the V-ATPase

Abstract

The vacuolar H⁺-ATPase (V-ATPase) is a multi-subunit protein complex, required for the acidification of intracellular compartments. The formation of a functional complex and the underlying mechanisms of the assembly of the V-ATPase subcomplexes V₀ and V₁ still remain largely elusive. Here, we explored the role of the potential *Arabidopsis thaliana* assembly factors *AtVMA12*, and *AtVMA22* in the assembly of the membrane bound V₀ subcomplex. In order to assess the functional relationship between the assembly factor candidates and the V-ATPase, we characterized T-DNA insertion lines of *AtVMA22* and *AtVMA12*. We were unable to detect homozygous plants, due to a lethality as it is also observed for V-ATPase knock-out alleles. In order to complement this phenotype, we transformed genomic construct of *AtVMA22*-GFP as well as overexpressing constructs of *AtVMA12*-RFP and *AtVMA22*-GFP. To study the localization and the interaction between *AtVMA12* and *AtVMA22*, the proteins were expressed transiently in *Arabidopsis* protoplasts and *Nicotiana benthamiana*. We demonstrate that *AtVMA22* is recruited to the endoplasmic reticulum (ER) by *AtVMA12*. We used inducible artificial microRNA constructs against *AtVMA22* and *AtVMA12* and assessed their effect on the V-ATPase. Activated amiRNA constructs led to impaired cell expansion and changed Golgi morphology characteristic for plants with reduced V-ATPase activity. Using CO-IP experiments we could demonstrate that both assembly factors directly associate with components of the V-ATPase.

Introduction

In a eukaryotic cell, most proteins do not act in isolation, but interact with other proteins to fulfill a dedicated cellular task (Ye et al., 2011). The assembled protein complexes are essential for the survival of the cell. Nevertheless our understanding of the coordinated formation of these protein complexes is limited. For soluble proteins it is well-known that hydrophobic effects are the driving forces behind the aggregation and association of proteins (Iwasaki et al., 2009). For membrane-embedded proteins however a thermodynamic view of the subunits constituting a complex is insufficient. Instead membrane-embedded proteins rely on the varying properties of the membrane as well as on the presence of folding and assembly chaperones (Yasuda et al., 2009). These chaperones physically interact with complex intermediates, to prevent their aggregation and subsequent degradation. One example for this interaction represents the bacterial F_1F_0 -ATPase (F-ATPase), whose membrane-embedded F_0 subcomplex is assembled with the coordinated help of the assembly factors Uncl, ATP10 and ATP23 (Descamps et al., 2009; Gruber et al., 2009; Wagner and Mittag, 2009). Structurally and mechanistically similar to the F-ATPase are the V-ATPases. The first indications that assembly factors interact with the V-ATPase came subcellular fractionation analysis of yeast mutants lacking Vma22p. Vma22p is a cytosolic protein, yet in wild-type cells, it was found associated with the ER. In *vma12 Δ* cells, the fractionation profile of Vma22p changed, now being localized in the cytosol (Hill and Stevens, 1995). Further investigation revealed that the ER association of Vma22p depended on the presence of Vma12p. Vma12p and Vma22p form a stable hetero-complex assisting in the assembly of the V_0 subcomplex in the ER. Both proteins were not detected in the final V-ATPase holo-complex, which led to the conclusion that they only transiently interact with the V-ATPase, before it is transported to the vacuole (Graham et al., 1998).

Despite the strong conservation in overall V-ATPase composition, localization, and function, in plants and other higher eukaryotes the assembly of the V-ATPase is largely unaddressed. We have identified one potential *Arabidopsis thaliana* orthologue of Vma12p and of Vma22p. Here we report that both putative orthologues are essential for plant development. BIFC analysis revealed that AtVMA22 is recruited to the ER membrane by AtVMA12. We present biochemical evidence that AtVMA12 directly interacts with components of the V_0 subcomplex in the ER. Finally, reduction of transcript levels of both assembly factors led to impaired V-ATPase activity shown by reduced hypocotyl length and

aberrant Golgi morphology. In addition, we observe pro-vacuolar structures within meristematic root cells. Our analysis indicates that AtVMA12 and AtVMA22 are required in the plant cell ER to assemble a functional V-ATPase.

Results

Identification of Vma12p and Vma22p orthologues

Based on low sequence similarity but similar protein size and topology potential orthologues of Vma12p and Vma22p of *Arabidopsis thaliana* (AtVMA12 [At5g52980](#); AtVMA22 [At1g20770](#)) and *Drosophila melanogaster* (DmVMA12 [CG7071](#), DmVMA22 [CG14671](#)) have been identified (Fig. 4A and B). The Vma12p orthologues from *Drosophila* and *Arabidopsis* share ~11 % amino acids (aa) identity and ~24 % aa similarity. AtVMA12 with 25,4 kDa is similar in size to Vma12p with 25,2 kDa, while DmVMA12 with 34,52 kDa is larger than its orthologues. The difference in size can be explained by the presence of the 65 aa longer N-terminus of DmVMA12. Similar to the yeast Vma12p, the *Arabidopsis* and the *Drosophila* orthologue are predicted to have two transmembrane domains. The alignment in Fig. 4A also highlights the membrane topology of the VMA12 proteins based on predictions of SignalP4.0 (Petersen et al., 2011). AtVMA12 possesses a strong C-terminal dilysine (KK) - motif, whereas the yeast orthologue possesses only a weak KITL C-terminal retention signal (Jackson et al., 1990). The DmVMA12 lacks a classical ER retention motif. The VMA22 proteins also share weak aa identity (~9 %) and a similarity (~23 %). All VMA22 proteins have a similar size with ~20 kDa (DmVMA22 17,3 kDa; Vma22p 20,1 kDa; AtVMA22 23,8 kDa). There are no putative membrane spanning domains in AtVMA22, Vma22p and DmVMA22 as predicted by hydropathy analysis (Kyte and Doolittle, 1982).¹

We analyzed the expression pattern of *AtVMA12* and *AtVMA22* using the data set of AtGenExpress Developmental series (Schmid et al., 2005). Both assembly factors show similar expression profiles in seedlings, roots, shoots, leaves and flowers. The transcript levels of *AtVMA22* are slightly stronger than the expression of *AtVMA12* in all of the previous named organs. In the ripening seeds however the correlation of the expression between the assembly factors is lost. While *AtVMA12* expression increased fourfold, expression of *AtVMA22* decreased by half (Fig. S. 3).

¹ Further characterization of the *Drosophila* candidates was done in collaboration with Dr. Fani Papagiannouli, 2011-2012 and will be described and discussed elsewhere.

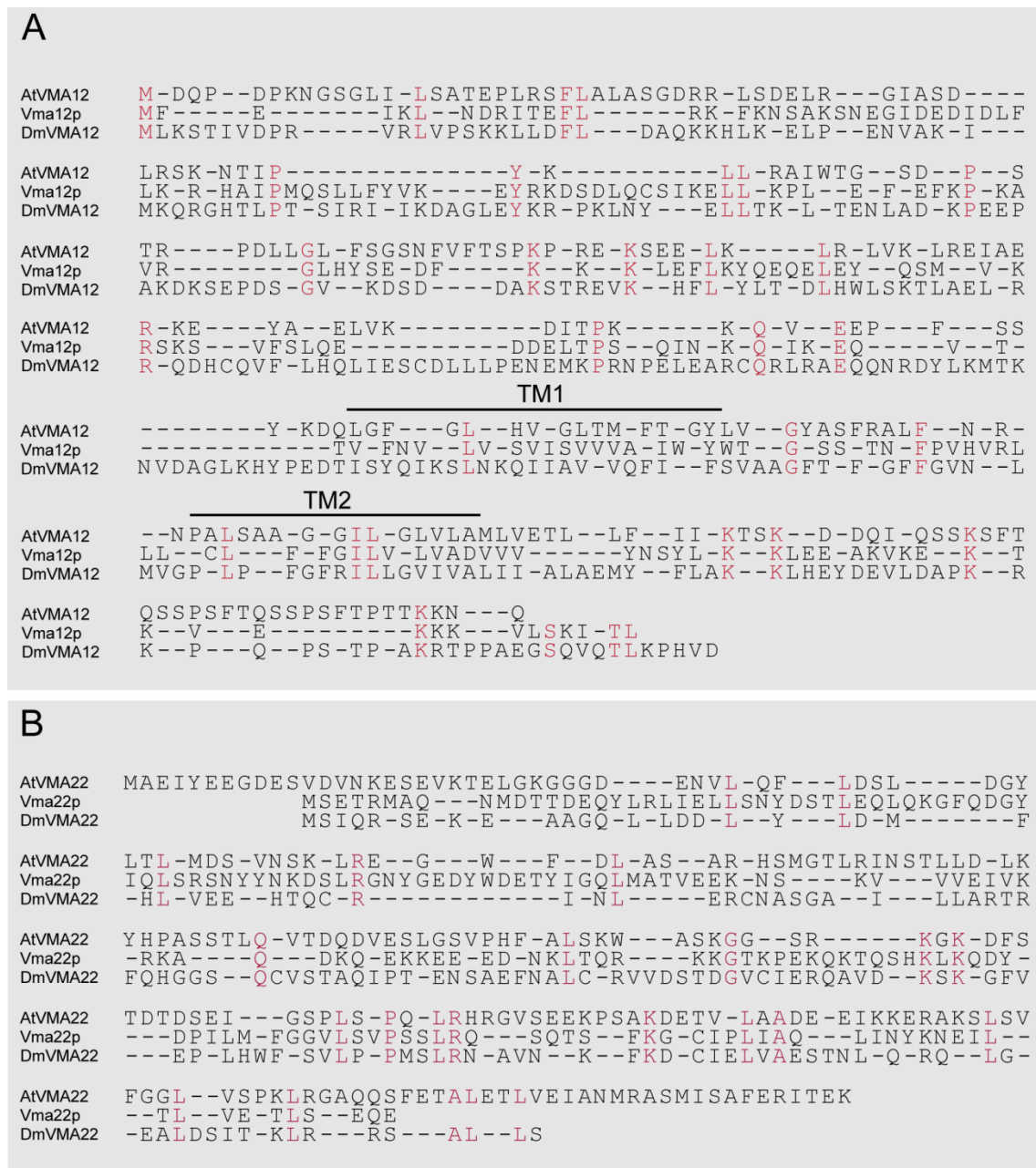


Fig. 4: Alignment of Vma12p and Vma22p with candidate proteins from *Arabidopsis thaliana* and *Drosophila melanogaster*. Identity between the proteins is indicated by red letters, similarity between the proteins is not highlighted. (A) Amino acid sequences of yeast Vma12p, AtVMA12 (At2g31710) and DmVMA12 (CG7071) were aligned using the Clustal W algorithm. The VMA12 proteins share 11% amino acid identity. Transmembrane domains are marked as TM1 and TM2. Topology was predicted using TMHMM. (B) Amino acid sequences of yeast Vma22p and AtVMA22 (At2g31710) and *Drosophila* DmVMA22 were aligned using the Clustal W algorithm. The VMA22 proteins share 9% amino acid identity.

Localization and interaction of AtVMA12 and AtVMA22

In yeast, the membrane-integral Vma12p interacts directly with the soluble Vma22p recruiting it onto the cytosolic face of the ER membrane. The interaction results in the formation of a hetero-complex assisting in the assembly of the V_0 subcomplex (Graham et

al., 1998). To determine the subcellular localization of AtVMA22 and AtVMA12, we created overexpressing constructs for AtVMA12 and AtVMA22, both under the control of the Ubiquitin promoter (UBI10) (Norris et al., 1993), thereby guaranteeing a ~100 higher and ubiquitous expression of our constructs. Due to the potential C-terminal ER di-lysine motif, AtVMA12 was tagged with mRFP at the N-terminus. AtVMA22 was tagged at the N-terminus with GFP.

GFP-AtVMA22 was transiently expressed together with RFP-AtVMA12 or as a control with AtVMA21-RFP (Neubert et al., 2008). We used *Arabidopsis* suspension culture protoplasts (FIG. S. 2) and *Nicotiana benthamiana* plants for the transient expression of the constructs. GFP-AtVMA22 is localized to the cytosol, if co-expressed with AtVMA21-RFP (Fig. 5A-C). The co-expression of GFP-AtVMA22 and RFP-AtVMA12 resulted in the recruitment to the ER surface (Fig. 5D-E), indicating that the two proteins interact *in planta*.

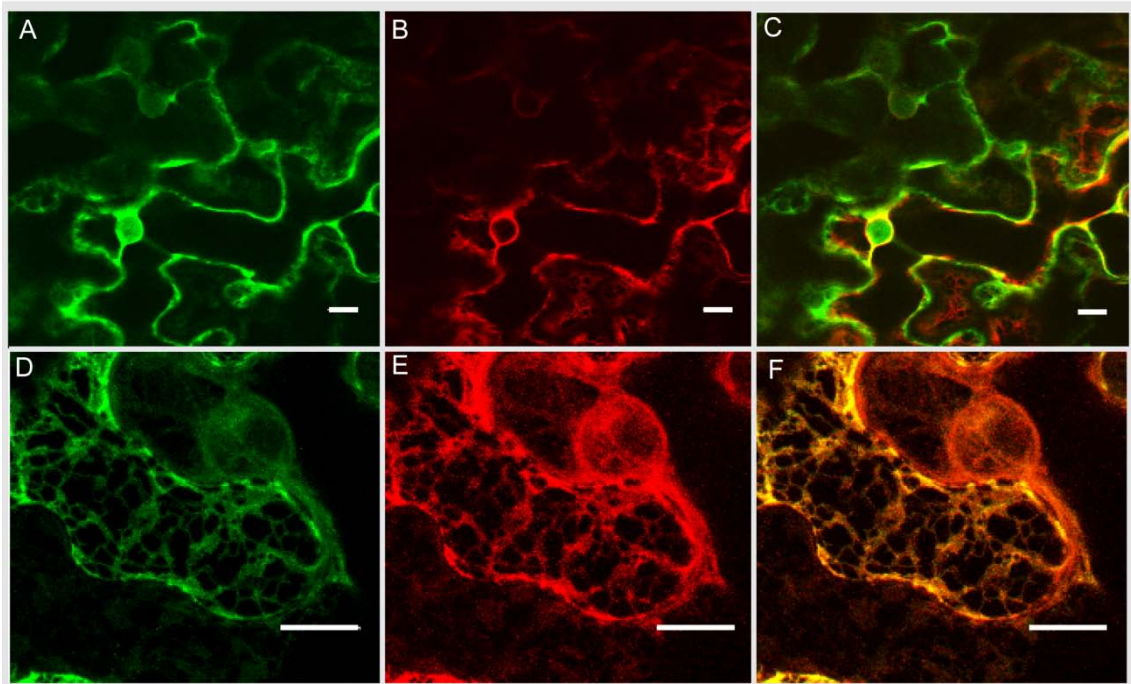


Fig. 5: GFP-AtVMA22 is recruited to the ER, when co-expressed with RFP-AtVMA12. Three week old plants of *Nicotiana benthamiana* were transiently expressed with (A) GFP-AtVMA22 and (B) AtVMA21-RFP or (D) GFP-AtVMA22 and (E) RFP-AtVMA12. Figure C depicts an overlay of A and B. Figure F depicts an overlay of D and E. Bars represent 10 μ m

In yeast, the recruitment of Vma22p to the ER membrane is a result of the direct interaction between Vma12p and Vma22p. We were interested whether the recruitment of GFP-AtVMA22 to the ER membrane was the result of a direct interaction between RFP-AtVMA12 and GFP-AtVMA22. To answer this question, we used the bimolecular fluorescence complementation (BIFC) technique for visualization of protein-protein interaction (Hu et al., 2002).

AtVMA22 and *AtVMA12* cDNAs were cloned into pxYC (p22YC) and pYNx (pYN12), respectively. As control, we cloned the cDNA of *AtVMA21* into the pYNx (pYN21). We observed YFP fluorescence, when the combination of p22YC and pYN12 were expressed (Fig. 6A). Notably, we were unable to detect any fluorescence signals when pYN12 was co-expressed with a construct where the YFP-fragment was fused N-terminal to cDNA of *AtVMA22* (pYC22) (data not shown). Expression of p22YC with pYN21 however induced no fluorescence signals (Fig. 6C). Immuno-blot analysis of protein samples prepared from tobacco leaf material was performed to determine if the proteins were expressed. We used c-myc-tag- (pYN12 and pYN21) and HA-specific (p22YC) antibodies to demonstrate the expression of all fusion proteins in tobacco cells (Fig. 6B and D).

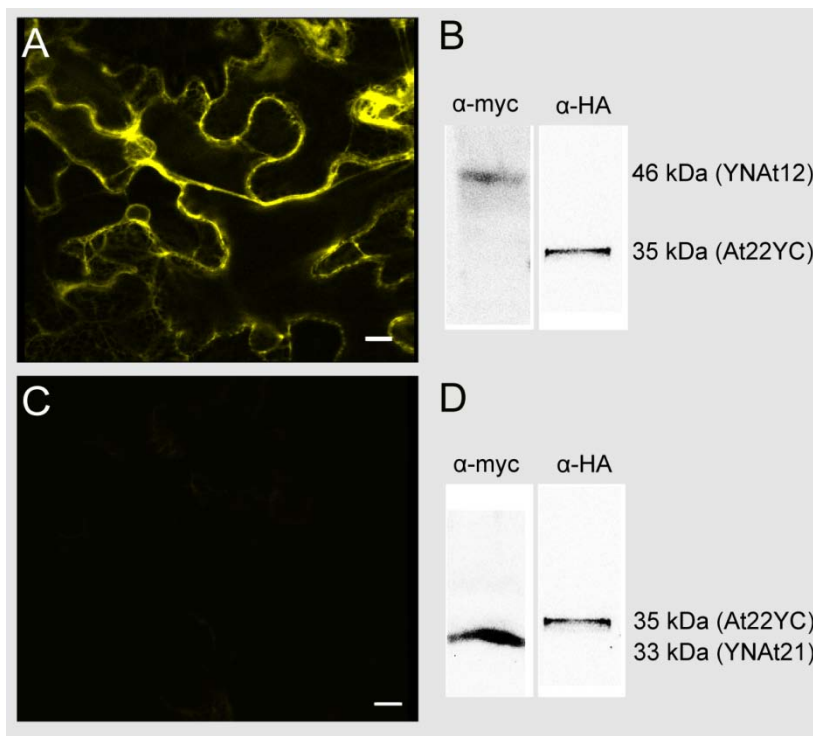


Fig. 6 *AtVMA22* interacts directly with *AtVMA12* in the ER membrane. Three week old plants of *Nicotiana benthamiana* transiently expressed (A) pYN12 and p22YC or (C) pYN21 and p22YC. The presence of the expressed fusion proteins was demonstrated by immunodetection with anti-c-myc (α -myc) antibodies for YN fusions and anti-HA (α -HA) for YC fusions (B and D). Bars represent 10 μ m

Do *AtVMA12* and *AtVMA22* function in V-ATPase assembly in yeast?

In order to determine if *AtVMA12* and *AtVMA22* are functional orthologs of the yeast assembly factors Vma12p and Vma22p, we tested whether *AtVMA12* alone or in conjunction with *AtVMA22* could complement yeast cells lacking Vma12p (*vma12 Δ*). The *vma12 Δ* null mutant exhibits a characteristic *vma $\bar{1}$* phenotype, including an increased sensitivity to high concentrations of Ca^{2+} in the medium and an inability to grow on media buffered to pH 7.5 (Graham et al., 1998). We compared the growth phenotype of yeast lacking the assembly factor Vma12p with cells expressing either *AtVMA12*, or co-

expressing AtVMA12 and AtVMA22. All proteins were expressed by a CEN plasmid under the control of the *Vma12* promoter. An HA-epitope tag was introduced at the N-terminus of AtVMA12. As shown in Fig. 7, yeast cells lacking *Vma12p* (*vma12Δ*), do not grow on rich media supplemented with 60 mM Ca^{2+} , due to a lack of functional V-ATPases. Neither the expression of the *Arabidopsis* assembly factor AtVMA12, nor the co-expression of AtVMA12 and AtVMA22 together in *vma12Δ* cells restored growth in the presence of elevated calcium. Total cell proteins were extracted from *vma12Δ* cells transformed with AtVMA12::HA and separated using SDS-PAGE. We were unable to detect AtVMA12::HA using anti-HA antibodies, from which we concluded that AtVMA12 could not be expressed in yeast cells (data not shown).

Taken together, unlike AtVMA21 (Neubert et al., 2008), the two *Arabidopsis* candidates fail to complement the respective yeast mutants indicating a higher degree of functional divergence (Fig. 7). Although the assembly factors lack the amino acid conservation known from components of the V-ATPase, we hypothesized that there is a structural conservation among the assembly factors. We therefore generated *AtScVMA12* chimeric constructs, by either replacing the yeast N-terminus or C-terminus of ScVMA12 with the respective portion of AtVMA12 (*AtScVMA12_N*/ *AtScVMA12_C*). We were unable to complement the yeast mutant *vma12Δ* and *vma12Δvma22Δ* with the chimeric *AtScVMA12* constructs (Fig. S. 1).

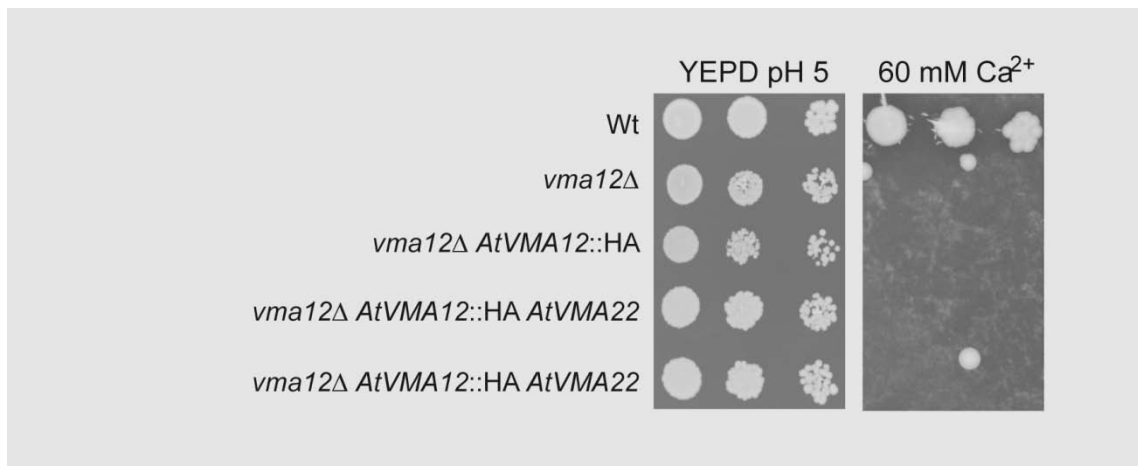


Fig. 7: The *Arabidopsis* assembly factors AtVMA12/22 do not complement the compromised growth phenotype of the yeast mutant *vma12Δ*. *vma12Δ* cells transformed with either AtVMA12::HA or with AtVMA12::HA and AtVMA22 were grown in SD-URA medium to $\text{OD}_{600} = 1$. As a control Wt (SF 838-1) cells were grown in YEPD medium to an $\text{OD}_{600} = 1$. The cultures were serially diluted (1:10, 1:100) and spotted onto YEPD medium buffered to pH 5 and on YEPD media containing and 60 mM CaCl_2 .

AtVMA22 and AtVMA12 are essential for the plant

Neither *AtVMA12* alone, nor in conjunction with *AtVMA22* were able to rescue the *vma12Δ* phenotype. To prove that *AtVMA12* and *AtVMA22* are true assembly factor of the plant V-ATPase, we characterized T-DNA insertion lines for *AtVMA22* (SALK_031513) and *AtVMA12* (SAIL_634_F09). To rule out the possibility of chromosomal rearrangements and to determine the exact insertion site, both T-DNA/genomic DNA junctions of the insertion allele of *atvma12* and *atvma22* were sequenced (Fig. 8A and B).

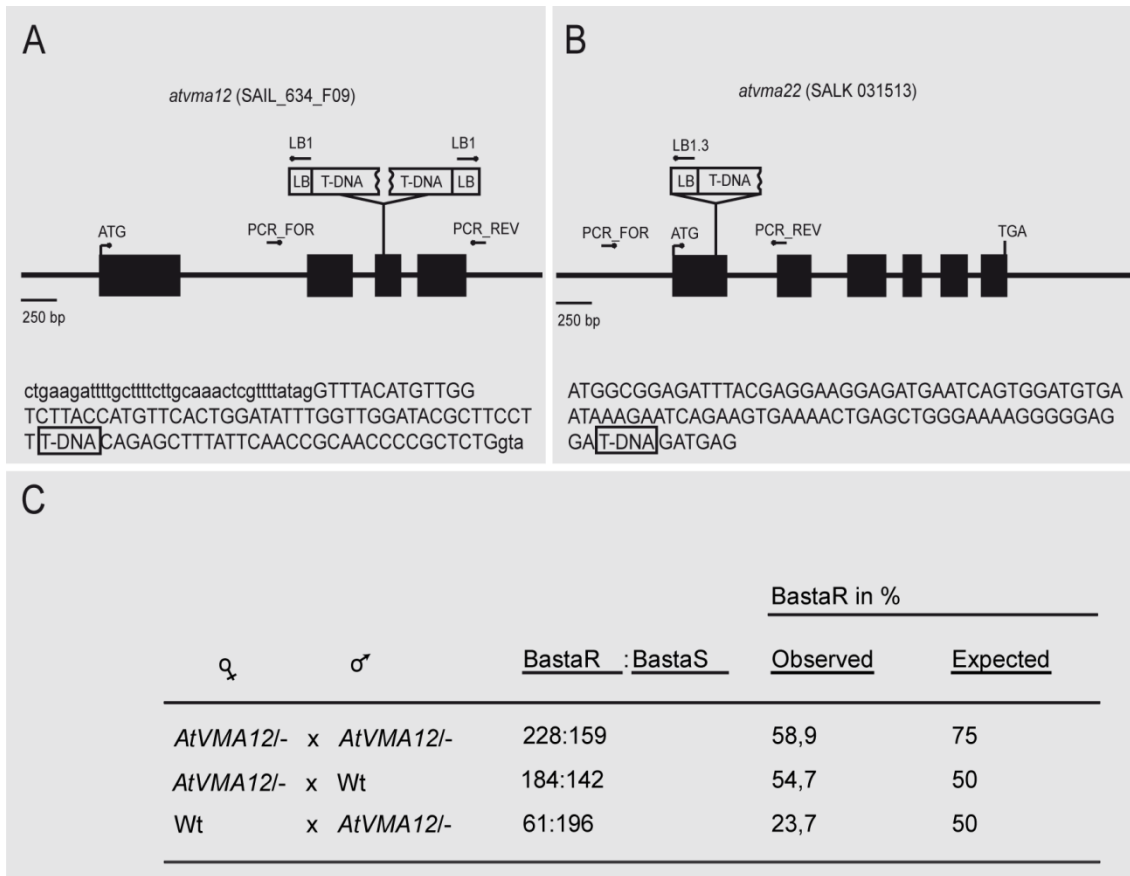


Fig. 8: Structure of the *AtVMA22* T-DNA allele and structure and segregation *AtVMA12* T-DNA allele. (A-B) Schematic representation of the T-DNA insertion allele *atvma12* (T-DNA insertion line SAIL_634_F09) and *atvma22* (T-DNA insertion line SALK_031513). Primers used to sequence T-DNA junctions are indicated as either LB1.3 (T-DNA specific), or PCR_FOR/REV (genome specific). Below: Position of T-DNA insertion (black box “T-DNA”) is shown within the genomic sequence, exon (capital letters) and intron (small letters). (A) The T-DNA is inserted in the third exon (exons are indicated as black boxes) of *AtVMA12*. Position 21482702 – 21482624 of chromosome 5 is shown as sequence below. T-DNA insertion is highlighted. (B) The T-DNA is inserted in the first exon of *AtVMA22*. Position 7216742 – 7216520 of chromosome 1 is shown as sequence. T-DNA insertion is highlighted (C) Segregation analysis of heterozygous *AtVMA12*^{-/-} plants.

We established that a tandem T-DNA insertion with inverted orientation, where the left border (LB) of the T-DNA is facing the genomic DNA has been integrated in the third exon of *AtVMA12* (Fig. 8A). For *AtVMA22*, a single T-DNA is inserted in the first exon, its LB

facing towards the 5' upstream region of the genomic DNA (Fig. 8B). Out of 140 and out of 260 individuals we were unable to detect homozygous plants for the null mutant of *atvma22* and *atvma12*, respectively, indicating either gametophyte or embryo lethality. Previous research on V-ATPase mutants has shown that single copy V-ATPase knock-out alleles lead to gametophyte or embryo lethality (Dettmer et al., 2005; Strompen et al., 2005). We proceeded with a genetic analysis of the heterozygous *AtVMA12*^{-/-} line using the Basta-Resistance (BastaR) on the T-DNA to observe the segregation. For *AtVMA22*^{-/-} plants the resistance gene has been silenced, therefore segregation analysis based on the kanamycin resistance (KanR) could not be employed. Analysis of the progeny of self-fertilized *AtVMA12*^{-/-} plants showed a decreased transmission of the BastaR gene (Fig. 8C). We asked whether the decreased transmission was due to a female or the male gametophyte lethality. We performed reciprocal crosses between *AtVMA12*^{-/-} and wild-type plants. Analysis of BastaR of the resulting progeny showed that transmission through the male gametophyte was impaired whereas transmission through the female gametophyte was not affected (Fig. 8C). One explanation for this might be that microgametogenesis of the null allele microspores can be sustained by sporophytic gene products, provided by the anther wall (Maitrejean et al., 2011). As a consequence subsequent fertilization of the female gametophyte can occur, but embryo development for individuals homozygous for the null allele is arrested, after the sporophytic gene product has been consumed. To rule out that reduced transmission of the T-DNA was not caused by a second-site mutation, but indeed by a lack of *AtVMA12*, BastaR *AtVMA12*^{-/-} plants were transformed with *RFP* tagged *AtVMA12* constructs carrying a KanR gene. 20 KanR T₁ plant lines were self fertilized; the T₂ progeny was subjected to kanamycin and BASTA selection, to obtain homozygous individuals for the null allele and for the *RFP-AtVMA12* insertion. Homozygous individuals were confirmed via PCR (Fig. 9A). Expression of *RFP-AtVMA12* was confirmed by CLSM analysis (Fig. 9B). Heterozygous *AtVMA22*^{-/-} plants were identified via PCR and transformed with *GFP* tagged *AtVMA22* constructs linked to a BastaR gene. Homozygous individuals for the null allele were confirmed via PCR (Fig. 9C). We were unable to detect any fluorescent signals in 20 independent *GFP-AtVMA22* lines (Fig. 9D). Unlike the *RFP-AtVMA12* construct, which was driven by the UBI10 promotor, the *GFP-AtVMA22* construct was expressed under the control of the endogenous *AtVMA22* promotor. Using the data set of the AtGenExpress Developmental series (Schmid et al., 2005), we analyzed the expression pattern of *AtVMA22* (Fig. S. 3).

From this data we concluded that the expression of GFP-AtVMA22 was too low to be detected.

Taken together our results indicate that observed lethality is due to the absence of the putative assembly factors *AtVMA22* and *AtVMA12*, respectively.

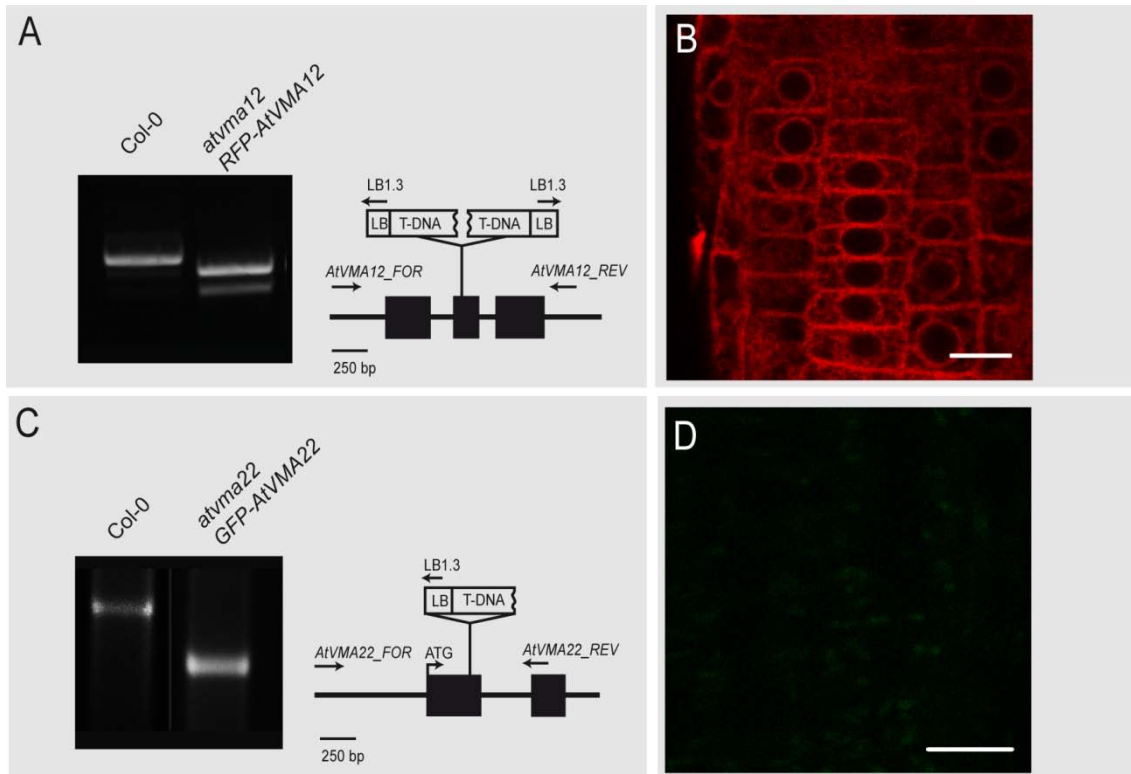


Fig. 9: *GFP-AtVMA22* and *RFP-AtVMA12* complement the *atvma12* and the *atvma22* null allele. Heterozygous *AtVMA12*^{-/-} and *AtVMA22*^{-/-} plants were transformed with *RFP-AtVMA12* and *GFP-AtVMA22* constructs respectively. (A) Plants homozygous for the null allele (*atvma12*) were identified via PCR using three primers (*AtVMA12_FOR/REV* and *LB1.3*). Due to the tandem T-DNA insertion, two bands were expected. (B) Root tips of 5 day old seedlings expressing *RFP-AtVMA12* were subjected to confocal laser scanning microscopy (CLSM) analysis. (C) Homozygous plants for the *GFP-AtVMA22* construct were selected on BastaR. Among these plants, homozygous plants for the null allele (*atvma22*) were identified by PCR using gene specific primers (*AtVMA22_FOR/_REV*) and T-DNA specific primers (*LB1.3*). (D) Root tips of 5 day old seedlings expressing *GFP-AtVMA22* were subjected to confocal laser scanning microscopy (CLSM) analysis. CLSM bars represent 10 μm.

Are *AtVMA12* and *AtVMA22* functional assembly factors of the V-ATPase?

Similar to null alleles of V-ATPase single copy genes, which exhibit either gametophyte or embryo lethality (Dettmer et al., 2005; Strompen et al., 2005), null alleles of *AtVMA12* and *AtVMA22* are lethal, suggesting that they function in V-ATPase assembly. In order to understand whether *AtVMA12* and *AtVMA22* are functional assembly factors of the V-ATPase, phenotypic analyses of weak mutant alleles in *Arabidopsis thaliana* were employed.

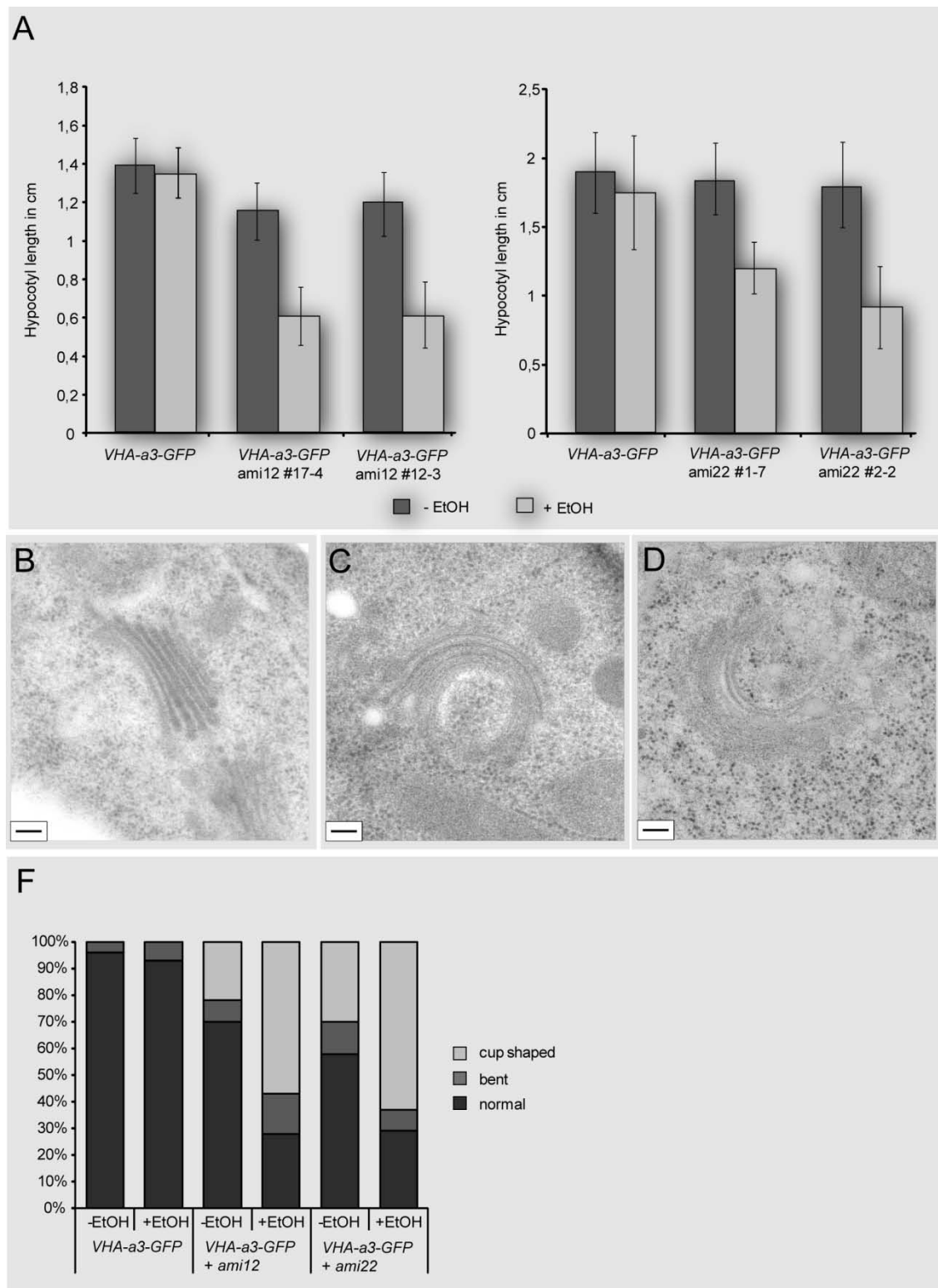


Fig. 10: Ethanol-induced expression of artificial microRNA against *AtVMA12* (*ami12*) and *AtVMA22* (*ami22*) respectively leads to a V-ATPase-deficient phenotype. (A) Hypocotyl length of 4d old etiolated seedlings grown in the absence or presence of EtOH. Shown are the results for *VHA-a3-GFP* and two independent transgenic lines expressing the ami-constructs against *AtVMA12* (*ami12*) and *AtVMA22* (*ami22*), respectively. At least 30 seedlings of each line were measured, error bars represent standard error. (B) Normal Golgi morphology is depicted in high-pressure frozen *VHA-a3-GFP* samples. Golgi morphology is altered in samples expressing the amiRNA against (C) *AtVMA12* and (D) *AtVMA22*. (F) Quantitative analysis of the amiRNA effects on Golgi morphology. Roots of the indicated lines were analyzed counting the number of Golgis in 100 sectioned cells per root. Bars represent 100 nm.

Homozygous plants expressing the tonoplast-localized subunit of the V-ATPase VHA-a3-GFP and *ami12* or *ami22* exhibit a reduced hypocotyl growth, which has been shown to reflect a reduction of the V-ATPase activity (Brüx et al., 2008; Neubert et al., 2008)(Fig. 10A). Ultrastructural analysis of *Arabidopsis* seedlings co-expressing *ami12* and *ami22* with VHA-a3-GFP revealed an aberrant Golgi morphology (Fig. 10C and D) as it has been previously described for V-ATPase knockout alleles and ConcA treatment (Dettmer et al., 2005; Strompen et al., 2005; Brüx et al., 2008). Statistical analysis showed a significant increase in aberrant shaped Golgi stacks in plants with induced *ami12* and *ami22* constructs, while only mild changes in Golgi morphology could be observed in plants with non-induced *ami* constructs (Fig. 10F). The mild induction of the *ami* constructs under non-inducing conditions can be explained with a leakiness of the AlcR/AlcA two component system (Roslan et al., 2001; Roberts et al., 2005). Confocal laser scanning microscopy (CLSM) analysis of 5 day old *Arabidopsis ami12* and *ami22* seedlings demonstrated that VHA-a3-GFP is localized to tubular structures (Fig. 11B and C). Previous work has suggested that mature vacuoles form as a result of branching ER tubules that sequester the cytoplasm (Hilling and Amelunxen, 1985). These pro-vacuoles have been identified in meristematic root cells of oat seedlings. Alternatively these tubules could represent vacuoles that are retarded in growth, possibly due to reduced V-ATPase activity. We applied immuno electron microscopy to further characterize these VHA-a3-GFP labeled tubules. We used meristematic cells in root tips probing with *Arabidopsis* vacuolar H⁺-pyrophosphatase (AVP1) antibodies. Gold particles were present at numerous tubular structures (Fig. 11D). Together, the IEM and the confocal laser scanning microscopy data indicate that the tubular structures could either represent pro-vacuoles or immature vacuoles. The CLSM data shows the presence of these tubular structures in plants, co-expressing VHA-a3-GFP and the *ami*RNA against the assembly factors (Fig. 11B,C).

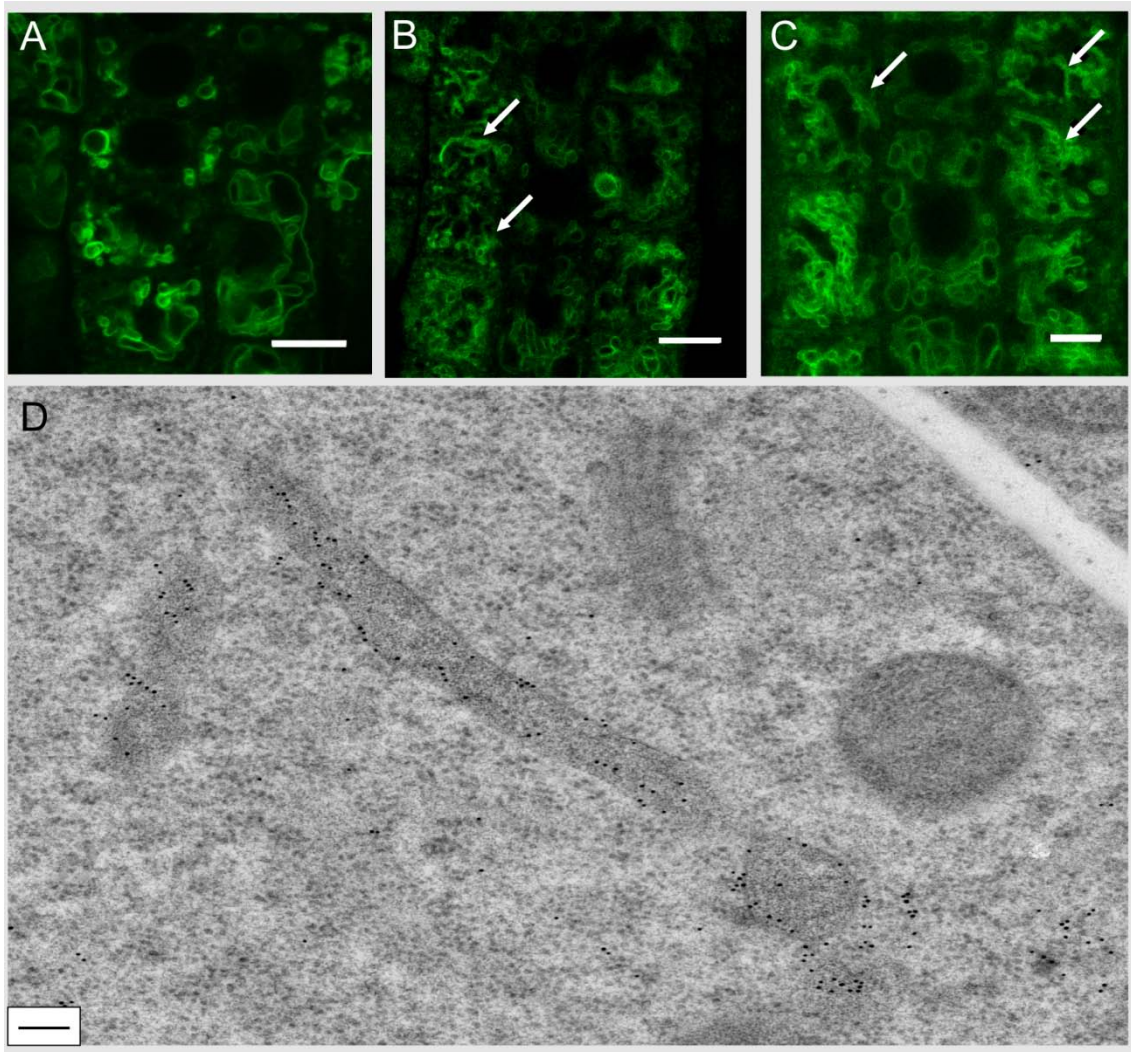


Fig. 11 Knock-down of the assembly factors *AtVMA12/AtVMA22* results in localization of VHA-a3-GFP to tubular structures. Root tips of 5 day old seedlings grown in the presence of ethanol (EtOH) were subjected to confocal laser scanning microscopy (CLSM) analysis and immuno electron microscopy (Biermann et al.). (A) VHA-a3-GFP is localized to mature vacuoles. Expression of (B) *ami12* and (C) *ami22* resulted in an increased number of pro-vacuoles labeled by VHA-a3-GFP (arrowheads). (D) AVP1 labeled pro-vacuoles. CLSM Bars represent 10 μm ; IEM bar represents 100 nm.

The maturation of vacuoles is a process including multiple fusion events of smaller vesicles and osmotic swelling due to water uptake. The role of the V-ATPase in the vacuolar maturation process has yet not been addressed in *Arabidopsis*. Our data suggests that the knockdown of the assembly factors *AtVMA22* and *AtVMA12* either directly interferes with the maturation of pro-vacuoles or the absence of an efficient assembly machinery delays the maturation by affecting V-ATPase assembly and/or function. To test whether these tubular structures can be attributed towards the loss of functional V-ATPases, we assayed the protein stability of VHA-a3-GFP in amiRNA lines.

Knockdown of AtVMA22 or AtVMA12 does not affect vacuolar V-ATPase stability

Knockout of *VMA12* and *VMA22* results in a severe destabilization of the Vph1p, leading to the degradation of the entire V_0 subcomplex (Kane, 1992). We were unable to detect a reduction of the protein levels of VHA-a3-GFP in *Arabidopsis* seedlings co-expressing VHA-a3-GFP and the amiRNA against the assembly factors (Fig. 12). We hypothesize that knock-down of the assembly factors was incomplete and therefore V_0 subcomplexes are still formed. In order to monitor V_0 subcomplex degradation we subjected induced and non-induced ami22 lines to Cycloheximide (CHX). CHX is a well established antibiotic inhibiting protein biosynthesis. After 2h CHX treatment of VHA-a3-GFP lines with activated artificial microRNA against AtVMA22 protein levels were not changed, implying that the knockdown does not affect the stability of VHA-a3-GFP (Fig. 12).

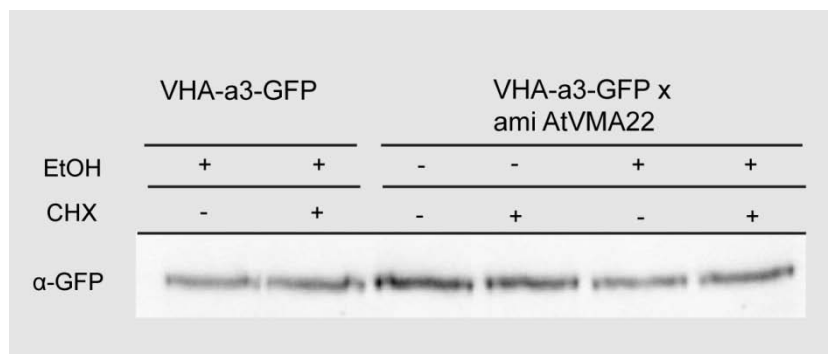


Fig. 12: VHA-a3-GFP protein stability is not affected after knockdown of AtVMA22. 6 day old plants grown on MS medium either supplemented with 0.3% of EtOH were subjected to 300 μ M CHX treatment for 2h.

AtVMA12 interacts with the V_0 subcomplex

In yeast, cross-linking experiments have proven a direct interaction of the heterocomplex Vma12p/Vma22p with Vph1p. The interaction between the V_0 subcomplex and the assembly factors has been reported to occur with a half-life of less than 5 min, due to rapid trafficking of V_0 subcomplexes out of the ER (Graham et al., 1998).

Our results so far indicate that AtVMA12 and AtVMA22 play a critical role for the function of the V-ATPase complex. In order to better understand how AtVMA12 and AtVMA22 facilitate the assembly process, we asked whether AtVMA12 directly interacts with V_0 subunits. To answer this question, we co-immunoprecipitated RFP-AtVMA12 from plants co-expressing RFP-AtVMA12 and VHA-a3-R729N-GFP. The mutation in the *VHA-a3* isoform renders the V-ATPase non-functional, while protein complex assembly is not affected (Refer chapter II). In contrast to Wt Col-0 plants, expressing VHA-a3-GFP, V_0 complexes containing VHA-a3R729N-GFP are retained in the ER, not reaching the vacuole (Fig. 13A and B). As can be seen in Fig. 13B RFP-AtVMA12 and VHA-a3R729N-GFP co-localized in the

ER to a very high degree. We extracted total microsomal membranes from 5 day old etiolated *Arabidopsis* seedlings either co-expressing VHA-a3-GFP/-R729N and RFP-AtVMA12, or RFP-AtVMA12 alone. Using an anti-RFP antibody we were able to detect a ~50 kDa protein, which corresponds to the expected size of RFP-AtVMA12 (Fig. 13C).

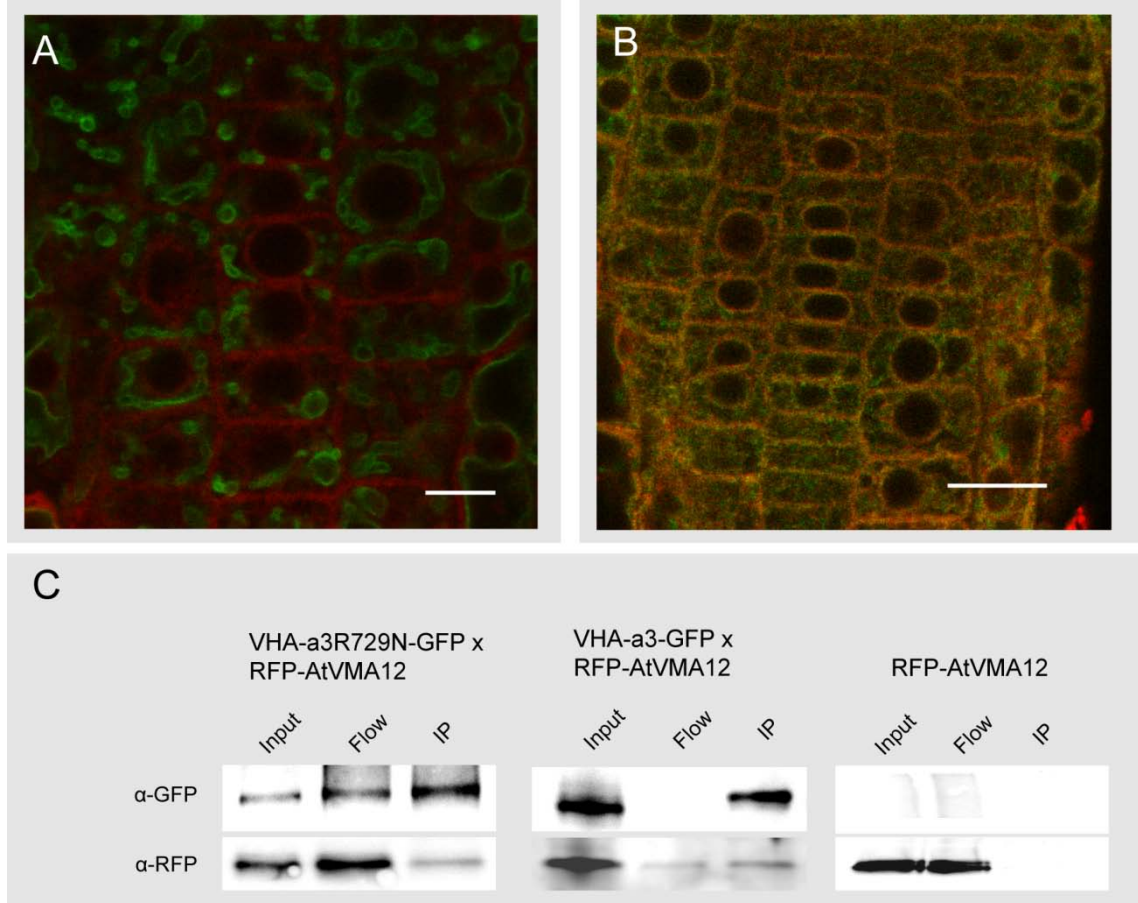


Fig. 13 RFP-AtVMA12 directly interacts with VHA-a3R729N-GFP in the ER membrane. *Arabidopsis* root tips of 5 day old seedlings (A) co-expressing of RFP-AtVMA12 and VHA-a3-GFP and (B) co-expressing RFP-AtVMA12 and VHA-a3R729N-GFP. (C) GFP immunoprecipitation from 5 day old etiolated *Arabidopsis* seedlings co-expressing RFP-AtVMA12 and VHA-a3R729N-GFP, or RFP-AtVMA12 and VHA-a3-GFP, or expressing RFP-AtVMA12 alone, using GFP-TRAP[®] coupled magnetic particles. Total microsomal extracts (Input), unbound protein flow (Flow) and immunoprecipitates (IP) were subjected to immunoblots using anti-GFP and anti-RFP antibodies. CLSM bars represent 10 μ m.

In a control experiment of plants only expressing RFP-AtVMA12, the 50 kDa band could only be detected in the Input and Flow, while it was not recovered in the actual IP, indicating that RFP-AtVMA12 specifically binds to VHA-a3-GFP and VHA-a3R729N-GFP (Fig. 13C). Interestingly, the protein amount of RFP-AtVMA12 co-immunoprecipitating with VHA-a3R729N-GFP was almost equal to the amount of RFP-AtVMA12 co-immunoprecipitating with VHA-a3-GFP (Fig. 13C), indicating that the retention of VHA-a3R729N-GFP in the ER did not prolong the interaction between AtVMA12 and the V_0 subcomplex.

Taken together we conclude that AtVMA12 interacts with the V_0 subcomplex in the ER. The retention of the V_0 subcomplex, in the case of the VHA-a3R729N, in the ER does not change the kinetics of the V_0 – AtVMA12 interaction.

AtVMA22 interacts with the V_1 subcomplex

Our results so far indicate that AtVMA22 is recruited by AtVMA12 which in turn interacts with the V_0 subcomplex. Interactome studies indicated that AtVMA22 interacts with the V_1 subcomplex (Back et al., 2005). We therefore asked whether AtVMA22 can also interact with the V_1 subcomplex. To answer this question, we generated total protein extracts from 5 day old etiolated *Arabidopsis* seedlings expressing either GFP under the control of the Ubi10 promotor, or AtVMA22-GFP under its endogenous promotor. Protein extracts were subjected to immunoprecipitation experiments using GFP-Trap® magnetic beads followed by western blotting. Using an anti-VHA-C antibody we detected a ~41 kDa protein, which was present in the IP of AtVMA22-GFP, while it was absent in protein extracts of plants expressing GFP (Fig. 14). From these results we conclude that AtVMA22-GFP interacts with the V_1 subcomplex, whereas unbound GFP cannot co-immunoprecipitate VHA-C.

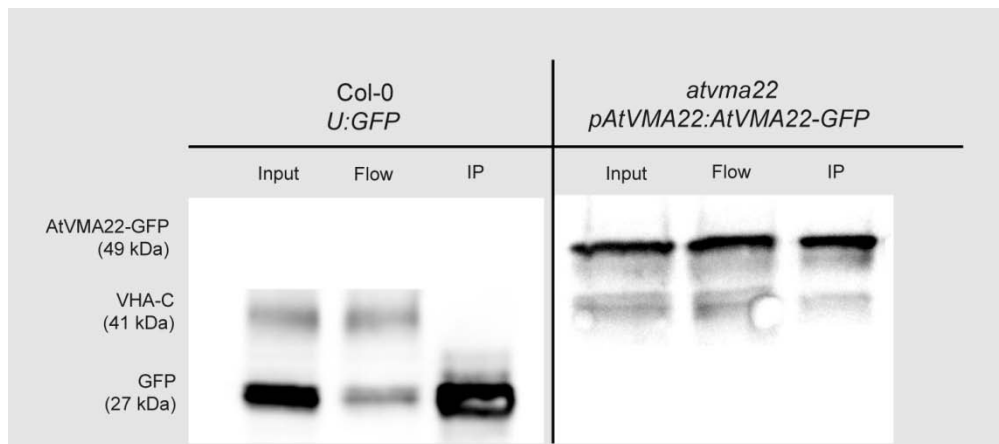


Fig. 14: AtVMA22 interacts with the V_1 subcomplex. GFP immunoprecipitations using anti- GFP-TRAP® coupled magnetic particles from 5 day old etiolated wild-type seedlings expressing free GFP under the control of the Ubi10 promotor and seedlings expressing AtVMA22-GFP under the endogenous promotor. Total protein extracts (Input), unbound protein flow (Flow) and immunoprecipitations (IP) were subjected to immunoblot using anti-GFP and anti-VHA-C antibodies.

It remains to be shown if the interaction of AtVMA22 with the V_1 subcomplex occurs in the cytosol or at the ER membrane.

Appendix

Appendix A

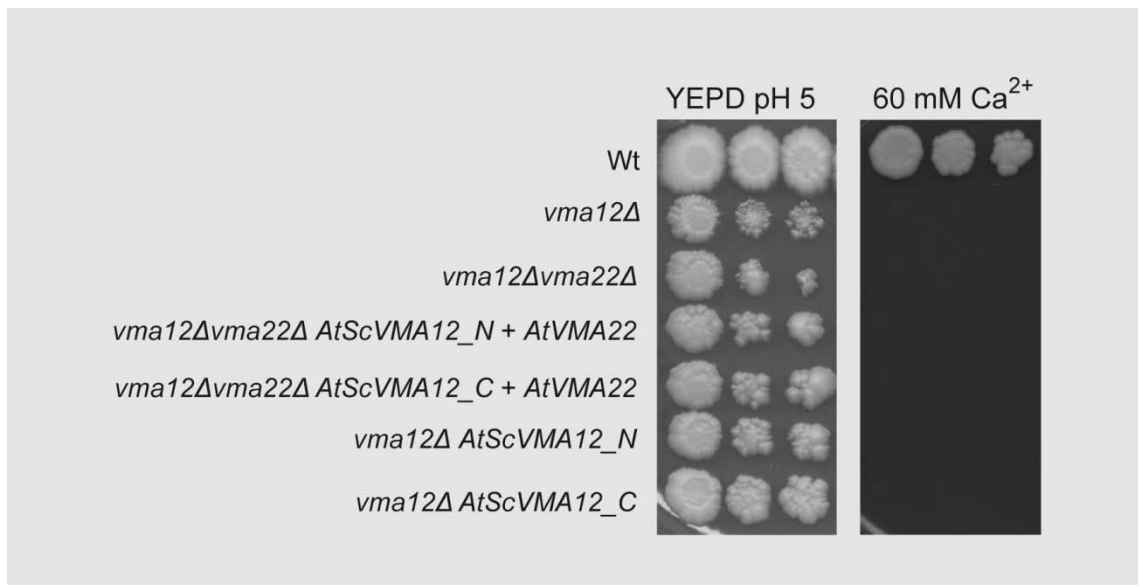


Fig. S. 1 *vma12Δ* cells transformed with either *AtVMA12_N* or with *AtVMA12_C* were grown in SD-URA medium to OD₆₀₀ = 1. *vma12Δvma22Δ* cells transformed either with *AtVMA12_N* and *AtVMA22* or with *AtVMA12_C* and *AtVMA22* were grown in SD-URA medium to OD₆₀₀ = 1. As a control Wt (SF 838-1) cells were grown in YEPD medium to an OD₆₀₀ = 1. The cultures were serially diluted (1:10, 1:100) and spotted onto YEPD medium buffered to pH 5 and on YEPD media containing and 100 mM CaCl₂.

Appendix B

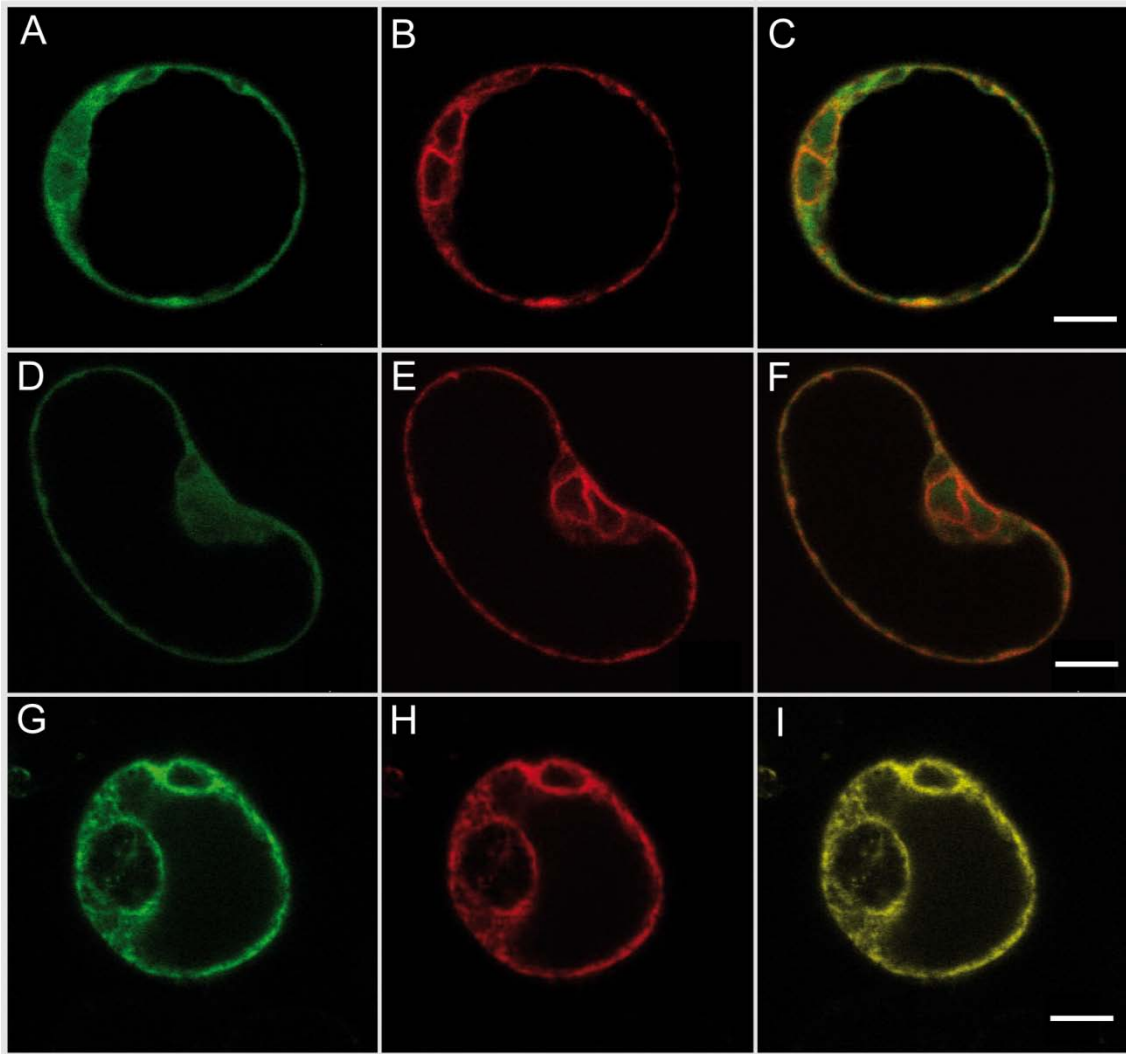


Fig. S. 2 GFP-AtVMA22 is recruited to the ER membrane by AtVMA12-RFP. Transient expression of fluorescently tagged AtVMA12 (RFP-AtVMA12), AtVMA21 (AtVMA21-RFP), AtVMA22 (GFP-AtVMA22) and p24 (p24-RFP; (Langhans et al., 2008)) in *Arabidopsis* root protoplasts. Fluorescence signals were detected 3 days after transformation. (A) GFP-AtVMA22 was co-expressed with (B) the ER marker p24-RFP. (C) Overlay of GFP-AtVMA22 and p24-RFP. Both markers were separate from each other. (D) GFP-AtVMA22 was co-expressed with (E) the assembly factor AtVMA21-RFP. (F) The overlay of both channels .. Co-expression of (G) GFP-AtVMA22 and (H) AtVMA12-RFP. The once cytosolic GFP-AtVMA22 is recruited to the ER membrane as can be seen in the (I) overlay.

Appendix C

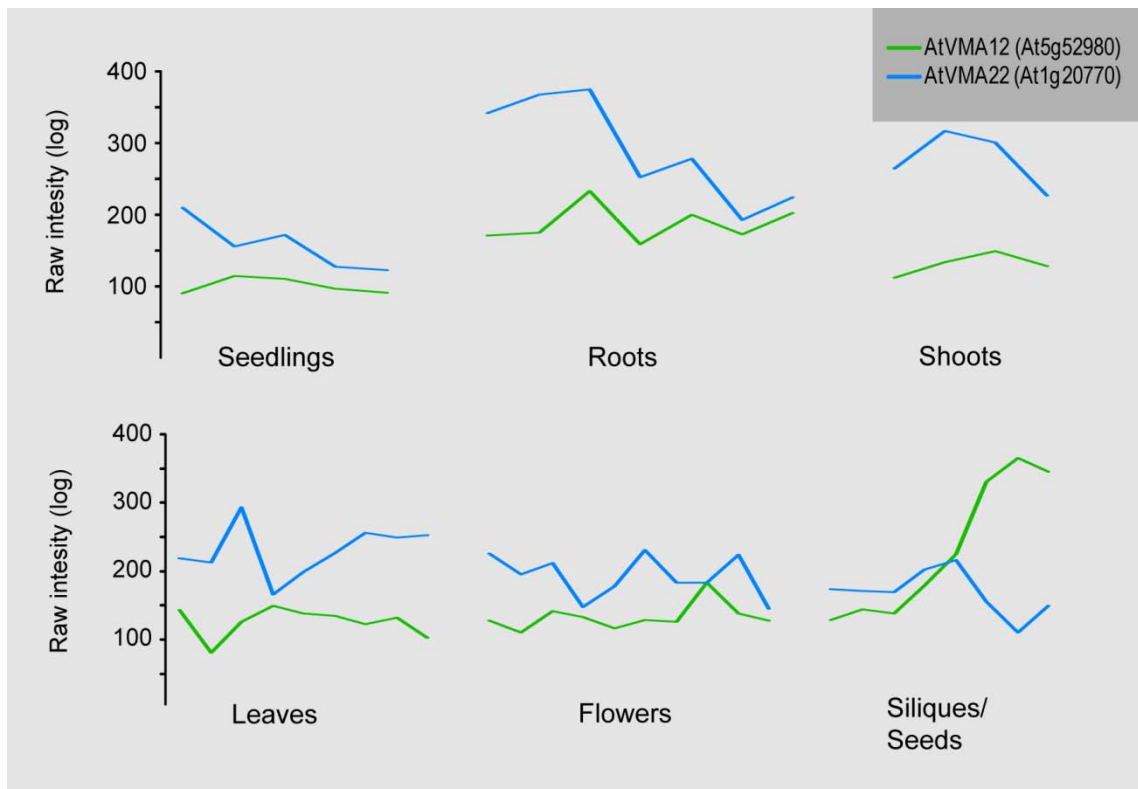


Fig. S. 3: *AtVMA12* and *AtVMA22* expression profile correlates during development. The line graphs show raw intensity values with a logarithmic scale. *AtVMA12* (green line) and *AtVMA22* (blue line) expression is correlated during development with the siliques. Expression data were obtained from the AtGenExpress Developmental series (Schmid et al., 2005).

Discussion

Protein folding and protein complex assembly in the endoplasmic reticulum takes place in a crowded environment, in which the protein concentration is estimated to be around 100 $\mu\text{g}/\mu\text{l}$ (Winnay and Kahn, 2011). In this environment hydrophobic domains within membrane-embedded proteins can interact non-specifically, forming unwanted aggregates. ER resident chaperones and assembly factors are known to shield hydrophobic protein patches and preserve assembly intermediates for subsequent processing.

Here, we show that *Arabidopsis* has one gene for *AtVMA12* and for *AtVMA22* which are predicted to encode proteins with $\sim 18\%$ amino acid identity with yeast *Vma12p* and $\sim 26\%$ amino acid identity with *Vma22p* respectively. Expression of a RFP-tagged *AtVMA12* together with an GFP-tagged *AtVMA22* revealed that both proteins interact with each other in the ER membrane. Further biochemical analysis showed that *AtVMA12* and *AtVMA22* interact with components of the V_0 and the V_1 subcomplex of the vacuolar H^+ -ATPase.

Despite our efforts to unravel the molecular role of the assembly factors, it is still unclear how the membrane bound *AtVMA12* and the cytosolic *AtVMA22* co-assist in the assembly of the V_0 subcomplex. Loss of *Vma12p* or *Vma22p* in yeast exposes *Vph1p* to rapid degradation. Interestingly artificial microRNAs directed against *AtVMA12* and *AtVMA22* had no effect on the stability on the *Arabidopsis* *Vph1p* orthologue *VHA-a3*. From these results we concluded that the knockdown of the assembly factors was incomplete, therefore not affecting *VHA-a3* protein levels. However, it cannot be ruled out that the assembly factors in plants function differently, thus possibly affecting other subunits of the V_0 subcomplex. In contrast to yeast, all the *Arabidopsis* V_0 subunits are encoded by gene families suggesting a requirement for a more accurate coordination to incorporate the correct isoform with respect to a complex developmental program. In the light of this evolutionary subunit diversification, the question arises whether the assembly factors have different affinities for the three *VHA-a* isoforms. Furthermore, high throughput yeast two-hybrid (Y-2-H) screens show that *Vma22p* interacts with subunit F of the V_1 subcomplex (Schroder and Kaufman, 2005), suggesting a role of *Vma22p* apart from V_0 subcomplex assembly. Interactome studies for *Arabidopsis* proteins confirmed a putative interaction of *AtVMA22* with subunit F of the V-ATPase (Back et al., 2005). Interestingly,

unlike any other deletion in any of the V_1 subunits, yeast mutants lacking *Vma7p* (subunit F) affect the stability of the V_0 subcomplex (Graham et al., 1994). In the light of the interactome studies, it seems likely that the VMA22 proteins have a pivotal function, possibly on the one hand recruiting the V_1 subcomplex to the ER and on the other hand modifying the V_0 subcomplex in a way to become competent for V-ATPase holo-complex assembly. Biochemical evidence from Co-IP experiments presented in this work supports this hypothesis of AtVMA22 interacting with the cytosolic V_1 subcomplex. However further characterization is necessary to elucidate whether AtVMA22 interacts with the V_1 subcomplex in conjunction with AtVMA12 at the ER membrane or independent of AtVMA12 in the cytosol.

Furthermore the interactome studies suggest an interaction of AtVMA22 and *Vma22p* with components of the conserved oligomeric Golgi complex (COG complex). The COG complex seems to be essential for maintaining or establishing the structure and function of the Golgi. This complex is proposed to function in retrograde transport within the Golgi (Schroder et al., 2004), but also in ER to Golgi trafficking (Schroder et al., 2003; Wiederkehr et al., 2004). Although the exact mode of action of COG is unclear, it is thought to affect the intraluminal pH of the Golgi (Kaufman et al., 2002). Judging from these studies, it seems possible that AtVMA22 could interplay with COG at the Golgi, regulating V-ATPase activity, thereby affecting intraluminal pH. Indeed, our studies show that reduced transcript levels of *AtVMA22* resulted in swollen and bent Golgi cisterna in a way typical for plant cells with reduced V-ATPase function (Strompen et al., 2005; Dettmer et al., 2006; Brück et al., 2008; Neubert et al., 2008). In the light of the interactome studies, it does not seem too farfetched that the aberrant Golgi morphology could be the result of fewer assembled V_1V_0 subcomplexes at the Golgi. If AtVMA22 is acting at the ER as well as at the Golgi, how does AtVMA22 cycle between these compartments? The carboxy-terminus of AtVMA12 contains a di-lysine (KK) – motif, which has previously been reported to be required for ER localization of type I and type II membrane proteins (Jackson et al., 1990). Previous studies have shown that the carboxy-terminal KK-motif is directly recognized by COPI coat components and that KK containing proteins are incorporated into COPI-coated vesicles which travel from the Golgi to the ER (Wieland and Harter, 1999; McMahon and Mills, 2004). So far, our data does not exclude cycling of a complex of AtVMA12 and AtVMA22 between the ER and the Golgi. However, mutating the KK-motif did not alter the localization of AtVMA12, indicating that the C-terminal di-lysine motif is

not a functional retention/recycling signal (data not shown). Nevertheless this does not entirely disprove the possibility of AtVMA12 cycling between the ER and the Golgi. We have shown that AtVMA12 specifically interacts with AtVMA22 and components of the V_0 subcomplex. But are both assembly factors specific chaperones for the plant V-ATPase? In *vma22Δ* and *vma21Δ* mutant cells, indirect immunofluorescence staining pattern for the yeast plasma membrane ATPase Pma1p and for the vacuolar integral membrane protein alkaline phosphatase (Alp) were indistinguishable from wild-type cells (Hill and Stevens, 1994, 1995), indicating no defect in transport efficiency. Also quantitative analysis of Alp revealed no general defect in vacuolar transport efficiency, but it was neglected in general that total protein amount of Alp was decreased in *vma22Δ* and *vma21Δ* mutant cells. Whether this decrease in protein amount is a consequence of the poor growth of these mutant cells, or the absence of the assembly factors affects protein stability of other proteins is still unclear.

Model for V-ATPase assembly

The characterization of three ER localized chaperones, assisting in the assembly of the plant V-ATPase suggests that the assembly process is carefully organized. Based on our findings, we propose the following model for the assembly of the V-ATPase. AtVMA22 is recruited to the membrane by AtVMA12. We cannot exclude at this point that the formation of the AtVMA12-AtVMA22 heterocomplex precedes the interaction of AtVMA12 with the V_0 subcomplex. AtVMA22 interacts with the V_1 subcomplex. At what point AtVMA22 interacts with the V_1 subcomplex is unclear. AtVMA22 could be recruited to the ER in conjunction with the V_1 subcomplex, thereby serving as a guiding protein, facilitating the holo-complex assembly. Alternatively AtVMA22-AtVMA12 heterocomplex formation precedes the interaction of AtVMA22 with the V_1 subcomplex. Based on this model AtVMA22 could function as a plug, possibly controlling V-ATPase holo-complex assembly in the ER. The third assembly factor AtVMA21 associates independently with the V_0 subcomplex. The role of AtVMA12 and AtVMA22 in the further transport of the V-ATPase is unclear. AtVMA12 could together with AtVMA22 and the V-ATPase be packed into COPII coated vesicles and transported together with AtVMA21 to the Golgi. AtVMA21 disassociates and is recycled to the ER membrane. Whether AtVMA12 or a heterocomplex of AtVMA12/AtVMA22 is also part of this transport process or whether AtVMA22 is able to interact with the COG complex at the Golgi, fulfilling regulatory functions is unclear.

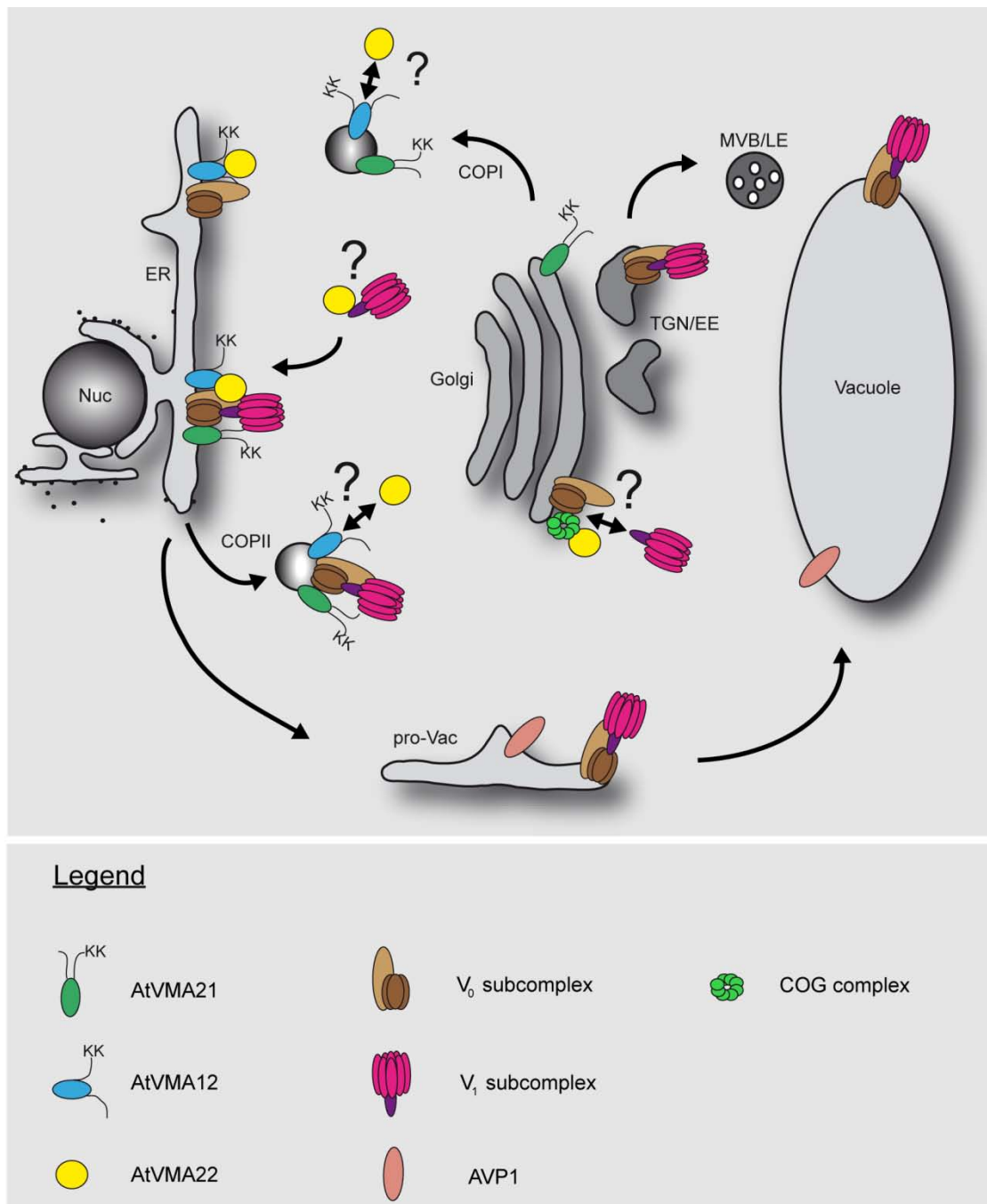


Fig. 15 Model of the V-ATPase assembly in the ER. AtVMA12 and AtVMA22 associate to form a heterocomplex that interacts directly with the V₀ subcomplex in the ER membrane. AtVMA22 can interact with the V₁ subcomplex either independent of AtVMA12 or in conjunction with AtVMA12. AtVMA21 assists in the assembly of the proteolipid ring of the V₀ subcomplex. Since VHA-a3-GFP cannot exit the ER in the absence of other V₀ subunits, we propose that the V-ATPase complex must be assembled completely before it exits the ER. The precise role of AtVMA12 and AtVMA22 in the assembly and release of the V-ATPase V₀ subcomplex is not yet clear.

Material and Methods

Plant Materials and Growth Conditions

Arabidopsis (*Arabidopsis thaliana*) ecotype Columbia 0 (Col-0) plants were grown on nutrient solid MS medium as described previously (Xiong et al., 2005) under long-day conditions (16 h light) at 22°C, unless described otherwise. *Arabidopsis* seeds were surface sterilized in 70% (v/v) Ethanol and 0.1% (v/v) Triton X-100 solution for 20 min followed by 10 min sterilization with 95% (v/v) Ethanol. Seeds containing ethanol-inducible alc gene-expression constructs were surface sterilized using 6 % sodium hypochlorite (NaClO) for 5 min followed by several washing steps with ddH₂O. Sterilized seeds were exposed to cold treatment for at least 2 d. For concanamycin A and MG132 treatment, 4-d-old seedlings grown on nutrient solid MS medium were transferred to liquid MS medium 1 μ M concanamycin A or 50 μ M MG132 and incubated for the indicated times.

Staining of Seedlings with FM4-64 and Microscopy

5 day old seedlings were transferred into liquid MS medium (1/2 MS + 0.5% sucrose; pH 5.8) and stained with a final concentration of 1 μ M FM4-64. FM4-64 was dissolved in DMSO and stored at -20°C.

Constructs generated for this study

Generation of pURT2Kan

For the pURT2Kan, we generated a 678 bp DNA fragment encoding the ORF of monomeric red fluorescent protein (mRFP) by PCR amplification using Ara6-mRFP (Ueda et al., 2004) as template. BamHI restriction sites were introduced with primers RFP_BamHI_f and RFP_BamHI_r. The fragment was subcloned into the pJET1.2/blunt Cloning Vector (Thermo Fisher Scientific Inc) for sequencing and then ligated into the *BamHI-BamHI* digested pUTkan, which is a derivative of the pJH212 vector.

Generation of pUTbar+

All basic plant binary vectors that confer Basta resistance in plants are based on the pTbar vector, a derivative of pPZP312 based on pPZP vectors (Pierce et al., 2007). We introduced a new MCS into the pTbar vector. The oligonucleotides MCS_for and MCS_rev were

annealed by stepwise lowering the temperature from 99 °C to room temperature and phosphorylated at the 5'-ends using the T4 polynucleotide kinase (Fermentas). The pTbar+ was generated by restriction digestion of pTbar *BamHI-Sall* and subsequent ligation of the doublestranded oligo containing 5'-*BamHI* and 3'-*Sall* overhangs. Next a 647 bp fragment of the Ubiquitin-10 promoter sequence was PCR-amplified using the primer pair UBIQ10_*BamHI_for* and UBIQ10_*BamHI_rev* adding *BamHI* restriction sites on both ends. pTbar+ was digested with *BamHI* to ligate the Ubiquitin-10 fragment and generate pUTbar+.

Generation of pUGT2kan

For the pUGT2kan, the GFP5 (S65T) gene (kindly provided by C. Fankhauser, Geneva) was PCR amplified with the forward primer GFP_*BglIII_f* and reverse primer GFP_*BamHI_r*. The 721 bp fragment was subcloned into the pJET1.2/blunt Cloning Vector for sequencing. The GFP5 sequence was isolated using *BglIII* and *BamHI* restriction enzymes, and ligated into the *BamHI* digested pUTkan, which is a derivative of the pJH212.

Generation of pAtVMA22:AtVMA22-GFP

For *AtVMA22* (At1g20770) a 497bp DNA fragment encoding the promoter-sequence plus the 5'UTR was obtained by PCR amplification from genomic plant DNA material. A *BamHI* and *SacII* restriction site have been introduced with the primers 22_Prom_*BamHI_f* and 22_Prom_*SacII_r*. The genomic sequence containing five introns and the terminator of *AtVMA22* were amplified using primers 22_gen_*SpeI_f* and 22_gen_*Sall_r*. For an N-terminal fusion of *AtVMA22*, the GFP5 (S65T) gene was PCR amplified with the forward primer GFP_*SacII_f* and reverse primer GFP_*SpeI_r*. In order to obtain the *AtVMA22*-GFP rescue construct the promoter sequence was isolated via *SpeI-Sall* restriction digest, ligated to the GFP5 sequence and subcloned into the pJET1.2/blunt Cloning Vector. The promoter-GFP fusion was isolated using *BamHI* and *SpeI* restriction enzymes, and ligated together with the genomic *AtVMA22* sequence, which was isolated via restriction digest using *SpeI* and *Sall* into the binary vector pPZP312.

Generation of U:AtVMA12-RFP

For AtVMA12 (At5g52980), the cDNA from Col-0 plants was amplified using primers 12_for and 12_rev. The 669 bp fragment was subcloned into the pJET1.2/blunt Cloning Vector. *XmaI* and *SacII* restriction sites were introduced by PCR amplification using primers At12_XmaI_f and At12_SacII_rev. The fragment was ligated into the *XmaI-SacII* digested pURT2kan, which is a derivative of the pJH212 vector.

Generation of AlcA:amiAtVMA22 and AlcA:amiAtVMA12

For the generation of artificial microRNA (amiRNA) constructs against AtVMA22 and AtVMA12, we used the WMD3 - Web app for the automated design of artificial microRNAs (<http://wmd.weigelworld.org>), where the principles for the design amiRNAs have been integrated into a Web-based tool (Schwab et al., 2006). In brief, At5g52980 (AtVMA12) and At1g20770 (AtVMA22) have been selected as target genes. The amiRNA sequences were selected, which were predicted to target specifically AtVMA12 and AtVMA22 respectively.

Four oligonucleotides were used for each target gene to engineer the amiRNA into the endogenous miR319a precursor by site-directed mutagenesis. As a template for the PCR, the plasmid pRS300, containing the miR319a precursor in the pBluescript (Stratagene) was used (plasmids were kindly provided by Detlef Weigl). The amiRNA sequence was digested using *EcoRI* and *BamHI* restriction enzymes and ligated into the *EcoRI-BamHI* digested pHanAlcA, a derivative of the pHANNIBAL (Wesley et al., 2001), in which the 35S promoter has been replaced by an ethanol-inducible promoter pAlcA (Roslan et al., 2001). The pAlcA:amiAtVMA12 and pAlcA:amiAtVMA22 cassette was digested *NotI* and ligated into the binary plant vector pBart_Alcr, which contains the coding sequence for the transcriptional activator Alcr, which activates the ethanol-inducible promoter pAlcA in the presence of ethanol. Transgenic plants were selected based on the phosphinothricin (BASTA) resistance conferred by the bar gene contained in pBART_Alcr. Homozygous lines were established, and hypocotyl length of etiolated seedlings grown on MS plates containing 0.2% ethanol was compared with seedlings grown in the absence of ethanol.

Generation of the binary BIFC vectors pYNx, pxYN, pxYC, pYCx

We amplified a 683 bp fragment via PCR containing the MCS, the c-myc tag and the N-terminal 155aa of the e-YFP using the 35S:SPYNE173 (Accession-No: EU796363) as

template (Sze et al., 2002). A *Bam*HI and a *Bgl*III restriction site have been introduced using primers YN173_*Bgl*III_f and YN173_*Bam*HI_r. In order to generate the *pYNx* vector, we ligated the cassette containing the MCS, myc tag and the N-terminal fragment of the e-YFP into the *Bam*HI digested pUTkan vector, which is a derivative of the pJH212.

For *pxYN*, we ligated a 575bp PCR fragment generated with the primers cYN_*Spe*I_for and cYN_*Xba*I_rev, using the *35S:SPYNE* (Accession-No: EU796373) as template (Sze et al., 2002) into the *Spe*I digested pUTkan.

The pYCx and the pxYC vectors were generated based on pUTbar+ described previously. For pYCx the primers nYC_*Aat*II_For and nYC_*Aat*II_Rev was used to PCR-amplify the eYFP-HA cassette from the SPYCE(MR) template (Sze et al., 2002). The PCR fragment was subcloned into the pJET1.2/blunt vector and sequenced. Finally the eYFP-HA cassette was isolated from pJET and ligated into the *Aat*II digested pUTbar+. Correct orientation of the insert was confirmed by test digestion. For the generation of pxYC the HA-eYFP cassette was PCR-amplified from SPYCE(M) using cYC_*Sal*I_For and cYC_*Sal*I_Rev. The fragment, flanked by *Sal*I restriction sites was sub-cloned into the pJET1.2/blunt vector and subjected to sequence analysis. After digestion with *Sal*I the HA-eYFP fragment was ligated into the *Sal*I digested pUTbar+, designated pxYC.

Generation of U:YN-AtVMA12

A 678 bp fragment was separated from the *U:AtVMA12:RFP* (described above) construct via *Xma*I-*Sac*II. The fragment was ligated into the *Xma*I-*Sac*II digested *pYNx* to generate the *U:YN:AtVMA12* construct.

Generation of U:AtVMA22-YC

A 660 bp PCR fragment was amplified using primers *Aat*II_At22_f and *Spe*I_22_r introducing *Aat*II-*Spe*I restriction sites. The vector pxYC was digested *Aat*II-*Spe*I and the fragment containing AtVMA22 was ligated to generate the construct *U:AtVMA22-YC*.

Generation of U:YN-AtVMA21

We amplified AtVMA21, using pJet-AtVMA21a as a template (Neubert et al., 2008) introducing two *Eco*RV restriction sites. The fragment was ligated into the *Sma*I digested *pYNx*.

Generation of pVMA12:AtScVMA12_N

For the *pVMA12:AtScVMA12_N*, a 461 bp PCR fragment encoding the ORF of *AtVMA12* until the first predicted transmembrane domain plus 40 bp of the 5'UTR of the yeast *ScVMA12* promotor was generated using primers *AtVMA12_P_f* and *AtVMA12_TMD1_r*. As a template we used the *U:AtVMA12:RFP*. In a second PCR reaction a 350 bp fragment containing the ORF of *ScVMA12* starting at the first predicted transmembrane domain plus 40 bp of the 3'UTR of *ScVMA12* was amplified using primers *Vma12_TMD1_f* and *ScVma12_ter_r*. We used the pDJ2 as template (Jackson and Stevens, 1997). Both PCR fragments were used in a third PCR reaction to generate one chimeric construct *AtScVMA12_N* by using primers *AtVMA12_P_f* and *ScVma12_ter_r*.

Generation of pVMA12:AtScVMA12_C

For the *pVMA12:AtScVMA12_C*, a 732 bp PCR fragment encoding the ORF of *ScVMA12* until the second predicted transmembrane domain plus 40 bp of the 5'UTR of the yeast *ScVMA12* promotor was generated using primers *ScVMA12_P_f* and *AtVMA12_TMD2_r*. As a template we used the pDJ2. In a second PCR reaction a 154 bp fragment containing the ORF of *AtVMA12* starting at the second predicted transmembrane domain plus 40 bp of the 3'UTR of *ScVMA12* was amplified using primers *Vma12_TMD1_f* and *AtVma12_ter_r*. We used the pDJ2 as template (Jackson and Stevens, 1997). Both PCR fragments were used in a third PCR reaction to generate one chimeric construct *AtScVMA12_C* by using primers *ScVMA12_P_f* and *AtVma12_ter_r*.

Blast searches were carried out using the TAIR database (<http://www.arabidopsis.org>) and the databases at the NCBI (<http://www.ncbi.nlm.nih.gov>).

Molecular complementation

Complementation of the atvma22 and atvma12 mutant

The transgenic lines SALK_031513 (*atvma22*) and Sail_634_F09 (*atvma12*) were identified by SALK institute and by Nottingham Arabidopsis Stock Centre. The rescue constructs *pAtVMA22:AtVMA22:GFP* and *U:AtVMA12:RFP* were introduced into the *Agrobacterium* strain GV3101::pMP90. Col-0, *atvma12/+*, *atvma22/+* plants were transformed using standard procedures. Transformants were selected by spraying 0.1% BASTA (AgrEvo, Düsseldorf, Germany) and screened via PCR for presence of the T-DNA disrupting the *AtVMA12* and *AtVMA22* gene. Seeds of BASTA-resistant *atvma22/+* plants and *atvma12/+*

plants were germinated on MS plates containing $50 \mu\text{g ml}^{-1}$ kanamycin. *AtVMA22/+* plants were transferred to soil and then sprayed with Basta. To identify homozygous *AtVM22* plants the following primers were used: Salk_l, Salk_r and LB1.3.

To identify homozygous *AtVMA12* plants the following primers were used: Sail_12r, Sail_12l, LB1.

Protein Extraction

Frozen plant tissue (100 mg) was ground in liquid nitrogen. The powder was transferred into a 2 ml Eppendorf tube and 500 μl of Extraction buffer (0.35 M Saccharose, 70 mM pH 8.8 Tris-HCl,

10 % v/v Glycerol, 3 mM Na_2EDTA , 1.5 % w/v PVP-40, 0.5 % Triton X-100, 0.15 v/v BSA, 4 mM DTT, 1x Complete Protease Inhibitor [Roche Diagnostics GmbH]) was added. The homogenate was vigorously vortexed and then centrifuged at 10.000 *g* for 15 min at 4°C. The supernatant was afterwards transferred into a new Eppendorf tube and centrifuged again. Protein concentration of the supernatant was determined using Bradford assay (Bradford, 1976).

Co-Immunoprecipitation

Protein extracts subjected to Co-immunoprecipitation were obtained as described with some modifications (Schumacher et al., 1999). Plant tissue (1g/ml buffer) from 5 day etiolated Arabidopsis plants was homogenized in liquid nitrogen using extraction buffer (50 mM Tris pH 8, 50 mM NaCl, 10% Glycerol and 1 x Complete Protease Inhibitor [Roche Diagnostics GmbH]). The homogenate was centrifuged at 10.000 *g* at 4°C for 10 min. The supernatant was centrifuged at 150.000*g* for 30 min at 4°C. The supernatant was discarded and the pellet homogenized with a *Potter-Elvehjem* tissue grinder in extraction buffer. Protein concentration was determined using Bradford assay (Bradford, 1976). For immunoprecipitation, 100 μg protein was solubilized and incubated for 1 h at 4°C using 3 % NP40. Solubilized proteins were separated from non-solubilized proteins by centrifugation at 150.000 *g* for 30 min. The supernatant was loaded on GFP-Trap[®] coupled to agarose beads (ChromoTek GmbH, München, Germany) and incubated for 2h at 4°C. Beads were washed three times and then proteins were eluted with SDS-sample buffer (4 % SDS, 140 mM Tris-HCl pH 6.8, 20 % Glycerol, 0.01 % Bromophenolblue, 10 % β -Mercaptoethanol) at 50°C for 5 min.

Fluorescence Microscopy

Fluorescence microscopy was performed using a Leica TCS SP5 confocal laser-scanning microscope. All CLSM images were obtained using the Leica Confocal software and a 63x water-immersion objective. The excitation wavelength was 488 nm; emission was detected for GFP between 500 and 530 nm, for RFP between 565 and 600 nm, and for FM4-64 between 620 and 680 nm. Adobe Photoshop was used for image processing. Quantification of colocalization was assessed using the Leica Confocal software.

Primer used

Name	Sequence
RFP_BamHI_f	5'- GGATCCATGGCCTCCTCCGAGGACGT-3'
RFP_BamHI_r	5'- GGATCCGGCGCCGGTGGAGTGGC-3'
MCS_for	5'- GATCCGACGTCTCTAGATTAATTAACCATGGACTAGTG-3'
MCS_rev	5'- TCGACACTAGTCCATGGTTAATTAATCTAGAGACGTCG-3'
UBIQ10_BamHI_for	5'- CTAGGATCCCGACGAGTCAGTAATAAACG-3'
UBIQ10_BamHI_rev	5'- CATGGATCCGCTGTTAATCAGAAAACTC-3'
GFP_BglII_f	5'- ATAAGATCTAAGGAGATATAATCATGAG-3'
GFP_BamHI_r	5'- ATAGGATCCTTTGTATAGTTCATCCATGCC-3'
22_Prom_BamHI_f	5'- CTTGGATCCAGAAGAAGATGGGTTGAAG-3'
22_Prom_SacII_r	5'- CATCCGCGGCGAAATTTAGCTCCAAC-3'
22_gen_SpeI_f	5'- ATGACTAGTGCGGAGATTTACGAGGAAGG-3'
22_gen_Sall_r	5'- AATGTGACCGTCGTGGATAAGAGATTAA-3'
GFP_SacII_f	5'- CCGCGGATGAGTAAAGGAGAAGAAC-3'
GFP_SpeI_r	5'- ACTAGTTTTGTATAGTTCATCCATGC-3'
12_for	5'- GTGTTTGGACCCGATCAAAGATCGATA-3'
12_rev	5'- GGAAAAGAATGCAAACAAAGTTCTACTCGAG-3'
At12_XmaI_f	5'- CATCCCGGGATGGATCAACCCGACCCG-3'
At12_SacII_rev	5'- CTACCGCGGTTGATTTTTCTTAGTAGTGGGAG-3'
YN173_BglII_f	5'- ACTAGATCTATGGTGAGCAAGGGCGAGGAG-3'
YN173_BamHI_r	5'- GAAGGATCCAAGATCCTCCTCAGAAATC-3'
cYN_SpeI_for	5'- CCAACTAGTATGGAGCAAAAGTTGATTTTC-3'
cYN_XbaI_rev	5'- CATTCTAGACTACTCGATGTTGTGGCGGATC-3'

nYC_AatII_For	5' -CATGACGTCATGGACAAGCAGAAGAAC-3'
nYC_AatII_Rev	5'- CCTGACGTCAGCGTAATCTGGAACATCG-3'
cYC_Sall_For	5'- CATGTCGACATGTACCCATACGATGTTC-3'
cYC_Sall_Rev	5'- GATGTCGACTTACTTGTACAGCTCGTC-3'
AatII_At22_f	5'- GACGTCATGGCGGAGATTTACGAGG-3'
SpeI_22_r	5'- ACTAGTCTTCTCTGTGATCGCTC-3'
AtVMA12_P_f	5'- GGATAATTGACGATTGGCATCACATAAAAGAACTCTAATG GATCAACCCGACCCG-3'
AtVMA12_TMD1_r	5'- CAAGAACGTTGAAAACAGTGGTAACGAGCTGGTCTTTGTA-3'
Vma12_TMD1_f	5'- GTTACCACTGTTTTCAACGTTCTTGTAAGTGCATATCGG-3'
ScVma12_ter_r	5'- GCTCTCGGATCTCGGAGTTCTTATTTATAAAATGATCAGTTAA GCGTAATCTGGAACGT-3'
ScVMA12_P_f	5'-GATAGGATAATTGACGATTGGCATCACATAAAAGAACTCTAA TGTTGAAATTAAGT-3'
AtVMA12_TMD2_r	5'- GTTATACACAACCACATCTGCTACTAAGACCAATATTCC-3'
Vma12_TMD1_f	5'- GTAGCAGATGTGGTTGTGTATAACAAAACGTCTAAAGATG-3'
AtVma12_ter_r	5'- GCTCTCGGATCTCGGAGTTCTTATTTATAAAATGA TCAGCTATTGATTTTTCTTAGTAG-3'
Salk_l	5'- CGGTTTGACCCGAAAGAGGTA-3'
Salk_r	5'- GATCAAACCATCCCTGCAAAA-3'
LB1.3	5'- ATTTTGCCGATTTGGAAC-3'
Sail_12r	5'-GGATGCTTCTGGGTTTCTTTC
Sail_12l	5'-TCAGTAGGAAAAGAATGCAAACAAA -3'
LB1	5'-GCCTTTTCAGAAATGGATAAATAGCCTTGCTTCC -3'

II – Quality control of the plant V-ATPase

Abstract

In a eukaryotic cell approximately one-third of all proteins are targeted to the secretory pathway, thus making the endoplasmic reticulum (ER) the first organelle they encounter (Ghaemmaghami et al., 2003). In this crowded environment the ER provides a safe environment for protein folding and oligomerisation. In a sophisticated quality control (QC) system, so-called chaperones monitor the maturation process of the proteins, ensuring that only correctly folded proteins are secreted (Ellgaard and Helenius, 2003). The ERQC been defined as a system controlling folding and maturation of proteins (Brodsky and McCracken, 1999; Ellgaard and Helenius, 2001), but so far no system has been described monitoring the function of proteins. Here we have presented data on three VHA-a3 point mutations reducing V-ATPase activity to a varying degree, depending on the mutation. Further characterization of these mutations has led us to assume that the presence of active V-ATPase complexes determines the fate of non-functional V-ATPase complexes. To decipher the mechanism behind this function dependent ER quality control (FERQCL), we showed that the ER chaperone calnexin is required to retain non-functional V-ATPase complexes in the ER. The impaired growth phenotype associated with inactive V-ATPase complexes not being retained in the ER emphasizes the biological relevance of a FERQCL system.

Introduction

Malfunctioning and defective products in today's world are often the reason for customer complaints leading to subsequent trials, costs and a ruined reputation for the company. By installing a highly accurate quality control within the production line of a company, defective products can be sorted out before they ever reach a customer. Therefore a quality control is essential for the survival of a company in a competitive market. In biology, eukaryotes have installed this economic principle and employed a variety of mechanisms to monitor the quality of their cellular products (proteins). For almost one-third of all eukaryotic proteins, which are destined for the secretory pathway the endoplasmic reticulum (ER) is the first organelle they encounter (Ghaemmaghami et al., 2003; Kanapin et al., 2003). Here, an ER quality control (ERQC) system ensures that only correctly folded proteins reach the Golgi (Ellgaard and Helenius, 2003). Primary quality control identifies structural and biophysical features that allow distinction of mature molecules and immature proteins. Malformed proteins are retained, while correctly folded proteins leave the ER. The efficiency of this system is mainly determined by conformational stability of the folded protein, which is defined as the free energy of folding (Shusta et al., 1999). In other words, the higher the free-energy barrier between native and non-native structure, the lower the fraction that is retained in the ER. Mutant as well as wild-type proteins are present in a folding equilibria transiently unfolding, exposing chaperone binding sites and returning to their native conformation (Englander et al., 2007; Liu and Howell, 2010). Due to the lower conformational stability the incompletely folded form of a mutant protein is favored, making chaperone binding more frequent. Although the conformational stability provides an explanation for the retention of non-native proteins, the molecular mechanisms guiding chaperones, like calnexin and calreticulin to their target molecules are not well understood. In addition, it remains to be shown, whether non-functional but correctly folded proteins can be recognized by the ERQC and if so, how this machinery discriminates between functional and non-functional substrates.

We have designed a pH-sensor by generating an *Arabidopsis* mutant VHA-a3 protein (VHA-a3R729N) fused to the pH-sensitive orange seapen *Ptilosarcus gurneyi* GFP (PtGFP) (Schulte et al., 2006). In yeast, introduction of this very specific amino acid change abolished V-ATPase activity and proton translocation, while assembly of the V-ATPase complex is not affected (Leng et al., 1996; Kawasaki-Nishi et al., 2001a). When expressed

in the yeast *vph1/stv1Δ* mutant strain, all mutant V-ATPase complexes were transported to the vacuolar membrane, passing normal ERQC despite their impaired functionality.

We expressed VHA-a3R729N-ptGFP in wild-type *Arabidopsis thaliana* and in *vha-a2vha-a3* double mutants, lacking both tonoplast-localized isoforms (VHA-a2 and VHA-a3) and as a result has no tonoplast V-ATPase activity (Krebs et al., 2010). Interestingly, VHA-a3R729N-ptGFP was retained in the ER in wild-type plants, while the mutant protein was efficiently transported to the vacuolar membrane in the *vha-a2vha-a3* double mutant (data not shown). To gain insight into the mechanism controlling the localization of the same protein in different genetic backgrounds, we repeated these experiments using *GFP* fusion constructs.

Results

The VHA-a3R729N-GFP containing V-ATPase complexes are retained in the ER and degraded by the 26S Proteasome in wild type plants

We expressed the VHA-a3R729N-GFP protein under the control of the UBI10 promotor in Col-0 and *vha-a2vha-a3 Arabidopsis* plants. Plants carrying the construct were indistinguishable from the wild-type and the *vha-a2vha-a3* mutant. (Fig. S. 4).

Using CLSM analysis, VHA-a3R729N-GFP was localized in the ER in cells of the root differentiation and elongation zone in wild-type seedlings (Fig. 16A, D). In contrast, VHA-a3R729N-GFP in the *vha-a2vha-a3* double mutant localized to the tonoplast (Fig. 16B, E). Total proteins were extracted from 5 day old seedlings expressing VHA-a3R729N-GFP or VHA-a3-GFP. Immunoblotting with anti-GFP antibodies revealed that the signal intensity of independent plant lines expressing VHA-a3R729N-GFP was considerably lower than in plants expressing VHA-a3-GFP (Fig. 16G). We found that the low signal intensity corresponded to low protein levels of VHA-a3R729N-GFP (Fig. 16G). We were curious whether the low protein amount in *Arabidopsis* could be ascribed to a degradative process. *Arabidopsis* seedlings were treated for 2 h with proteasome inhibitor MG132 (Fig. 16G). The levels of VHA-a3R729N-GFP in wild-type Col-0 increased 4 fold after treatment, suggesting that VHA-a3R729N-GFP is degraded by the 26S proteasome (Fig. 16G). To rule out that the degradation is caused by VHA-a3 outcompeting VHA-a3R729N-GFP for available V_0 subunits, we asked whether the mutant protein has been incorporated into the V-ATPase holo-complex.

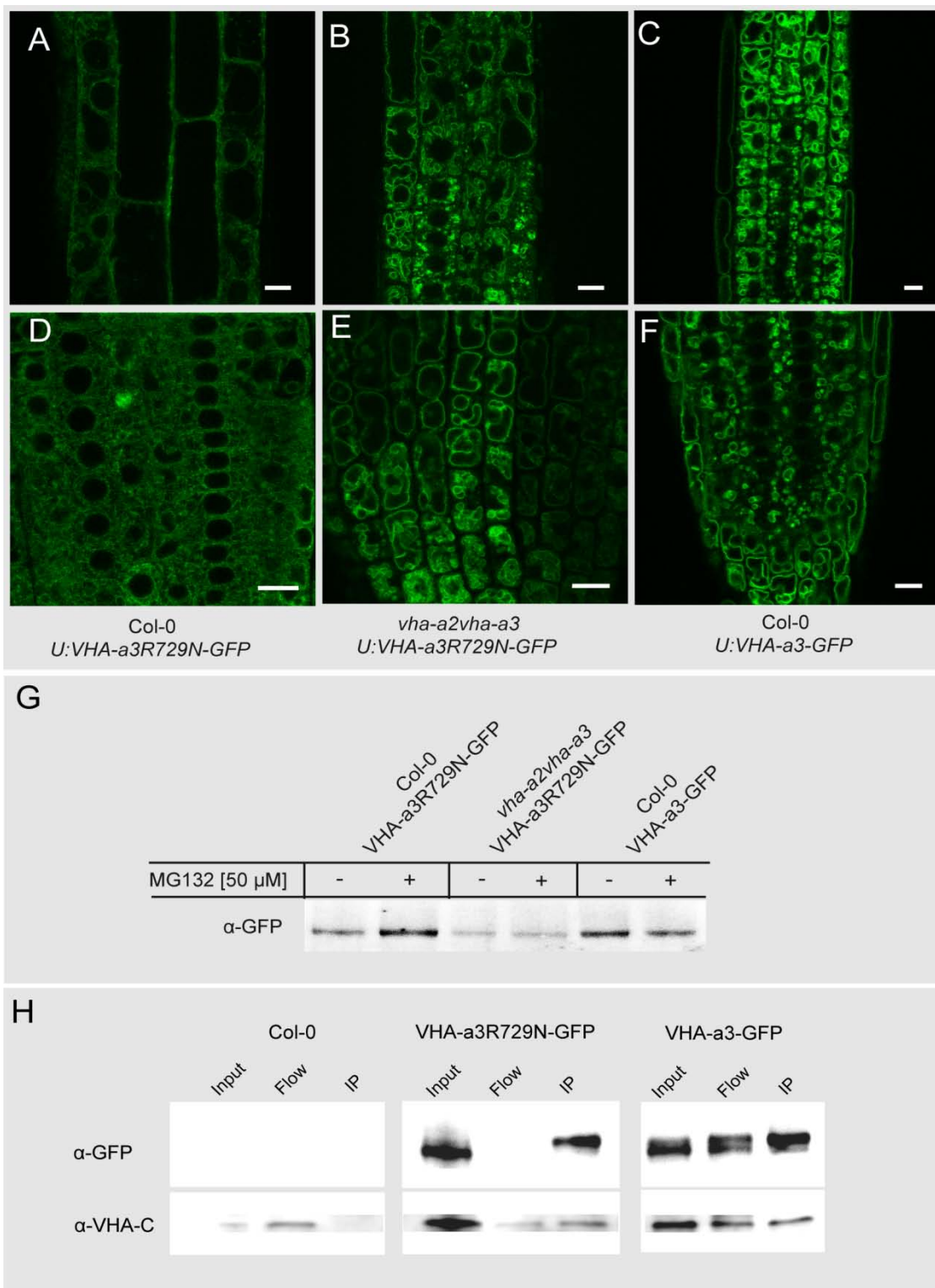


Fig. 16 VHA-a3R729N-GFP is retained in the ER in wild-type Col-0 plants and localizes to the tonoplast in the *vha-a2vha-a3* double mutant. (A-F) Root tips of 5-day old *Arabidopsis* seedlings were subjected to CLSM analysis (plant lines as indicated). (G) VHA-a3R729N-GFP is stabilized after MG132 treatment. 5 day old *Arabidopsis* seedlings have been treated with 50 μ M of MG132 (+). In control lanes (-) no MG132 was applied. After 2h total protein extracts were made from 50 seedlings. (H) VHA-a3 interacts with the V_1 subcomplex at the ER. GFP immunoprecipitations using anti- GFP-TRAP[®] coupled magnetic particles from 5 day old etiolated wild-type seedlings (Col-0) expressing VHA-a3R729N-GFP or VHA-a3-GFP. Total microsomal membranes (Input), unbound protein flow (Flow) and immunoprecipitations (IP) were subjected to immunoblot using anti-GFP and anti-VHA-C antibodies.

Subunit VHA-C co-immunoprecipitated with VHA-a3R729N-GFP and VHA-a3-GFP as shown in Fig. 16H. We inferred that the co-immunoprecipitation of subunit VHA-C with VHA-a3-GFP/VHA-a3-GFP729N reflects the assembly of the V_1 and the V_0 subcomplex. This simplification is justified from previous experiments, demonstrating that only assembled V_1 subcomplexes are able to associate with fully assembled V_0 subcomplexes (Ho et al., 1993).

Taken together, VHA-a3R729N-GFP is incorporated into the V-ATPase holo-complexes and transported to the vacuole in the *vha-a2vha-a3* background. In contrast, in wild-type plants V-ATPase complexes containing VHA-a3R729N-GFP are retained in the ER and degraded by the 26S proteasome. Consistent with these results from *Arabidopsis* we observed a similar behavior of the mutated Vph1p yeast orthologue. In wild-type cells Vph1R735N-GFP is retained in the ER, while in the *vph1/stv1Δ* mutant, Vph1R735N-GFP localizes in the ER (Upendo Lupanga, Masterthesis, 2011). We assumed that the retention of V-ATPase complexes containing VHA-a3R729N-GFP resulted from the presence of functional V-ATPase complexes. We therefore asked, whether V-ATPase activity might be a required for the retention of VHA-a3R729N-GFP.

V-ATPase activity is required to retain VHA-a3R729N-GFP in the ER

If V-ATPase activity is required to retain VHA-a3R729N-GFP in the ER, we assumed that by preventing proton translocation VHA-a3R729N-GFP would be released from the ER into the endocytic pathway.

Concanamycin A (ConcA) has been proven to be a specific inhibitor of the V-ATPase (Drose and Altendorf, 1997). In addition, ConcA interferes with both endocytic and secretory trafficking, resulting in an accumulation of cargo from both pathways in the ConcA-induced vesicle aggregates (Dettmer et al., 2006). 5 day old wild-type seedlings expressing VHA-a3R729N-GFP were incubated with 5 μ M ConcA for 2h. VHA-a3R729N-GFP containing V-ATPase complexes exited the ER, now accumulating in dots. To investigate the nature of these dots, we incubated ConcA treated plants with the lipophilic styryl dye FM4-64. FM4-64 is endocytosed and labels endosomal, prevacuolar and vacuolar compartments over 15 min to 2 h (Dettmer et al., 2006). After 15 min co-localization between VHA-a3R729N-GFP and the FM4-64 at the *trans*-Golgi network (TGN) was observed (Fig. 17B), whereas no colocalization could be observed for the untreated control (Fig. 17A). Quantification of CLSM images revealed that ~70% of the pixels with signal intensities above the chosen threshold overlapped between the red and green channels. In comparison to the

untreated plants, this overlap represents a genuine colocalization of the FM and GFP signal at the TGN (Fig. 17D). Consistent with these results, relocation of Vhp1R735N-GFP to the Golgi after ConcA treatment was observed in wild-type yeast (U.Lupanga, Masterthesis, 2011).

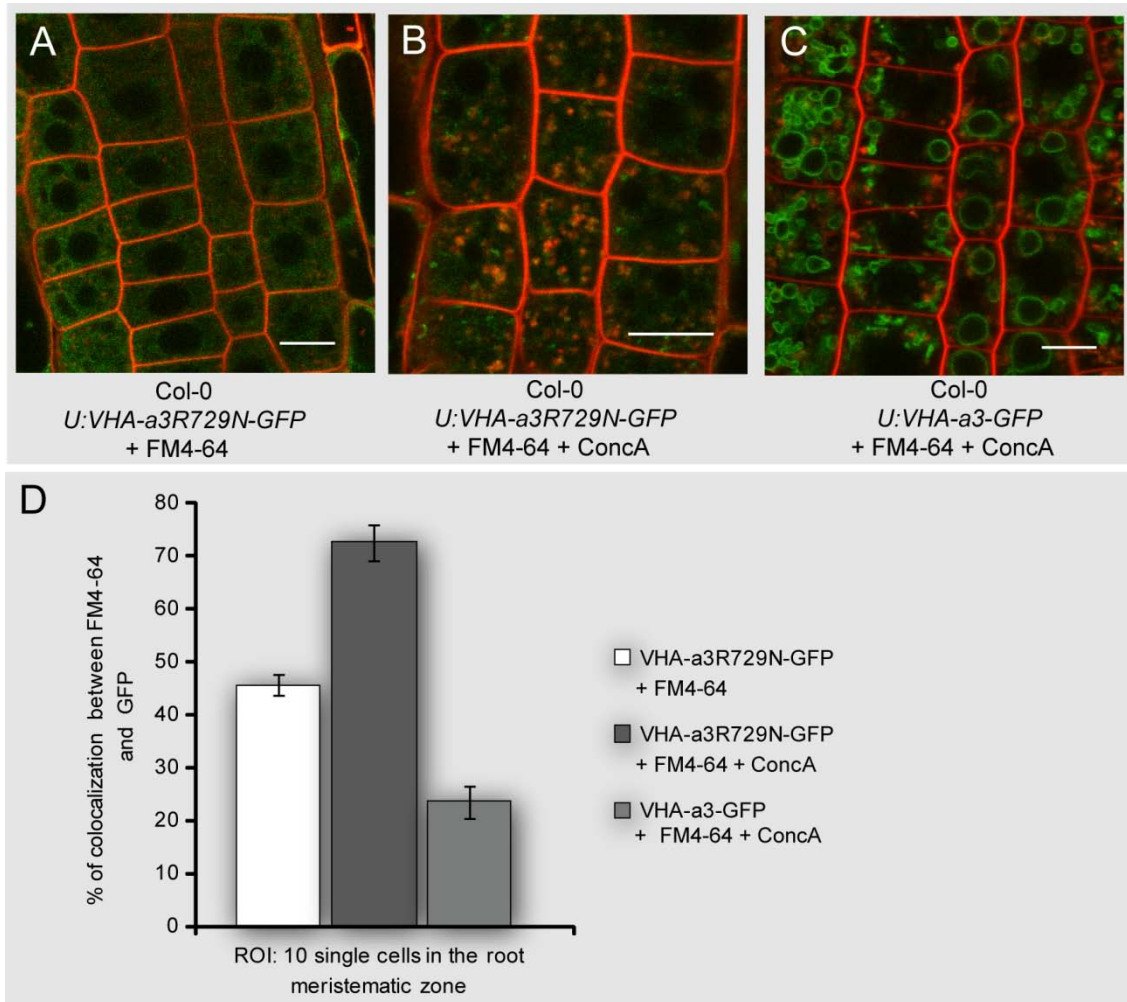


Fig. 17 The VHA-a3R729N-GFP exits the ER upon Concanamycin A treatment. CLSM analysis of 5 day old *Arabidopsis* wild-type Col-0 seedlings. (A) Root expressing VHA-a3R729N-GFP incubated with FM4-64 for 15 min. (B) Root expressing VHA-a3R729N-GFP treated with 5 μM Concanamycin A (ConcA) and incubated with FM4-64 for 15 min. (C) Root expressing VHA-a3-GFP, treated with 5 μM ConcA and incubated with FM4-64 for 15 min. (D) Quantification of colocalization between VHA-a3R729N-GFP and FM4-64, treated with and without ConcA. Data represent the means of 10 independent experiments ±SD. CLSM bars = 10 μm

From these results, we concluded that V-ATPase activity is a required for the retention of non-functional complexes in the ER in yeast and in plant. Interestingly 2h ConcA treated VHA-a3-GFP plants did not show any colocalization with the FM4-64 (Fig. 17C). Extending ConcA treatment from 2h to 6h up to 12h did not change the exclusive vacuolar localization of VHA-a3-GFP (data not shown), indicating a TGN-independent transport route of VHA-a3-GFP to the vacuole.

VHA-a3E780Q-GFP is transported to the vacuole

Having shown that the inactive V-ATPases are retained in the ER in the presence of active V-ATPase complexes, we were interested if there was an activity threshold controlling the release or the retention. To that end, we replaced the glutamic acid with a glutamine at amino acid position 789 within the VHA-a3 protein. The particular exchange within Vph1p has been shown to reduce V-ATPase activity to ~ 20 % in yeast (Leng et al., 1996). The VHA-a3E780Q-GFP protein was expressed under the control of the UBI10 promotor in wild-type Col-0 and in the *vha-a2vha-a3* double mutant. Plants were indistinguishable from untransformed control plants (Fig. S. 4). Five independent homozygous plant lines were used for CLSM analysis for each genetic background. In wild-type plants we observed a clear labeling of the vacuolar membrane (Fig. 18A). In the *vha-a2vha-a3* mutant VHA-a3E780Q-GFP was also localized to the tonoplast (Fig. 18B).

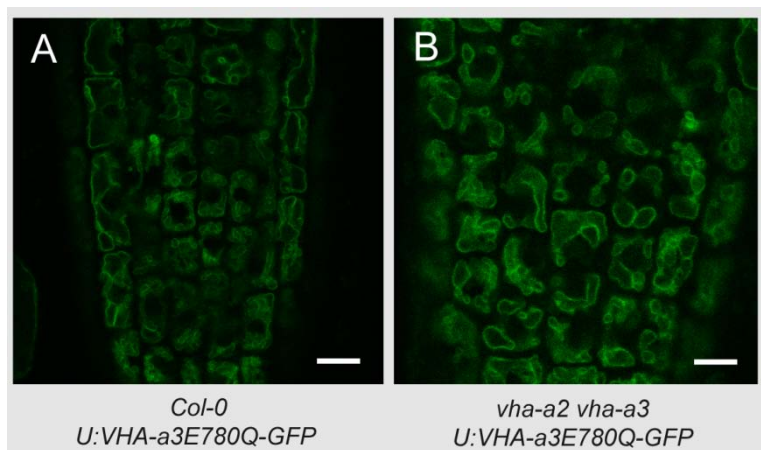


Fig. 18 VHA-a3E780Q-GFP localizes to the vacuolar membrane. (A) CLSM analysis of Col-0 seedling root tip expressing VHA-a3E780Q-GFP. (B) CLSM analysis of *vha-a2vha-a3* seedling root tip expressing VHA-a3E780Q-GFP. CLSM bars = 10 µM

VHA-a3R790K-GFP localized to the trans-Golgi network and the vacuole

Our results so far showed that V-ATPases, possessing only 20 % of activity exit the ER, reaching the tonoplast. The exchange of another conserved amino acid residue allowed us to lower the V-ATPase activity further. According to Kawasaki-Nishi et al. the exchange of this conserved arginine residue at amino acid position 790 to a lysine residue reduces V-ATPase activity to ~10 % and ~5 % proton translocation activity (Kawasaki-Nishi et al., 2001a). We expressed the VHA-a3R790K-GFP under the control of the UBI10 promotor in wild-type Col-0 and in the *vha-a2vha-a3* mutant. Except for one plant line, all plants carrying the construct were indistinguishable from the untransformed control (Fig. S. 4). One line expressing VHA-a3R790K-GFP in the wild-type background showed a growth phenotype similar to the *vha-a2vha-a3* mutant (*v23*-like) (Fig. 19D). We reasoned that this

negative effect was caused by an overexpression of the VHA-a3R790K-GFP protein. Therefore we generated total protein extracts from 5-day old etiolated *VHA-a3-GFP* wild-type and *VHA-a3R790K-GFP* mutant seedlings and probed with anti-GFP antibodies.

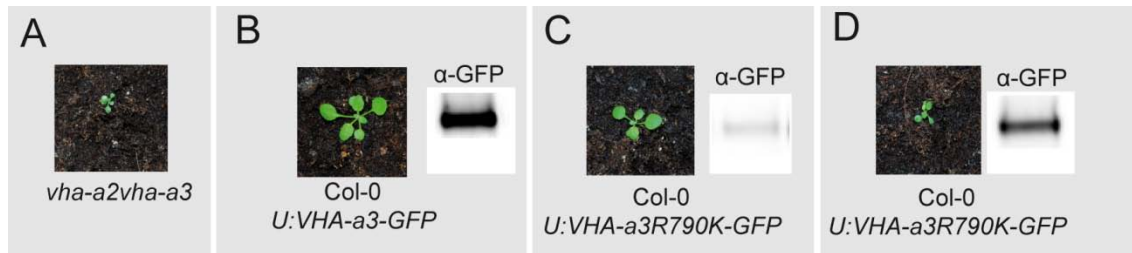


Fig. 19 VHA-a3R790K-GFP has a negative effect on plant growth. *Arabidopsis* wild-type and *vha-a2vha-a3* plants grown on soil with 16-h light/ 8-h dark cycle. (A) *vha-a2vha-a3* double mutant. (B) Wild-type Col-0 plant expressing VHA-a3-GFP. (C-D) Wild-type Col-0 expressing VHA-a3R790K-GFP. (B-D) The presence of the expressed protein was demonstrated by immunodetection with anti-GFP-antibodies.

Immunoblots showed a high abundance of the VHA-a3R790K-GFP protein in the wild-type line with the v23-like phenotype (Fig. 19D). We next assayed the localization of VHA-a3R790K-GFP in both genetic backgrounds. In 5 day old seedlings, we observed that the majority of VHA-a3R790K-GFP localized to the vacuolar membrane and to a punctuate pattern in root cells of the differentiation zone and elongation zone in wild-type and in the *vha-a2vha-a3* double mutant. To determine the identity of the dots we incubated seedlings for 15 min with FM4-64. We observed a colocalization between the VHA-a3R790K-GFP and FM4-64 at the TGN (Fig. 20C). The localization of VHA-a3R790K-GFP in plants exhibiting the v23-like phenotype was indistinguishable from plants with an unremarkable phenotype. No colocalization was observed for wild-type VHA-a3-GFP control plants incubated with FM4-64 (Fig. 20A).

Taken together, based on the localization and the level of expression, we assume that the v23-like phenotype is caused by a competition between VHA-a3R790K-GFP and VHA-a3 for available V-ATPase complexes. This competition lowers the total proton translocation efficiency and as a consequence reduces plant growth. Whereas ~20% of V-ATPase activity seems to be sufficient to correctly target V-ATPase complexes to the tonoplast, a reduction to 10 % results in dual labeling of the TGN and the vacuolar membrane. Inactive V-ATPase complexes are retained in the ER in the presence of active V-ATPase complexes by a yet unknown mechanism.

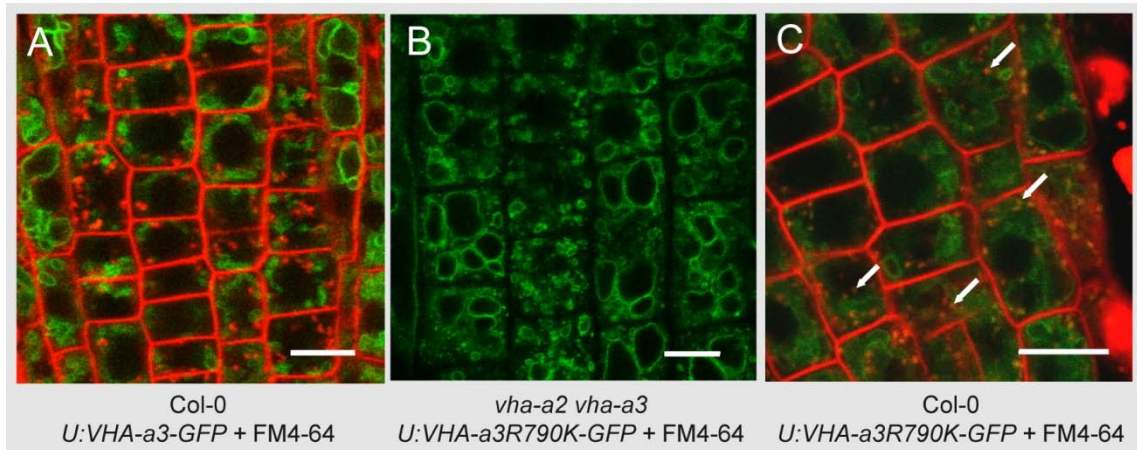


Fig. 20 VHA-a3R790K-GFP localizes to the TGN and to the vacuolar membrane. (A) CLSM analysis of a wild-type Col-0 seedling root tip expressing VHA-a3-GFP incubated with FM4-64 for 15min. (B) CLSM analysis of a *vha-a2vha-a3* seedling root tip expressing VHA-a3R790K-GFP. (C) CLSM analysis of a wild-type Col-0 seedling root tip expressing VHA-a3R790K-GFP incubated with FM4-64 for 15min. Colocalization indicated by arrows. CLSM bars = 10 μ M

What molecular components are required to retain non-functional V-ATPase complexes?

Having shown that V-ATPase activity is required to retain non-functional V-ATPase complexes in the ER, we wanted to understand the molecular mechanism of action that retains non-functional complexes. One promising candidate marked calnexin, an ER chaperone, necessary for retaining non-native proteins in the ER (Ellgaard and Helenius, 2003). Calnexin has been found to co-immunoprecipitate with V_0 subcomplexes isolated from oat seedlings (Li et al., 1998). The genome of *Arabidopsis thaliana* encodes two paralogous genes for calnexin (*AtCNXI* [At5g61790.1](#); *AtCNXII* [At5g07340](#)). We have designed inducible artificial microRNA (amiRNA) against calnexin I and II (*amiCNX*). Expression of a construct was either controlled by the ethanol-inducible promoter AlcA (Roslan et al., 2001) or by the UBI10 promoter. *VHA-a3R729N-GFP* and *VHA-a3-GFP* plants were transformed and T2 lines were established. The efficiency of the calnexin knockdown was determined by western blot analysis using an anti-calnexin antibody (Fig. 21A). Lines that showed a significant decrease in the protein level of calnexin were used for CLSM analysis. *Arabidopsis* seedlings were grown five days on MS plates and on MS plates containing 0.2% ethanol (EtOH) for induction. Plant lines only expressing VHA-a3-GFP showed vacuolar labeling under both growth conditions (Fig. 21B-C). VHA-a3R729N-GFP was localized in the ER independent of the growth condition (Fig. 21D-E).

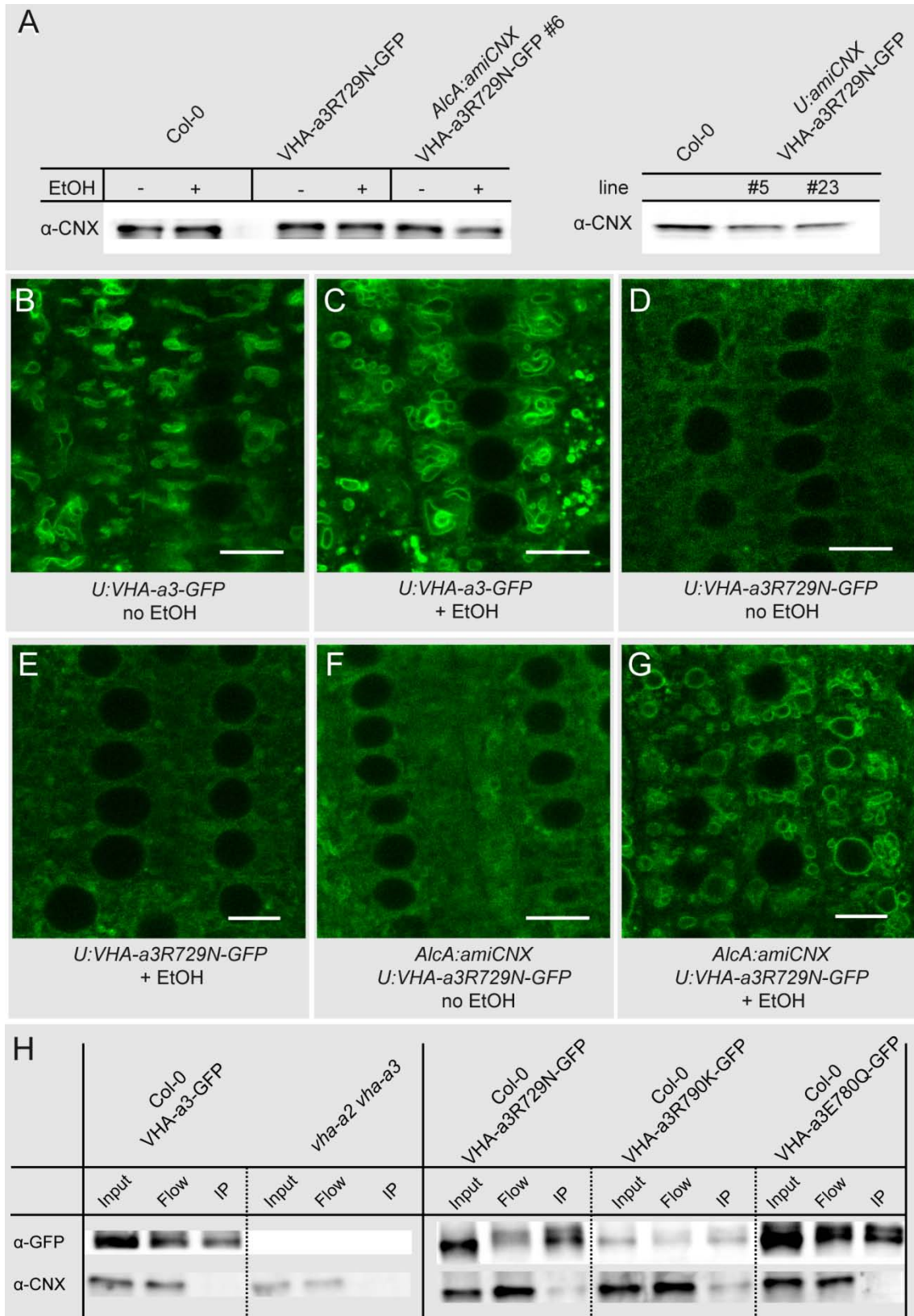


Fig. 21 Calnexin I and calnexin II retain VHA-a3R729N-GFP in the ER. (A) Calnexin protein levels are reduced in independent lines expressing the amiRNA construct. Total proteins were extracted from 5-day old *Arabidopsis* seedlings. Calnexin protein levels were detected using anti-calnexin (α -CNX) antibodies. (B-G) CLSM analysis of wild-type seedlings, grown on MS medium with and without 0.2% Ethanol (EtOH), expressing (B-C) VHA-a3-GFP, (D-E) VHA-a3R729N-GFP and (F-G) VHA-a3R729N-GFP with amiCNX. (H) GFP immunoprecipitation from 5 day old etiolated *Arabidopsis* seedlings co-expressing VHA-a3-GFP, VHA-a3R729N-GFP, VHA-a3R790K-GFP and VHA-a3E780Q-GFP using GFP-TRAP® coupled magnetic particles. Total microsomal extracts (Input), unbound protein flow (Flow) and immunoprecipitates (IP) were subjected to immunoblots using anti-GFP and anti-Calnexin (CNX) antibodies.

However, lines co-expressing VHA-a3R729N-GFP and the amiCNX under inducing conditions showed relocalization of VHA-a3R729N-GFP to the vacuolar membrane (Fig. 21G), indicating that in the wild type calnexin is required for the retention of VHA-a3R729N-GFP in the ER. The relocalization was observed in two independent lines with the inducible promoter and in two independent lines, where the construct was driven by the UBI10 promoter. Due to the general role of calnexin in the primary ERQC system, the knockdown could have decreased overall ERQC efficiency, releasing VHA-a3R729N-GFP and potentially other aberrant proteins from the ER. We therefore asked whether the retention of VHA-a3R729N-GFP required a direct interaction with calnexin. Total microsomal membranes from 5 day old etiolated *Arabidopsis* seedlings expressing VHA-a3/-R729N/-R790K/-E780Q -GFP were extracted. We were unable to co-immunoprecipitate calnexin with VHA-a3-GFP and VHA-a3E780Q-GFP, while a faint calnexin band was detected in the IP lane of VHA-a3R729N-GFP and VHA-a3R790K-GFP (Fig. 21H). From this we conclude that non-functional complexes specifically interact with calnexin, while functional complexes are competent to leave the ER. VHA-a3E780Q-GFP and VHA-a3-GFP might be transported to the tonoplast very efficiently, thus not allowing a detectable interaction of calnexin with these proteins. We observed a growth phenotype for the *R729N* mutation in the *amiCNX* background (Fig. 22B). In lines, where the *amiCNX* construct was driven by the UBI10 promoter and VHA-a3R729N-GFP was localized to the vacuole, plant growth was reduced. From this we conclude that the non-functional V-ATPase V_0 subcomplexes at the tonoplast compete with wild-type subcomplexes for available V_1 subcomplexes, thus reducing overall V-ATPase activity, leading to the observed growth phenotype.



Fig. 22 VHA-a3R729N-GFP plants expressing the *amiCNX* construct show a growth phenotype. (A) VHA-a3-GFP plant expressing the artificial microRNA against calnexin under the control of the UBI10 promotor. (B) VHA-a3R729N-GFP plant expressing artificial microRNA against calnexin under the control of the UBI10 promotor.

If the V-ATPase is already assembled in the ER, is it active?

We have seen that the retention of the non-functional V-ATPase complexes is dependent on V-ATPase activity, yet it remains to be shown, whether the V-ATPase complexes are active in the ER. To determine if and to which extent the *Arabidopsis* ER might be acidified and if this is due to the activity of the V-ATPase, we used the pH-sensitive GFP from the orange seapen *Ptilosarcus gurneyi* (PtGFP). To ensure the retention of the PtGFP to the lumen of the ER we generated a PtGFP construct with an N-terminal signal peptide derived from an *Arabidopsis* vacuolar basic chitinase (SP) and the C-terminal amino acid sequence KDEL. Expression of the protein was controlled by the UBI10 promotor. Previous experiments using normal GFP fusions efficiently targeted SP-GFP-HDEL to the ER lumen in *Arabidopsis* (Matsushima et al., 2003b; Matsushima et al., 2003a). *Arabidopsis* protoplasts were transformed with the *U:SP-PtGFP-KDEL* construct and localization was monitored using CLSM analysis. As is shown in Fig. 23A the GFP fluorescence was observed in the ER lumen. We generated transgenic *Arabidopsis* bearing the *U:SP-PtGFP-KDEL* construct. All 20 T1 lines (à 8 individuals), which were screened failed to give any detectable

fluorescence above the autofluorescence level (data not shown). The expression of these proteins in *Arabidopsis* was below the detection level, due to either strong degradation or poor expression.

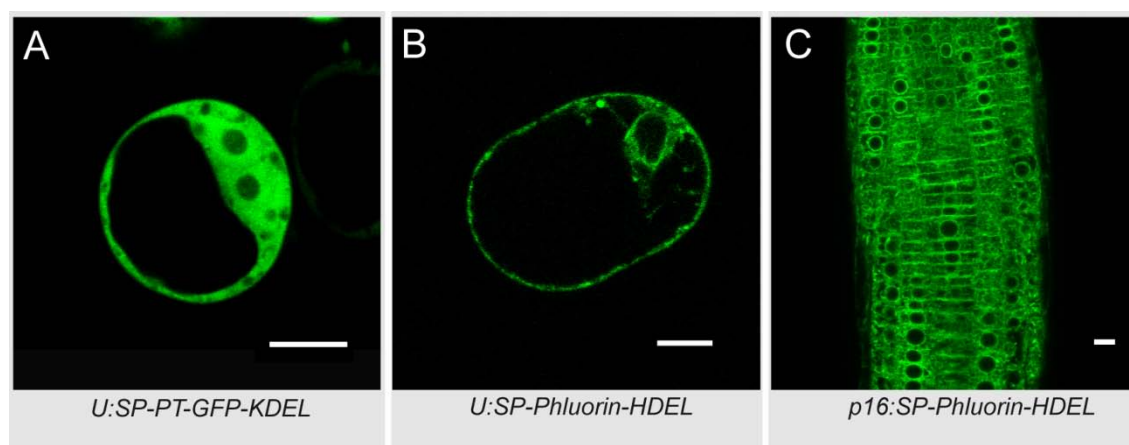


Fig. 23 Expression of SP-pHluorin-HDEL under control of the p16 promotor results in ER localization in stable transformed plants. (A) SP-PtGFP-KDEL was expressed under the control of the Ubiquitin10 promotor in *Arabidopsis* root protoplasts. (B) Sp-pHluorin-HDEL was expressed under the control of the Ubiquitin10 promotor in *Arabidopsis* root protoplasts. Fluorescence signals were detected 3 days after transformation. (C) *Arabidopsis* root tips of 5 day old seedlings stably expressing SP-pHluorin-HDEL under the control of the p16 promotor. CLSM bars represent 10 μ m.

Therefore, we exchanged the *PtGFP* and the C-terminal KDEL sequence for the ratiometric *pHluorin* and a C-terminal HDEL sequence, thus generating an *U:SP-pHluorin-HDEL* construct. Similar to the previous construct, ER localization of the pHluorin protein could be confirmed in transient experiments (Fig. 23B), while stable transformed plants lacked fluorescence signals (data not shown). From these experiments we concluded that high expression of the pH sensitive GFP is required for fluorescence detection in stable transformed *Arabidopsis* plants. Hence, we generated *SP-pHluorin-HDEL* construct under the control of the p16 ribosomal promotor. As can be seen in Fig. 23C, stable transformed *Arabidopsis* T1 plants exhibited robust ER localization of the SP-pHluorin-HDEL.

Is the V-ATPase part of the ERQC system?

We observed that VHA-a3R729N-GFP is retained in the ER, possibly due to absence of V-ATPase activity in the ER. We next ask, whether this loss of activity effects ERQC control in general. To answer this question we have transformed the *vha-a2vha-a3* double mutant with well established markers for ERQC. The mutant of *Arabidopsis thaliana* Carboxypeptidase Y (AtCPY*) is recognized by the ER associated degradation (ERAD) system retranslocated to the cytosol by AtCDC48 and degraded in a proteasome

dependent manner (Yamamoto et al., 2010). The structurally mutant, but biochemically functional brassinosteroid receptor *bri1-9* is retained in the ER due to the ERQC. Reduction of the fidelity of the retention-based ER quality control, allows *bri1-9* to be exported to the cell surface (Jin et al., 2007). If the V-ATPase activity in the ER is crucial for the recruitment of ERQC proteins like AtCDC48, we would expect a transport of AtCPY* along the secretory pathway to the vacuole, and the export of the *bri1-9* along the secretory pathway to the plasmamembrane.

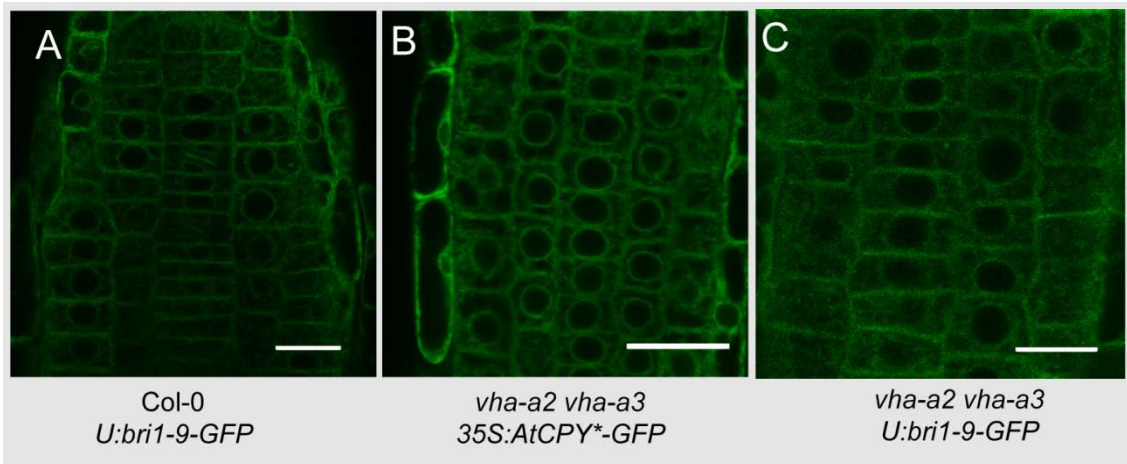


Fig. 24 The *vha-a2vha-a3* double mutant does not affect other ER quality control processes. Plants were grown for 5 days on MS medium. (A) Wild-type Col-0 plants expressing *bri1-9-GFP* under the control of the Ubiquitin10 promoter. (B) *AtCPY*-GFP* expressed under the control of the 35S promoter in *vha-a2vha-a3* double mutant. (C) *bri1-9-GFP* expressed under the control of the Ubiquitin10 promoter in *vha-a2vha-a3* plants

Appendix

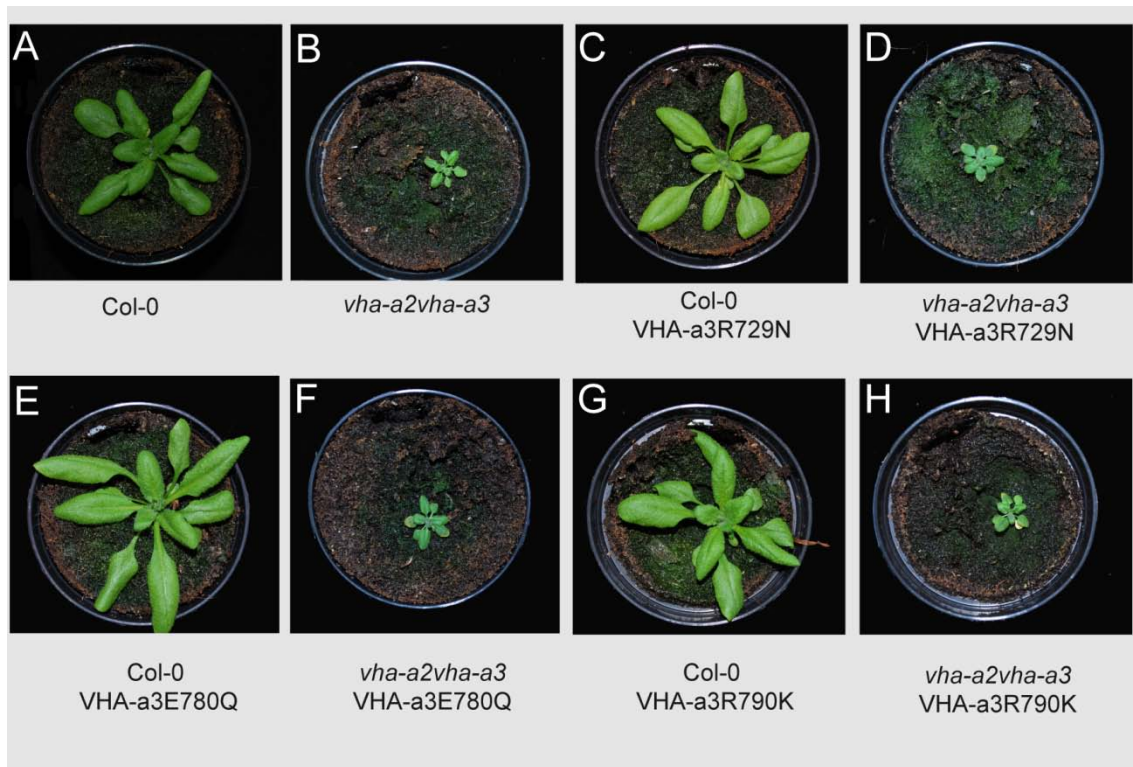


Fig. S. 4: VHA-a3 mutants do not complement the *vha-a2vha-a3* phenotype. (A-H) Phenotype of VHA-a3 mutants in Col-0 wild-type and *vha-a2vha-a3* 3 week old *Arabidopsis* plants (as indicated). 3 week old *Arabidopsis* wild-type and *vha-a2vha-a3* plants grown on soil with 16-h light/ 8-h dark cycle.

Discussion

V-ATPase activity determines the fate of non-functional complexes

In this study, we have demonstrated that VHA-a3R729N-GFP is part of the assembled V-ATPase complex in *Arabidopsis*. Previous experiments in yeast have stated that the mutation only affects V-ATPase activity, rendering the entire complex inactive, without affecting assembly or composition (Kawasaki-Nishi et al., 2001a). Complexes expressing VHA-a3R729N-GFP were not able to complement the growth phenotype of *vha-a2vha-a3* double mutant, from which we conclude that these complexes were inactive and non-functional in *Arabidopsis*. Intracellular localization of VHA-a3R729N-GFP was different, depending on whether it was expressed in the *vha-a2vha-a3* double mutant or in the wild-type Col-0. We showed that the protein was degraded by the proteasome in the wild-type, from which we conclude that VHA-a3R729N-GFP becomes poly-ubiquitylated prior to degradation. Once ubiquitylated, this polytopic membrane protein must be extracted from the membrane, but it is unclear how this is accomplished in the case of VHA-a3R729N-GFP. In a few cases, it has been reported that the proteasome is sufficient for retro-translocation (Lee et al., 2004). However it has been reported that polytopic membrane proteins can be extracted from the ER and targeted to the proteasome with the help of an AAA⁺-ATPase AtCDC48 complex (Marshall et al., 2008; Yamamoto et al., 2010). In contrast to the expression in wild-type plants we observed an overall low expression of the VHA-a3R729N-GFP in the *vha-a2vha-a3* background that could not be stabilized after MG132 treatment. It is possible that the low expression of VHA-a3R729N-GFP in the *vha-a2vha-a3* double mutant and its insensitivity to MG132 is the result of proteasome independent degradation. Until today, the mechanism responsible for the recognition and degradation of tonoplast integral membrane proteins is largely unknown. For the *Arabidopsis* tonoplast potassium channel AtTPK1 recent data suggests that AtTPK1 is degraded either via internalization into the vacuolar lumen or vesicles bud from the vacuole and fuse with multivesicular bodies (MVBs)(Maitrejean et al., 2011). The authors also suggest that this degradation might represent a general turnover pathway of tonoplast integral membrane proteins, thereby possibly also applying to VHA-a3R729N-GFP. Consistent with the results obtained in *planta*, we observed the same intracellular redistribution in yeast. Vph1R735Np-GFP was efficiently transported to the vacuolar membrane, while it was retained and degraded in the wild-type (Upendo Lupanga, Masterthesis, 2011).

How can this difference in localization of VHA-a3R729N-GFP (Vph1R735N-GFP) in two different genetic backgrounds be explained? When Vph1R735N was first described the mutation was shown to not affect V-ATPase assembly or localization (Kawasaki-Nishi et al., 2001a). In these studies the mutant protein was only expressed in the *vph1/stv1Δ* mutant, where Vph1R735N was not competing with wild-type Vph1p and Stv1p for available V_0 subunits. By expressing VHA-a3R729N-GFP (Vph1R735N-GFP) in the wild-type background, wild-type proteins might outcompete their mutant counterparts. Although we could not answer whether VHA-a3 is favored over VHA-a3R729N-GFP in V-ATPase assembly, we did show that VHA-a3R729N-GFP was incorporated into the V-ATPase complex. However the relocation of VHA-a3R729N-GFP in wild-type plants after ConCA treatment argues against a competition between mutant and wild-type VHA-a3 subunits. If VHA-a3R729N-GFP would compete with VHA-a3 for available V_0 subcomplexes, this competition would still be occurring after ConCA treatment, thereby not affecting localization. However VHA-a3R729N-GFP (Vph1R735N-GFP) exits the ER after ConCA treatment. Could ConCA have changed the conformation of VHA-a3R729N-GFP, thereby achieving export from the ER? ConCA has been found to bind in a pocket formed by helices 1, 2, and 4 of subunit c (Bowman et al., 2004). In addition, cytosolic amino acid residues within subunit a have been identified which, when mutated, confer decreased sensitivity to ConCA (Wang et al., 2005). None of these mutations have been shown to change the conformation and stability of the V-ATPase, making it unlikely that ConCA is responsible for conformational changes that induce relocation of VHA-a3R729N-GFP.

Alternatively the difference in localization in the wild-type and the mutant background could be explained with the fact that the V-ATPase itself functions as a pH sensor (Marshansky, 2007). It was previously demonstrated that the mammalian subunit a2 recruits the cytosolic Arf-GEF ARNO in an acidification dependent manner (Maranda et al., 2001). Structural analysis of Vph1p supports the hypothesis of Marshansky et al. by showing that the N-terminus of Vph1p is regulated by pH (Dechant and Peter, 2010). The authors suggest that intraluminal amino acid residues sense pH changes, transmitting the information to the N-terminus of the protein. Based on these findings, the N-terminus of VHA-a3R729N-GFP in wild-type plants could undergo conformational changes that result in the retention and degradation of this protein, while the absence of a proper pH, either after ConCA treatment or in the *vha-a2vha-a3* mutant suspends retention and degradation. This hypothesis could also explain the localization of VHA-a3R790K-GFP and

VHA-a3E780Q-GFP. Although in both mutants proton translocation is attenuated it still sufficient to attain an N-terminal conformation that allows ER export.

It remains to be shown what level of V-ATPase activity is required to retain non-functional complexes in the ER. In the yeast experimental setup we were able to express Vph1R735Np-GFP either in *vph1Δstv1Δ* mutant cells with 0% of V-ATPase activity, or in wild-type cells with 100% V-ATPase activity. Expression of Vph1R735Np-GFP in the *vph1Δ* or in the *stv1Δ* single mutant, both having reduced levels of V-ATPase activity could help determining the activity level.

Taken together our observation led us to conclude that we have a cross-kingdom conserved mechanism that distinguishes between non-functional and functional V-ATPase complexes at the ER. To our knowledge an ER quality control mechanism that is based on function than on folding has not been described so far. We therefore propose that the functionality of V-ATPase complexes is controlled by a function dependent ER quality control (FERQCL) mechanism.

Calnexin is required for a function dependent ER quality control (FERQCL)

Previous reports have shown that the ER lectin calnexin can associate with components of the V_0 and V_1 subcomplex in oat (Li et al., 1998). Using silencing of calnexin in *Arabidopsis* and yeast calnexin knock-out mutant *cneΔ* (U.Lupanga, Masterthesis, 2011), we observed a relocalisation of non-functional complexes to the tonoplast and vacuole. However, neither VHA-a3 nor VHA-a3R729N-GFP has any putative glycosylation sites. Although Vph1p has four predicted N-glycosylation sites, topological studies of the protein demonstrate that these sites are located in the cytoplasmic soluble domain of the protein, making it unlikely that any of these sites get N-glycosylated (Leng et al., 1999). We therefore propose that calnexin acts glycan-independent in the FERQCL. The precise role of calnexin in folding and quality control is still part of an ongoing debate. Most of the evidence of its glycan-independent substrate recognition was obtained from *in vitro* studies, using cytosolic proteins that would not encounter calnexin *in vivo* (Ihara and Williams, 1998). There is compelling evidence that calnexin can interact glycan-independent with proteins within the ERQC apparatus (Saito et al., 1999; Swanton et al., 2003). *In vivo* experiments done in human cell lines demonstrated that the transmembrane domain of calnexin is required to specifically recognize non-glycosylated transmembrane proteins (Swanton et al., 2003). Interestingly the exchange of a single

amino acid within the transmembrane domain of calnexin substrates is sufficient for the retention of these proteins to the ER membrane (Swanton et al., 2003). The mechanism of this retention is unclear, however it has been suggested that the introduction of a single polar amino acid within the hydrophobic environment of the lipid bilayer can be recognized by calnexin. The here presented single amino acid changes were all introduced in the transmembrane domain of VHA-a3. It is possible that these changes directly influenced the binding affinity of calnexin, or that the mutations exposed additional polar amino acid residues targeted by calnexin. As a consequence the mutations affected binding kinetics, resulting in a shift of unbound V_0 subcomplexes towards a calnexin-bound state. This hypothesis is supported by our Co-IP experiments. Proteins that were mistargeted co-immunoprecipitated calnexin, while VHA-a3-GFP and VHA-a3E780Q-GFP, which were targeted correctly to the vacuolar membrane did not co-immunoprecipitate calnexin.

Future research will focus on identifying additional factors apart from calnexin which are required for this mechanism. We are currently establishing an unbiased forward genetic approach by expressing VHA-a3R729N-GFP in a sensitized *vha-a3* background. *vha-a3* plants are indistinguishable from wild-type plants, however they have reduced V-ATPase activity at the tonoplast. Ethyl methanesulfonate (EMS) will be used to obtain diverse mutant alleles that play a critical role in the FERQCL system. We assume a relocalization of VHA-a3R729N-GFP to the vacuolar membrane, lowering V-ATPase activity and thereby reducing plant growth. In addition, we have employed screens of the yeast mutant library. So far, several ER quality control and ER associated degradation (ERAD) yeast mutants were tested for their impact on Vph1pR735N-GFP localization. However, we did not observe a relocalization of non-functional complexes in any of these mutants except for the calnexin mutant *cne1Δ* (U.Lupanga, Masterthesis, 2011).

VHA-a3-GFP is not transported to the tonoplast via the secretory pathway

In this study we show that VHA-a3R729N-GFP and VHA-a3R790K-GFP can localize to the TGN, while VHA-a3-GFP was not localized to the TGN after drug treatment. This could indicate that VHA-a3 is transported to the tonoplast via a TGN independent trafficking pathway. How is it possible that the structurally similar V-ATPase complexes that differ only in their activity are transported via different trafficking routes? For the TGN/ Golgi localizing V-ATPase complexes, unanimous studies in yeast and plant show that the N-

terminal cytosolic sequence of Stv1p and VHA-a1 contain the required targeting information for its localization, however it is still unclear how the specific localization is achieved (Kawasaki-Nishi et al., 2001c; Dettmer et al., 2006). Apart from the structural requirements, it might be sufficient to have correct activity for sorting. In yeast, V-ATPase complexes containing Stv1p has been shown to have a six times lower ratio of ATP hydrolysis to H⁺ transport than vacuolar protein complexes containing Vph1p (Kawasaki-Nishi et al., 2001b). Assuming the same coupling efficiencies are true for the *Arabidopsis* orthologues, VHA-a1 and VHA-a3 could be sorted via different transport pathways due to their activity. This hypothesis could also explain the localization of VHA-a3R70K-GFP and VHA-a3E780Q-GFP. With its higher V-ATPase activity VHA-a3E780Q-GFP reaches the tonoplast, while VHA-a3R790K exhibits a dual localization. How the sorting of differently active complexes is achieved remains elusive. Immunogold labeling of V-ATPase complexes in the ER in oat seedlings however revealed a spatial variation on the ER cisternae, which could according to the authors represent a regional specialization of the ER (Herman et al., 1994). V-ATPase complexes might be sorted to different trafficking routes in those ER “micro domains” according to activity and other not yet identified features.

The V-ATPase is assembled in the ER

The organelle of V-ATPase holo-complex assembly has been part of an ongoing debate. While work done in oat seedlings clearly demonstrated holo-complex assembly in the ER (Li et al., 1998), the yeast research community is divided. Co-IP experiments in temperature sensitive *sec18* mutant strains, where ER export is abrogated at restrictive temperatures (Graham and Emr, 1991) were employed to assay the level of association. Levels of Vph1p (V₀) that co-immunoprecipitate with Vma1p (V₁) are reduced, when compared to wild-type cells (Kane et al., 1999; Malkus et al., 2004). While Kane et al. interpret this data in favor of V-ATPase holo-complex assembly occurring in the ER, Malkus et al. object this model.

In addition to elucidate the FERQCL mechanism, we utilized VHA-a3R729N-GFP to demonstrate that the entire V-ATPase holo-complex is already assembled in the ER. Yet, it remains to be shown, whether this complex is active. Active V-ATPase complexes could greatly contribute to the overall ER luminal milieu, affecting downstream processes, i.e. PDI formation of disulphide-bonds, N-linked glycosylation and establishing favorable redox conditions. Recent research has revealed the presence of a PIN-FORMED5 (PIN5) auxin

efflux carrier in the ER membrane (Mravec et al., 2009), which is required for intracellular auxin homeostasis. Members of the PIN proteins belong to secondary active transporters (Feraru and Friml, 2008; Zažímalová et al., 2010). Their source of energy is unknown, however it has been suggested that PIN transport action is based on auxin/H⁺ antiport, which is fueled by an energizing proton pump. It therefore seems plausible that the V-ATPase is not only assembled, but also already active in the ER. The ConcA experiments presented here in this work support the idea that the V-ATPase is active in the ER. Although we did not observe any effect on general ERQC, which we monitored with bri1-9-GFP and AtCPY*-GFP, the change in luminal pH could just be sufficient to favor conformational stability of the VHA-a3 mutant proteins thus changing affinity for calnexin. In the future, we will be able to directly image the pH within the ER lumen with the here presented pH-sensor, thereby proving the hypothesis of an active V-ATPase in the ER.

Model of the FERQCL system

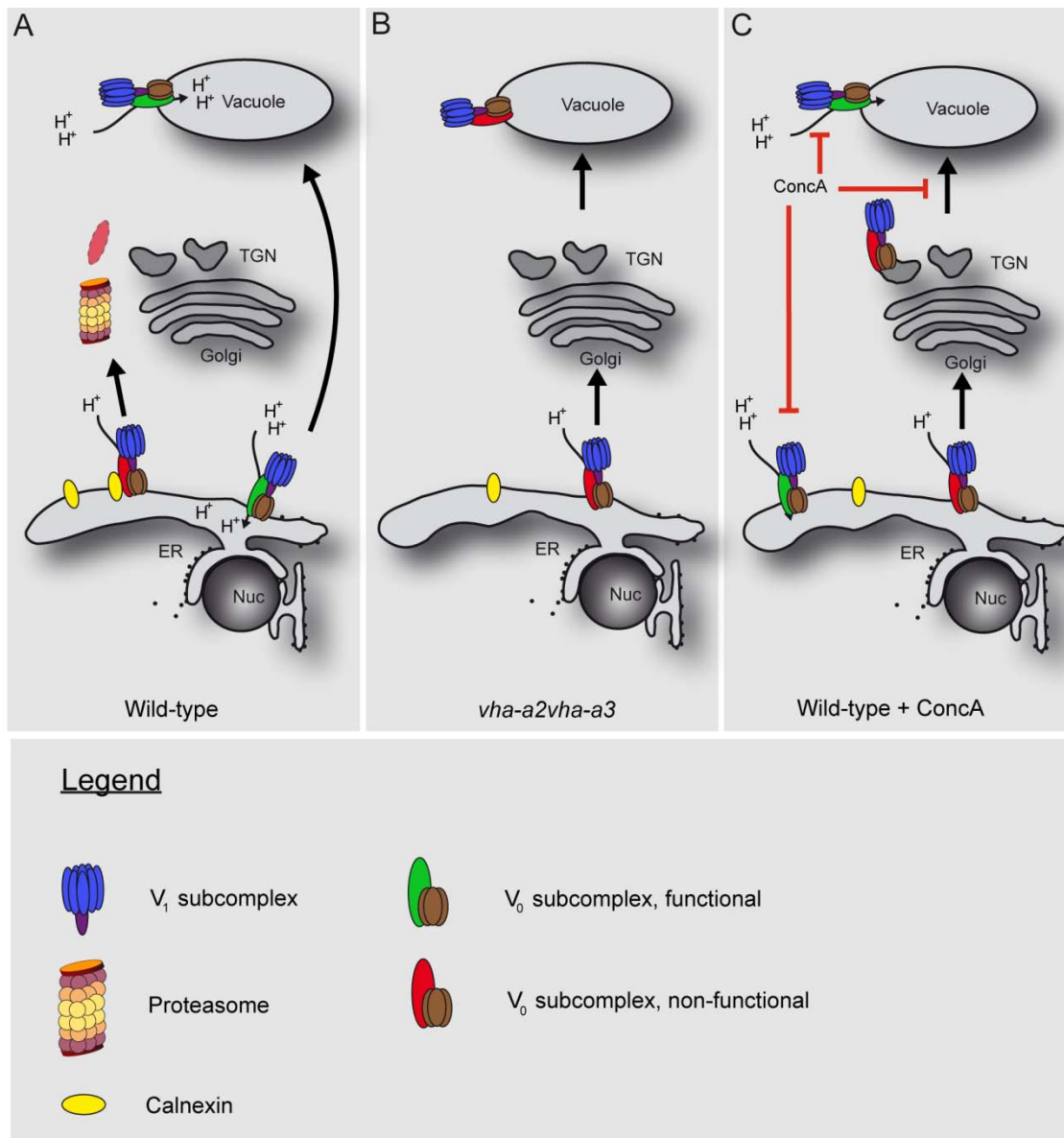


Fig. 25 Model for the function dependent ER Quality control (FERQCL). (A) In the presence of active V-ATPase complexes calnexin is recruited to non-functional complexes. The subunit a of the non-functional complexes is then exported from the ER and degraded by the proteasome, while still functional V-ATPase complexes are transported to the vacuole. (B) In the *vha-a2vha-a3* mutant V-ATPase activity has been reduced. Non-functional complexes cannot be recognized by calnexin and are therefore exported to the tonoplast. (C) If V-ATPase activity has been abolished by ConcA, calnexin cannot distinguish between functional and non-functional complexes. Therefore non-functional complexes leave the ER accumulating in the TGN.

Material and Methods

Plant Materials and Growth Conditions

Arabidopsis thaliana ecotype Columbia 0 (Col-0) plants were grown on nutrient solid MS medium as described previously (Xiong et al., 2005) under long-day conditions (16 h light) at 22°C, unless described otherwise. *Arabidopsis* seeds were surface sterilized in 70% (v/v) Ethanol and 0.1% (v/v) Triton X-100 solution for 20 min followed by 10 min sterilization with 95% (v/v) Ethanol. Seeds containing ethanol-inducible alc gene-expression constructs were surface sterilized using 6 % sodium hypochlorite (NaClO) for 5 min followed by several washing steps with ddH₂O. Sterilized seeds were exposed to cold treatment for at least 2 d. For concanamycin A and MG132 treatment, 4-d-old seedlings grown on nutrient solid MS medium were transferred to liquid MS medium 1 μM concanamycin A or 50 μM MG132 and incubated for the indicated times.

Constructs generated for this study

Generation of U:VHA-a3R790K-GFP, U:VHA-a3E780Q-GFP, U:VHA-a3R729N-GFP

A 364bp fragment was separated from the VHA-a3 cDNA with *Sall-EcoRI* and subcloned into the pJet1.2/blunt Cloning Vector generating the plasmid pa3Cterm. Site directed mutagenesis was performed on the pa3Cterm according to the manufacturer's protocol. For *U:VHA-a3R790K-GFP* the primers a3R790K_f and a3R790K_r were used, for *U:VHA-a3E780Q-GFP* the primers a3E780Q_f and a3E780Q_r were used and to obtain the fragment resulting in *U:VHA-a3R729N-GFP* primers R729N_for and R729N_rev were used. Fragments containing the indicated mutations were then substituted back into the pUGT2kan containing the wildtype VHA-a3 cDNA.

Generation of AlcA:amiCNX and U:amiCNX

For the generation of artificial microRNA (amiRNA) constructs against AtCNX1 and AtCNX2, we used the WMD3 - Web app for the automated design of artificial microRNAs (<http://wmd.weigelworld.org>), where the principles for the design amiRNAs have been integrated into a Web-based tool (Schwab et al., 2006). In brief, At5g61790 (*AtCNX1*) and At5g07340 (*AtCNX2*) have been selected as target genes. The amiRNA sequences were selected, which were predicted to target both *AtCNX1* and *AtCNX2* respectively.

Four oligonucleotides were used to engineer the amiRNA into the endogenous miR319a precursor by PCR amplification. As a template for the PCR, the plasmid pRS300, containing the miR319a precursor in the pBluescript (Stratagene) was used (plasmids were kindly provided by Detlef Weigl). The amiRNA sequence was digested using *EcoRI* and *BamHI* restriction enzymes and ligated into the *EcoRI-BamHI* digested pHanAlcA, a derivative of the pHANNIBAL (Wesley et al., 2001), in which the 35S promoter has been replaced by an ethanol-inducible promoter pAlcA (Roslan et al., 2001). The pAlcA:*amiAtCNX* cassette was digested *NotI* and ligated into the binary plant vector pBart_AlcR, which contains the coding sequence for the transcriptional activator AlcR, which activates the ethanol-inducible promoter pAlcA in the presence of ethanol. Transgenic *U:VHA- α 3R729N-GFP* Col0 plants were selected based on the phosphinothricin (BASTA) resistance conferred by the bar gene contained in pBART_AlcR. Homozygous lines were established, and seedlings were screened for GFP signals.

For the *U:amiCNX* construct the amiRNA sequence was digested using *ApaI* and *SacII* restriction enzymes and ligated into the *ApaI-SacII* digested pUTkan, which is a derivative of the pJH212. The amiRNA sequence was digested from the pUTkan using *Sall* restriction enzyme and ligated into a *Sall* digested pUTbar+, which is a derivative of pZP312.

Generation of U:SP-PtGFP-KDEL

We generated 751 bp fragment of *PtGFP* (Schmid et al., 2005) by PCR amplification adding the first 34 bp of the basic vacuolar chitinase signal sequence (SP-sequence) and a C-terminal KDEL sequence, using primers Sp-Pt_1for and Sp-pt_KDEL_rev. The resulting PCR fragment was used as template for a second PCR amplification adding 44 bp of the SP-sequence and a *BamHI* restriction site to the N-terminus using primers Sp-Pt_2for and Sp-pt_KDEL_rev. The fragment was subcloned into the pJet1.2/blunt Cloning Vector and sequenced. For the *U:Sp-PtGFP-KDEL* construct the *PtGFP-KDEL* sequence was digested using *BamHI* and *SacII* restriction enzymes and ligated into the BamHI-SacII digested pUTkan.

Generation of U:Sp-pHluorin-HDEL

We generated 803 bp fragment of *pHluorin* (Moseyko and Feldman, 2001) by PCR amplification adding the first 37 bp of the basic vacuolar chitinase signal sequence (SP-sequence) and a C-terminal HDEL sequence, using primers P1-Sp-for and HDEL_rev. The

resulting PCR fragment was used as template for a second PCR amplification adding 44 bp of the SP-sequence and a *Bam*HI restriction site to the N-terminus using primers P2-SP-2for and HDEL_rev. The fragment was subcloned into the pJet1.2/blunt Cloning Vector and sequenced. For the *U:Sp-pHluorin-HDEL* construct the *SP-pHluorin-HDEL* sequence was digested using *Bam*HI and *Sac*II restriction enzymes and ligated into the *Bam*HI-*Sac*II digested pUTkan.

Generation of pp16tkan

For the pp16tkan, we isolated the Atp16 promoter (At3g60245) from the pCS-015 plasmid (kindly provided by Christoph Schuster, Lohmann group) by restriction digestion using *Kpn*I and *Bam*HI. We digested the pUTkan vector *Kpn*I-*Bam*HI to replace the Ubiquitin10 promoter with the p16 fragment. The p16 fragment was ligated into the *Kpn*I-*Bam*HI digested pUTkan to generate the pp16Tkan.

Generation of p16:Sp-pHluorin-HDEL

For the *p16:Sp-pHluorin-HDEL*, we isolated the Sp-pHluorin-HDEL fragment from the *U:Sp-pHluorin-HDEL* by restriction digestion with *Bam*HI-*Sac*II. The fragment was ligated into the *Bam*HI-*Sac*II opened pp16tkan to generate the *p16:Sp-pHluorin-HDEL*.

Blast searches were carried out using the TAIR database (<http://www.arabidopsis.org>) and the databases at the NCBI (<http://www.ncbi.nlm.nih.gov>).

Protein Extraction

Frozen plant tissue (100 mg) was ground in liquid nitrogen. The powder was transferred into a 2 ml Eppendorf tube and 500 µl of Extraction buffer (0.35 M Saccharose, 70 mM pH 8.8 Tris-HCl, 10 % v/v Glycerol, 3 mM Na₂EDTA, 1.5 % w/v PVP-40, 0.5 % Triton X-100, 0.15 v/v BSA, 4 mM DTT, 1x Complete Protease Inhibitor [Roche Diagnostics GmbH]) was added. The homogenate was vigorously vortexed and then centrifuged at 10.000 g for 15 min at 4°C. The supernatant was afterwards transferred into a new Eppendorf tube and centrifuged again. Protein concentration of the supernatant was determined using Bradford assay (Bradford, 1976).

Co-Immunoprecipitation

Protein extracts subjected to Co-immunoprecipitation were obtained as described with some modifications (Schumacher et al., 1999). Plant tissue (1g/ml buffer) from 5 day etiolated Arabidopsis plants was homogenized in liquid nitrogen using extraction buffer (50 mM Tris pH 8, 50 mM NaCl, 10% Glycerol and 1 x Complete Protease Inhibitor [Roche Diagnostics GmbH]). The homogenate was centrifuged at 10.000 g at 4°C for 10 min. The supernatant was centrifuged at 150.000g for 30 min at 4°C. The supernatant was discarded and the pellet homogenized with a *Potter-Elvehjem* tissue grinder in extraction buffer. Protein concentration was determined using Bradford assay (Bradford, 1976). For immunoprecipitation, 100 µg protein was solubilized and incubated for 1 h at 4°C using 3 % NP40. Solubilized proteins were separated from non-solubilized proteins by centrifugation at 150.000 g for 30 min. The supernatant was loaded on GFP-Trap® coupled to agarose beads (ChromoTek GmbH, München, Germany) and incubated for 2h at 4°C. Beads were washed three times and then proteins were eluted with SDS-sample buffer (4 % SDS, 140 mM Tris-HCl pH 6.8, 20 % Glycerol, 0.01 % Bromophenolblue, 10 % β-Mercaptoethanol) at 50°C for 5 min.

Fluorescence Microscopy

Fluorescence microscopy was performed using a Leica TCS SP5 confocal laser-scanning microscope. All CLSM images were obtained using the Leica Confocal software and a 63x water-immersion objective. The excitation wavelength was 488 nm; emission was detected for GFP between 500 and 530 nm, for RFP between 565 and 600 nm, and for FM4-64 between 620 and 680 nm. Adobe Photoshop was used for image processing. Quantification of colocalization was assessed using the Leica Confocal software.

Primer used

<u>Name</u>	<u>Sequence</u>
a3R790K_f	5'-GAAACTCAACCCAGTGAAGTTTCAGCGC-3'
a3R790K_r	5'-CGCGTTCCTTACGCGCTGAAACTTCAC-3'
a3E780Q_f	5'-GAAGGAACGCGCTTAGTGTCTGCATCAC-3'
a3E780Q_r	5'-GGGAGTTTTGCTGGTGATGCAGACACTA-3'
R729N_for	5'-CTTACCTGAATCTATGGGCTCTCAGTCTTGCCC-3'

R729N_rev 5'-CCATAGATTCAGGTAAGAAGCGGTGTTGGAAACAGCTCC-3'

Sp-Pt_1for 5'-CTTTTCACTTCTCCTATCATTATCCTCGGCCGAATTC AACCGCAACGTG-3'

Sp-pt_KDEL_r 5'-CCGCGGTTACAGTTCATCCTTCACCCATTCATGCAGGCTGCC-3'

Sp-Pt_2for 5'- GGATCCATGAAGACTAATCTTTTTCTCTTTCTCATCTTTTCACTTCTCCT-3'

P1-Sp-for 5'-CTTTTCACTTCTCCTATCATTATCCTCGGCCGAATTCAGTAAAGGAG
AAGAAC-3'

HDEL_rev 5'-CCGCGGTTACAGTTCATCGTGTGGTATAGTTCATCCATGCC-3'

P2-SP-2for 5'-GGATCCATGAAGACTAATCTTTTTCTCTTTCTCATCTTTTCACTTCTCCT-3'

Concluding remarks and outlook

The compartment newly synthesized proteins destined for the secretory pathway first encounter is the endoplasmic reticulum. The ER has a dual function; it assists in folding and assembly, but also monitors the quality of newly formed proteins. It presents a challenging task to distinguish between a protein that is in the process of folding and a defective one that cannot fold or assemble. The ER is constitutively loaded with new proteins that are in the process of folding and assembly and hence these proteins could be considered transiently defective. To deal with this paradox, the ER hosts a battery of chaperones that identify misfolded proteins.

We have identified two novel *Arabidopsis* assembly factors, which are required for V-ATPase assembly and we have presented a quality control system that monitors the function of the V-ATPase. However it is difficult to draw a clear line that divides assembly from the function dependent ER quality control system (FERQCL). The assembly factors could be part of the machinery that recruits calnexin or, yet unidentified factors to non-functional complexes. With the help of AtVMA12/AtVMA22 mutated VHA-a3 could be maintained in a prolonged transitional state that allows association with calnexin or other ER chaperones, like the thiol oxidoreductase ERp57. The identification of three assembly factors in a higher eukaryote now allows a comparative analysis of assembly factors from yeast and *Arabidopsis* thus determining the underlying molecular mechanism in assembly and quality control. Having shown that the FERQCL system is conserved in both, yeast and *Arabidopsis*, research on other model organisms could be employed to extend and complete our understanding of this novel QC system.

References

- Back, S.H., Schroder, M., Lee, K., Zhang, K., and Kaufman, R.J.** (2005). ER stress signaling by regulated splicing: IRE1/HAC1/XBP1. *Methods* **35**, 395-416.
- Baerenfaller, K., Grossmann, J., Grobei, M.A., Hull, R., Hirsch-Hoffmann, M., Yalovsky, S., Zimmermann, P., Grossniklaus, U., Gruissem, W., and Baginsky, S.** (2008). Genome-scale proteomics reveals *Arabidopsis thaliana* gene models and proteome dynamics. *Science* **320**, 938-941.
- Biermann, M., Pixberg, M., Riemann, B., Schuck, A., Heinecke, A., Schmid, K.W., Willich, N., Dralle, H., and Schober, O.** (2009). Clinical outcomes of adjuvant external-beam radiotherapy for differentiated thyroid cancer - results after 874 patient-years of follow-up in the MSDS-trial. *Nuklearmedizin* **48**, 89-98; quiz N15.
- Bowman, E.J., Graham, L.A., Stevens, T.H., and Bowman, B.J.** (2004). The bafilomycin/concanamycin binding site in subunit c of the V-ATPases from *Neurospora crassa* and *Saccharomyces cerevisiae*. *J Biol Chem* **279**, 33131-33138.
- Bradford, M.M.** (1976). A rapid and sensitive method for the quantitation of microgram quantities of protein utilizing the principle of protein-dye binding. *Anal Biochem* **72**, 248-254.
- Brockmeier, A., and Williams, D.B.** (2006). Potent Lectin-Independent Chaperone Function of Calnexin under Conditions Prevalent within the Lumen of the Endoplasmic Reticulum. *Biochemistry* **45**, 12906-12916.
- Brodsky, J.L., and McCracken, A.A.** (1999). ER protein quality control and proteasome-mediated protein degradation. *Semin Cell Dev Biol* **10**, 507-513.
- Brodsky, J.L., Werner, E.D., Dubas, M.E., Goeckeler, J.L., Kruse, K.B., and McCracken, A.A.** (1999). The requirement for molecular chaperones during endoplasmic reticulum-associated protein degradation demonstrates that protein export and import are mechanistically distinct. *J Biol Chem* **274**, 3453-3460.
- Brüx, A., Liu, T.Y., Krebs, M., Stierhof, Y.D., Lohmann, J.U., Miersch, O., Wasternack, C., and Schumacher, K.** (2008). Reduced V-ATPase activity in the trans-Golgi network causes oxylipin-dependent hypocotyl growth inhibition in *Arabidopsis*. *Plant Cell* **20**, 1088-1100.
- Caramelo, J.J., Castro, O.A., Alonso, L.G., de Prat-Gay, G., and Parodi, A.J.** (2003). UDP-Glc:glycoprotein glucosyltransferase recognizes structured and solvent accessible hydrophobic patches in molten globule-like folding intermediates. *Proceedings of the National Academy of Sciences* **100**, 86-91.

- Cipriano, D.J., Wang, Y., Bond, S., Hinton, A., Jefferies, K.C., Qi, J., and Forgac, M.** (2008). Structure and regulation of the vacuolar ATPases. *Biochim Biophys Acta* **1777**, 599-604.
- Coleman, C.E., Lopes, M.A., Gillikin, J.W., Boston, R.S., and Larkins, B.A.** (1995). A defective signal peptide in the maize high-lysine mutant floury 2. *Proc Natl Acad Sci U S A* **92**, 6828-6831.
- Compton, M.A., Graham, L.A., and Stevens, T.H.** (2006). Vma9p (subunit e) is an integral membrane V0 subunit of the yeast V-ATPase. *J Biol Chem* **281**, 15312-15319.
- Dechant, R., and Peter, M.** The N-terminal domain of the V-ATPase subunit 'a' is regulated by pH in vitro and in vivo. *Channels (Austin)* **5**, 4-8.
- Dechant, R., and Peter, M.** (2010). The N-terminal domain of the V-ATPase subunit 'a' is regulated by pH in vitro and in vivo. *Channels (Austin)* **5**, 4-8.
- Denecke, J., Carlsson, L.E., Vidal, S., Hoglund, A.S., Ek, B., van Zeijl, M.J., Sinjorgo, K.M., and Palva, E.T.** (1995). The tobacco homolog of mammalian calreticulin is present in protein complexes in vivo. *Plant Cell* **7**, 391-406.
- Descamps, E., Petrault-Laprais, M., Maurois, P., Pages, N., Bac, P., Bordet, R., and Vamecq, J.** (2009). Experimental stroke protection induced by 4-hydroxybenzyl alcohol is cancelled by bacitracin. *Neuroscience research* **64**, 137-142.
- Dettmer, J., Hong-Hermesdorf, A., Stierhof, Y.D., and Schumacher, K.** (2006). Vacuolar H⁺-ATPase activity is required for endocytic and secretory trafficking in Arabidopsis. *Plant Cell* **18**, 715-730.
- Dettmer, J., Schubert, D., Calvo-Weimar, O., Stierhof, Y.D., Schmidt, R., and Schumacher, K.** (2005). Essential role of the V-ATPase in male gametophyte development. *Plant J* **41**, 117-124.
- Dixon, D.P., Van Lith, M., Edwards, R., and Benham, A.** (2003). Cloning and initial characterization of the Arabidopsis thaliana endoplasmic reticulum oxidoreductins. *Antioxidants & redox signaling* **5**, 389-396.
- Drose, S., and Altendorf, K.** (1997). Bafilomycins and concanamycins as inhibitors of V-ATPases and P-ATPases. *J Exp Biol* **200**, 1-8.
- Ellgaard, L., and Helenius, A.** (2001). ER quality control: towards an understanding at the molecular level. *Curr Opin Cell Biol* **13**, 431-437.
- Ellgaard, L., and Helenius, A.** (2003). Quality control in the endoplasmic reticulum. *Nat Rev Mol Cell Biol* **4**, 181-191.

- Ellgaard, L., Molinari, M., and Helenius, A.** (1999). Setting the standards: quality control in the secretory pathway. *Science* **286**, 1882-1888.
- Elliott, J.G., Oliver, J.D., and High, S.** (1997). The thiol-dependent reductase ERp57 interacts specifically with N-glycosylated integral membrane proteins. *J Biol Chem* **272**, 13849-13855.
- Englander, S.W., Mayne, L., and Krishna, M.M.** (2007). Protein folding and misfolding: mechanism and principles. *Q Rev Biophys* **40**, 287-326.
- Feraru, E., and Friml, J.Ā.** (2008). PIN Polar Targeting. *Plant Physiology* **147**, 1553-1559.
- Fillingame, R.H., Jiang, W., and Dmitriev, O.Y.** (2000a). The oligomeric subunit C rotor in the fo sector of ATP synthase: unresolved questions in our understanding of function. *J Bioenerg Biomembr* **32**, 433-439.
- Fillingame, R.H., Jiang, W., and Dmitriev, O.Y.** (2000b). Coupling H(+) transport to rotary catalysis in F-type ATP synthases: structure and organization of the transmembrane rotary motor. *J Exp Biol* **203**, 9-17.
- Finnigan, G.C., Hanson-Smith, V., Houser, B.D., Park, H.J., and Stevens, T.H.** (2011). The reconstructed ancestral subunit a functions as both V-ATPase isoforms Vph1p and Stv1p in *Saccharomyces cerevisiae*. *Mol Biol Cell* **22**, 3176-3191.
- Forgac, M.** (1989). Structure and function of vacuolar class of ATP-driven proton pumps. *Physiol Rev* **69**, 765-796.
- Forgac, M.** (2007). Vacuolar ATPases: rotary proton pumps in physiology and pathophysiology. *Nat Rev Mol Cell Biol* **8**, 917-929.
- Frydman, J., Nimmesgern, E., Ohtsuka, K., and Hartl, F.U.** (1994). Folding of nascent polypeptide chains in a high molecular mass assembly with molecular chaperones. *Nature* **370**, 111-117.
- Ghaemmaghami, S., Huh, W.K., Bower, K., Howson, R.W., Belle, A., Dephoure, N., O'Shea, E.K., and Weissman, J.S.** (2003). Global analysis of protein expression in yeast. *Nature* **425**, 737-741.
- Graham, L.A., Hill, K.J., and Stevens, T.H.** (1994). VMA7 encodes a novel 14-kDa subunit of the *Saccharomyces cerevisiae* vacuolar H(+)-ATPase complex. *J Biol Chem* **269**, 25974-25977.
- Graham, L.A., Hill, K.J., and Stevens, T.H.** (1998). Assembly of the yeast vacuolar H+-ATPase occurs in the endoplasmic reticulum and requires a Vma12p/Vma22p assembly complex. *J Cell Biol* **142**, 39-49.

- Graham, T.R., and Emr, S.D.** (1991). Compartmental organization of Golgi-specific protein modification and vacuolar protein sorting events defined in a yeast *sec18* (NSF) mutant. *The Journal of Cell Biology* **114**, 207-218.
- Gruber, C.W., Cemazar, M., Anderson, M.A., and Craik, D.J.** (2009). Enzyme mechanism and function of a novel plant PDI involved in the oxidative folding of cystine knot defense peptides. *Advances in experimental medicine and biology* **611**, 31-32.
- Hammond, C., Braakman, I., and Helenius, A.** (1994). Role of N-linked oligosaccharide recognition, glucose trimming, and calnexin in glycoprotein folding and quality control. *Proc Natl Acad Sci U S A* **91**, 913-917.
- Hartl, F.U.** (1996). Molecular chaperones in cellular protein folding. *Nature* **381**, 571-579.
- Hebert, D.N., Simons, J.F., Peterson, J.R., and Helenius, A.** (1995). Calnexin, calreticulin, and Bip/Kar2p in protein folding. *Cold Spring Harbor symposia on quantitative biology* **60**, 405-415.
- Herman, E.M., Li, X., Su, R.T., Larsen, P., Hsu, H., and Sze, H.** (1994). Vacuolar-Type H⁺-ATPases Are Associated with the Endoplasmic Reticulum and Provacuoles of Root Tip Cells. *Plant Physiology* **106**, 1313-1324.
- Hill, K., and Cooper, A.A.** (2000). Degradation of unassembled Vph1p reveals novel aspects of the yeast ER quality control system. *EMBO J* **19**, 550-561.
- Hill, K.J., and Stevens, T.H.** (1994). Vma21p is a yeast membrane protein retained in the endoplasmic reticulum by a di-lysine motif and is required for the assembly of the vacuolar H⁽⁺⁾-ATPase complex. *Mol Biol Cell* **5**, 1039-1050.
- Hill, K.J., and Stevens, T.H.** (1995). Vma22p is a novel endoplasmic reticulum-associated protein required for assembly of the yeast vacuolar H⁽⁺⁾-ATPase complex. *J Biol Chem* **270**, 22329-22336.
- Hirata, R., Umemoto, N., Ho, M.N., Ohya, Y., Stevens, T.H., and Anraku, Y.** (1993). VMA12 is essential for assembly of the vacuolar H⁽⁺⁾-ATPase subunits onto the vacuolar membrane in *Saccharomyces cerevisiae*. *J Biol Chem* **268**, 961-967.
- Ho, M.N., Hirata, R., Umemoto, N., Ohya, Y., Takatsuki, A., Stevens, T.H., and Anraku, Y.** (1993). VMA13 encodes a 54-kDa vacuolar H⁽⁺⁾-ATPase subunit required for activity but not assembly of the enzyme complex in *Saccharomyces cerevisiae*. *Journal of Biological Chemistry* **268**, 18286-18292.
- Hu, C.-D., Chinenov, Y., and Kerppola, T.K.** (2002). Visualization of Interactions among bZIP and Rel Family Proteins in Living Cells Using Bimolecular Fluorescence Complementation. *Molecular Cell* **9**, 789-798.
- Ihara, Y., and Williams, D.B.** (1998). [Calnexin is a molecular chaperone recognizing glycoproteins]. *Tanpakushitsu Kakusan Koso* **43**, 2450-2454.

- Ihara, Y., Cohen-Doyle, M.F., Saito, Y., and Williams, D.B. (1999). Calnexin Discriminates between Protein Conformational States and Functions as a Molecular Chaperone In Vitro. *Molecular Cell* **4**, 331-341.
- Iwasaki, K., Kamauchi, S., Wadahama, H., Ishimoto, M., Kawada, T., and Urade, R. (2009). Molecular cloning and characterization of soybean protein disulfide isomerase family proteins with nonclassic active center motifs. *FEBS J* **276**, 4130-4141.
- Jackson, D.D., and Stevens, T.H. (1997). VMA12 encodes a yeast endoplasmic reticulum protein required for vacuolar H⁺-ATPase assembly. *J Biol Chem* **272**, 25928-25934.
- Jackson, M.R., Nilsson, T., and Peterson, P.A. (1990). Identification of a consensus motif for retention of transmembrane proteins in the endoplasmic reticulum. *EMBO J* **9**, 3153-3162.
- Jefferies, K.C., Cipriano, D.J., and Forgac, M. (2008). Function, structure and regulation of the vacuolar (H⁺)-ATPases. *Arch Biochem Biophys* **476**, 33-42.
- Jessop, C.E., Tavender, T.J., Watkins, R.H., Chambers, J.E., and Bulleid, N.J. (2009). Substrate specificity of the oxidoreductase ERp57 is determined primarily by its interaction with calnexin and calreticulin. *J Biol Chem* **284**, 2194-2202.
- Jin, H., Yan, Z., Nam, K.H., and Li, J. (2007). Allele-specific suppression of a defective brassinosteroid receptor reveals a physiological role of UGGT in ER quality control. *Mol Cell* **26**, 821-830.
- Kanapin, A., Batalov, S., Davis, M.J., Gough, J., Grimmond, S., Kawaji, H., Magrane, M., Matsuda, H., Schonbach, C., Teasdale, R.D., and Yuan, Z. (2003). Mouse proteome analysis. *Genome Res* **13**, 1335-1344.
- Kane, P.M. (1992). Biogenesis of the yeast vacuolar H⁽⁺⁾-ATPase. *J Exp Biol* **172**, 93-103.
- Kane, P.M. (2006). The where, when, and how of organelle acidification by the yeast vacuolar H⁺-ATPase. *Microbiol Mol Biol Rev* **70**, 177-191.
- Kane, P.M., Tarsio, M., and Liu, J. (1999). Early steps in assembly of the yeast vacuolar H⁺-ATPase. *J Biol Chem* **274**, 17275-17283.
- Kaufman, R.J., Scheuner, D., Schroder, M., Shen, X., Lee, K., Liu, C.Y., and Arnold, S.M. (2002). The unfolded protein response in nutrient sensing and differentiation. *Nat Rev Mol Cell Biol* **3**, 411-421.
- Kawasaki-Nishi, S., Nishi, T., and Forgac, M. (2001a). Arg-735 of the 100-kDa subunit a of the yeast V-ATPase is essential for proton translocation. *Proc Natl Acad Sci U S A* **98**, 12397-12402.

- Kawasaki-Nishi, S., Nishi, T., and Forgac, M.** (2001b). Yeast V-ATPase complexes containing different isoforms of the 100-kDa a-subunit differ in coupling efficiency and in vivo dissociation. *J Biol Chem* **276**, 17941-17948.
- Kawasaki-Nishi, S., Nishi, T., and Forgac, M.** (2003). Proton translocation driven by ATP hydrolysis in V-ATPases. *FEBS Lett* **545**, 76-85.
- Kawasaki-Nishi, S., Bowers, K., Nishi, T., Forgac, M., and Stevens, T.H.** (2001c). The amino-terminal domain of the vacuolar proton-translocating ATPase a subunit controls targeting and in vivo dissociation, and the carboxyl-terminal domain affects coupling of proton transport and ATP hydrolysis. *J Biol Chem* **276**, 47411-47420.
- Krebs, M., Beyhl, D., Gorlich, E., Al-Rasheid, K.A., Marten, I., Stierhof, Y.D., Hedrich, R., and Schumacher, K.** (2010). Arabidopsis V-ATPase activity at the tonoplast is required for efficient nutrient storage but not for sodium accumulation. *Proc Natl Acad Sci U S A* **107**, 3251-3256.
- Kyte, J., and Doolittle, R.F.** (1982). A simple method for displaying the hydropathic character of a protein. *J Mol Biol* **157**, 105-132.
- Langhans, M., Marcote, M.J., Pimpl, P., Virgili-López, G., Robinson, D.G., and Aniento, F.** (2008). In vivo Trafficking and Localization of p24 Proteins in Plant Cells. *Traffic* **9**, 770-785.
- Lee, R.J., Liu, C.W., Harty, C., McCracken, A.A., Latterich, M., Romisch, K., DeMartino, G.N., Thomas, P.J., and Brodsky, J.L.** (2004). Uncoupling retro-translocation and degradation in the ER-associated degradation of a soluble protein. *EMBO J* **23**, 2206-2215.
- Leng, X.H., Nishi, T., and Forgac, M.** (1999). Transmembrane topography of the 100-kDa a subunit (Vph1p) of the yeast vacuolar proton-translocating ATPase. *J Biol Chem* **274**, 14655-14661.
- Leng, X.H., Manolson, M.F., Liu, Q., and Forgac, M.** (1996). Site-directed mutagenesis of the 100-kDa subunit (Vph1p) of the yeast vacuolar (H⁺)-ATPase. *J Biol Chem* **271**, 22487-22493.
- Li, X., Su, R.T., Hsu, H.T., and Sze, H.** (1998). The molecular chaperone calnexin associates with the vacuolar H⁽⁺⁾-ATPase from oat seedlings. *Plant Cell* **10**, 119-130.
- Liu, J.X., and Howell, S.H.** (2010). Endoplasmic reticulum protein quality control and its relationship to environmental stress responses in plants. *Plant Cell* **22**, 2930-2942.
- Lu, D.P., and Christopher, D.A.** (2008). Endoplasmic reticulum stress activates the expression of a sub-group of protein disulfide isomerase genes and AtbZIP60 modulates the response in *Arabidopsis thaliana*. *Mol Genet Genomics* **280**, 199-210.

- Ludwig, J., Kerscher, S., Brandt, U., Pfeiffer, K., Getlawi, F., Apps, D.K., and Schagger, H.** (1998). Identification and characterization of a novel 9.2-kDa membrane sector-associated protein of vacuolar proton-ATPase from chromaffin granules. *J Biol Chem* **273**, 10939-10947.
- Maitrejean, M., Wudick, M.M., Voelker, C., Prinsi, B., Mueller-Roeber, B., Czempinski, K., Pedrazzini, E., and Vitale, A.** (2011). Assembly and sorting of the tonoplast potassium channel AtTPK1 and its turnover by internalization into the vacuole. *Plant Physiol* **156**, 1783-1796.
- Malkus, P., Graham, L.A., Stevens, T.H., and Schekman, R.** (2004). Role of Vma21p in assembly and transport of the yeast vacuolar ATPase. *Mol Biol Cell* **15**, 5075-5091.
- Manolson, M.F., Wu, B., Proteau, D., Taillon, B.E., Roberts, B.T., Hoyt, M.A., and Jones, E.W.** (1994). STV1 gene encodes functional homologue of 95-kDa yeast vacuolar H(+)-ATPase subunit Vph1p. *JBC* **269**, 14064-14074.
- Maranda, B., Brown, D., Bourgoin, S., Casanova, J.E., Vinay, P., Ausiello, D.A., and Marshansky, V.** (2001). Intra-endosomal pH-sensitive recruitment of the Arf-nucleotide exchange factor ARNO and Arf6 from cytoplasm to proximal tubule endosomes. *J Biol Chem* **276**, 18540-18550.
- Marshall, R.S., Jolliffe, N.A., Ceriotti, A., Snowden, C.J., Lord, J.M., Frigerio, L., and Roberts, L.M.** (2008). The Role of CDC48 in the Retro-translocation of Non-ubiquitinated Toxin Substrates in Plant Cells. *Journal of Biological Chemistry* **283**, 15869-15877.
- Marshansky, V.** (2007). The V-ATPase $\alpha 2$ -subunit as a putative endosomal pH-sensor. *Biochem Soc Trans* **35**, 1092-1099.
- Matsushima, R., Kondo, M., Nishimura, M., and Hara-Nishimura, I.** (2003a). A novel ER-derived compartment, the ER body, selectively accumulates a beta-glucosidase with an ER-retention signal in Arabidopsis. *Plant J* **33**, 493-502.
- Matsushima, R., Hayashi, Y., Yamada, K., Shimada, T., Nishimura, M., and Hara-Nishimura, I.** (2003b). The ER body, a novel endoplasmic reticulum-derived structure in Arabidopsis. *Plant Cell Physiol* **44**, 661-666.
- McCracken, A.A., and Brodsky, J.L.** (1996). Assembly of ER-associated protein degradation in vitro: dependence on cytosol, calnexin, and ATP. *J Cell Biol* **132**, 291-298.
- McMahon, H.T., and Mills, I.G.** (2004). COP and clathrin-coated vesicle budding: different pathways, common approaches. *Curr Opin Cell Biol* **16**, 379-391.
- Moseyko, N., and Feldman, L.J.** (2001). Expression of pH-sensitive green fluorescent protein in Arabidopsis thaliana. *Plant Cell Environ* **24**, 557-563.
- Mravec, J., Skupa, P., Bailly, A., Hoyerova, K., Krecek, P., Bielach, A., Petrasek, J., Zhang, J., Gaykova, V., Stierhof, Y.D., Dobrev, P.I., Schwarzerova, K., Rolcik, J., Seifertova, D.,**

- Luschnig, C., Benkova, E., Zazimalova, E., Geisler, M., and Friml, J.** (2009). Subcellular homeostasis of phytohormone auxin is mediated by the ER-localized PIN5 transporter. *Nature* **459**, 1136-1140.
- Nelson, H., Mandiyan, S., and Nelson, N.** (1989). A conserved gene encoding the 57-kDa subunit of the yeast vacuolar H⁺-ATPase. *J Biol Chem* **264**, 1775-1778.
- Neubert, C., Graham, L.A., Black-Maier, E.W., Coonrod, E.M., Liu, T.Y., Stierhof, Y.D., Seidel, T., Stevens, T.H., and Schumacher, K.** (2008). Arabidopsis has two functional orthologs of the yeast V-ATPase assembly factor Vma21p. *Traffic* **9**, 1618-1628.
- Nishi, T., and Forgac, M.** (2002). The vacuolar (H⁺)-ATPases--nature's most versatile proton pumps. *Nat Rev Mol Cell Biol* **3**, 94-103.
- Norris, S.R., Meyer, S.E., and Callis, J.** (1993). The intron of Arabidopsis thaliana polyubiquitin genes is conserved in location and is a quantitative determinant of chimeric gene expression. *Plant Molecular Biology* **21**, 895-906.
- Ondzighi, C., Christopher, D.A., Cho, E.J., Chang, S.C., and Staehelin, L.A.** (2008). Arabidopsis protein disulfide isomerase-5 inhibits cysteine proteases during trafficking to vacuoles before programmed cell death of the endothelium in developing seeds. *Plant Cell* **20**, 2205-2220.
- Ou, W.J., Cameron, P.H., Thomas, D.Y., and Bergeron, J.J.** (1993). Association of folding intermediates of glycoproteins with calnexin during protein maturation. *Nature* **364**, 771-776.
- Parlati, F., Dominguez, M., Bergeron, J.J., and Thomas, D.Y.** (1995). *Saccharomyces cerevisiae* CNE1 encodes an endoplasmic reticulum (ER) membrane protein with sequence similarity to calnexin and calreticulin and functions as a constituent of the ER quality control apparatus. *J Biol Chem* **270**, 244-253.
- Parra, K.J., and Kane, P.M.** (1998). Reversible association between the V1 and V0 domains of yeast vacuolar H⁺-ATPase is an unconventional glucose-induced effect. *Mol Cell Biol* **18**, 7064-7074.
- Petersen, T.N., Brunak, S., von Heijne, G., and Nielsen, H.** (2011). SignalP 4.0: discriminating signal peptides from transmembrane regions. *Nat Meth* **8**, 785-786.
- Pierce, S.E., Davis, R.W., Nislow, C., and Giaever, G.** (2007). Genome-wide analysis of barcoded *Saccharomyces cerevisiae* gene-deletion mutants in pooled cultures. *Nat Protoc* **2**, 2958-2974.
- Powell, B., Graham, L.A., and Stevens, T.H.** (2000). Molecular characterization of the yeast vacuolar H⁺-ATPase proton pore. *J Biol Chem* **275**, 23654-23660.

- Roberts, G.R., Garoosi, G.A., Koroleva, O., Ito, M., Laufs, P., Leader, D.J., Caddick, M.X., Doonan, J.H., and Tomsett, A.B.** (2005). The alc-GR System. A Modified alc Gene Switch Designed for Use in Plant Tissue Culture. *Plant Physiology* **138**, 1259-1267.
- Roslan, H.A., Salter, M.G., Wood, C.D., White, M.R.H., Croft, K.P., Robson, F., Coupland, G., Doonan, J., Laufs, P., Tomsett, A.B., and Caddick, M.X.** (2001). Characterization of the ethanol-inducible alc gene-expression system in *Arabidopsis thaliana*. *The Plant Journal* **28**, 225-235.
- Ryan, M., Graham, L.A., and Stevens, T.H.** (2008). Voa1p functions in V-ATPase assembly in the yeast endoplasmic reticulum. *Mol Biol Cell* **19**, 5131-5142.
- Saito, Y., Ihara, Y., Leach, M.R., Cohen-Doyle, M.F., and Williams, D.B.** (1999). Calreticulin functions in vitro as a molecular chaperone for both glycosylated and non-glycosylated proteins. *EMBO J* **18**, 6718-6729.
- Sambade, M., and Kane, P.M.** (2004). The yeast vacuolar proton-translocating ATPase contains a subunit homologous to the *Manduca sexta* and bovine e subunits that is essential for function. *J Biol Chem* **279**, 17361-17365.
- Saroussi, S., and Nelson, N.** (2009). The little we know on the structure and machinery of V-ATPase. *J Exp Biol* **212**, 1604-1610.
- Schmid, M., Davison, T.S., Henz, S.R., Pape, U.J., Demar, M., Vingron, M., Scholkopf, B., Weigel, D., and Lohmann, J.U.** (2005). A gene expression map of *Arabidopsis thaliana* development. *Nature genetics* **37**, 501-506.
- Schroder, M., and Kaufman, R.J.** (2005). ER stress and the unfolded protein response. *Mutation research* **569**, 29-63.
- Schroder, M., Clark, R., and Kaufman, R.J.** (2003). IRE1- and HAC1-independent transcriptional regulation in the unfolded protein response of yeast. *Mol Microbiol* **49**, 591-606.
- Schroder, M., Clark, R., Liu, C.Y., and Kaufman, R.J.** (2004). The unfolded protein response represses differentiation through the RPD3-SIN3 histone deacetylase. *EMBO J* **23**, 2281-2292.
- Schulte, A., Lorenzen, I., Bottcher, M., and Plieth, C.** (2006). A novel fluorescent pH probe for expression in plants. *Plant Methods* **2**, 7.
- Schumacher, K., Vafeados, D., McCarthy, M., Sze, H., Wilkins, T., and Chory, J.** (1999). The *Arabidopsis det3* mutant reveals a central role for the vacuolar H(+)-ATPase in plant growth and development. *Genes Dev* **13**, 3259-3270.
- Schwab, R., Ossowski, S., Riester, M., Warthmann, N., and Weigel, D.** (2006). Highly Specific Gene Silencing by Artificial MicroRNAs in *Arabidopsis*. *The Plant Cell Online* **18**, 1121-1133.

- Shusta, E.V., Kieke, M.C., Parke, E., Kranz, D.M., and Wittrup, K.D.** (1999). Yeast polypeptide fusion surface display levels predict thermal stability and soluble secretion efficiency. *J Mol Biol* **292**, 949-956.
- Stevens, T.H., and Forgac, M.** (1997). Structure, function and regulation of the vacuolar (H⁺)-ATPase. *Annu Rev Cell Dev Biol* **13**, 779-808.
- Strompen, G., Dettmer, J., Stierhof, Y.D., Schumacher, K., Jurgens, G., and Mayer, U.** (2005). Arabidopsis vacuolar H-ATPase subunit E isoform 1 is required for Golgi organization and vacuole function in embryogenesis. *Plant J* **41**, 125-132.
- Swanton, E., High, S., and Woodman, P.** (2003). Role of calnexin in the glycan-independent quality control of proteolipid protein. *EMBO J* **22**, 2948-2958.
- Sze, H., Schumacher, K., Muller, M.L., Padmanaban, S., and Taiz, L.** (2002). A simple nomenclature for a complex proton pump: VHA genes encode the vacuolar H⁽⁺⁾-ATPase. *Trends Plant Sci* **7**, 157-161.
- Tamura, K., Yamada, K., Shimada, T., and Hara-Nishimura, I.** (2004). Endoplasmic reticulum-resident proteins are constitutively transported to vacuoles for degradation. *Plant J* **39**, 393-402.
- Tomashek, J.J., Garrison, B.S., and Klionsky, D.J.** (1997). Reconstitution in vitro of the V1 complex from the yeast vacuolar proton-translocating ATPase. Assembly recapitulates mechanism. *J Biol Chem* **272**, 16618-16623.
- Ueda, T., Uemura, T., Sato, M.H., and Nakano, A.** (2004). Functional differentiation of endosomes in Arabidopsis cells. *The Plant Journal* **40**, 783-789.
- Vitale, A., and Denecke, J.** (1999). The endoplasmic reticulum-gateway of the secretory pathway. *Plant Cell* **11**, 615-628.
- Wada, I., Rindress, D., Cameron, P.H., Ou, W.J., Doherty, J.J., 2nd, Louvard, D., Bell, A.W., Dignard, D., Thomas, D.Y., and Bergeron, J.J.** (1991). SSR alpha and associated calnexin are major calcium binding proteins of the endoplasmic reticulum membrane. *J Biol Chem* **266**, 19599-19610.
- Wagner, V., and Mittag, M.** (2009). Probing circadian rhythms in *Chlamydomonas reinhardtii* by functional proteomics. *Methods Mol Biol* **479**, 173-188.
- Wang, Y., Inoue, T., and Forgac, M.** (2005). Subunit a of the yeast V-ATPase participates in binding of bafilomycin. *J Biol Chem* **280**, 40481-40488.
- Ware, F.E., Vassilakos, A., Peterson, P.A., Jackson, M.R., Lehrman, M.A., and Williams, D.B.** (1995). The molecular chaperone calnexin binds Glc1Man9GlcNAc2 oligosaccharide as an initial step in recognizing unfolded glycoproteins. *J Biol Chem* **270**, 4697-4704.

- Watanabe, M., Kono, T., Matsushima-Hibiya, Y., Kanazawa, T., Nishisaka, N., Kishimoto, T., Koyama, K., Sugimura, T., and Wakabayashi, K.** (1999). Molecular cloning of an apoptosis-inducing protein, pierisin, from cabbage butterfly: possible involvement of ADP-ribosylation in its activity. *Proc Natl Acad Sci U S A* **96**, 10608-10613.
- Wesley, S.V., Helliwell, C.A., Smith, N.A., Wang, M., Rouse, D.T., Liu, Q., Gooding, P.S., Singh, S.P., Abbott, D., Stoutjesdijk, P.A., Robinson, S.P., Gleave, A.P., Green, A.G., and Waterhouse, P.M.** (2001). Construct design for efficient, effective and high-throughput gene silencing in plants. *The Plant Journal* **27**, 581-590.
- Wiederkehr, C., Basavaraj, R., Sarrauste de Menthiere, C., Hermida, L., Koch, R., Schlecht, U., Amon, A., Brachat, S., Breitenbach, M., Briza, P., Caburet, S., Cherry, M., Davis, R., Deutschbauer, A., Dickinson, H.G., Dumitrescu, T., Fellous, M., Goldman, A., Grootegoed, J.A., Hawley, R., Ishii, R., Jegou, B., Kaufman, R.J., Klein, F., Lamb, N., Maro, B., Nasmyth, K., Nicolas, A., Orr-Weaver, T., Philippsen, P., Pineau, C., Rabitsch, K.P., Reinke, V., Roest, H., Saunders, W., Schroder, M., Schedl, T., Siep, M., Villeneuve, A., Wolgemuth, D.J., Yamamoto, M., Zickler, D., Esposito, R.E., and Primig, M.** (2004). GermOnline, a cross-species community knowledgebase on germ cell differentiation. *Nucleic Acids Res* **32**, D560-567.
- Wieland, F., and Harter, C.** (1999). Mechanisms of vesicle formation: insights from the COP system. *Curr Opin Cell Biol* **11**, 440-446.
- Winnay, J.N., and Kahn, C.R.** (2011). PI 3-kinase regulatory subunits as regulators of the unfolded protein response. *Methods in enzymology* **490**, 147-158.
- Xiong, Y., Contento, A.L., and Bassham, D.C.** (2005). AtATG18a is required for the formation of autophagosomes during nutrient stress and senescence in *Arabidopsis thaliana*. *The Plant Journal* **42**, 535-546.
- Yamamoto, M., Kawanabe, M., Hayashi, Y., Endo, T., and Nishikawa, S.** (2010). A vacuolar carboxypeptidase mutant of *Arabidopsis thaliana* is degraded by the ERAD pathway independently of its N-glycan. *Biochem Biophys Res Commun* **393**, 384-389.
- Yasuda, H., Hirose, S., Kawakatsu, T., Wakasa, Y., and Takaiwa, F.** (2009). Overexpression of BiP has inhibitory effects on the accumulation of seed storage proteins in endosperm cells of rice. *Plant Cell Physiol* **50**, 1532-1543.
- Ye, C., Dickman, M.B., Whitham, S.A., Payton, M., and Verchot, J.** (2011). The unfolded protein response is triggered by a plant viral movement protein. *Plant Physiol* **156**, 741-755.
- Zažímalová, E., Murphy, A.S., Yang, H., Hoyerová, K., and Hořáček, P.** (2010). Auxin Transporters "Why So Many?". *Cold Spring Harbor Perspectives in Biology* **2**.
- Zerangue, N., Schwappach, B., Jan, Y.N., and Jan, L.Y.** (1999). A new ER trafficking signal regulates the subunit stoichiometry of plasma membrane K(ATP) channels. *Neuron* **22**, 537-548.

List of Abbreviations

°C	Degree Celsius
Aa	Amino acid
amiRNA	Artificial microRNA
Amp	Ampicillin
App.	Appendix
At	<i>Arabidopsis thaliana</i>
ATP	Adenosine-5'-triphosphate
ATPase	Adenosine-5'-triphosphatase
Bp	Base pairs
BIFC	Bimolecular fluorescence complementation
BSA	Bovine serum albumin
CaMV	Cauliflower mosaic virus
cDNA	Copy DNA
CLSM	Confocal laser scanning microscopy
ConcA	Concanamycin A
d	day(s)
DAG	Days after germination
DMSO	Dimethylsulfoxid
DNA	Desoxyribonucleic acid
<i>E.coli</i>	<i>Escherichia coli</i>
EE	Early endosome
EM	electron microscope
ERQC	ER quality control

et al.	<i>et alteri</i>
EtOH	Ethanol
FERQCL	Function dependent ER quality control
Fig.	Figure
Gent	Gentamycin
GFP	Green fluorescent protein
h	Hour(s)
Kan	Kanamycin
kDa	Kilodalton
mRFP	Monomeric red fluorescent protein
MS	Murashige-Skoog
MSX	L-Methionine-Sulfoximine
OD	Optical density
ORF	Open reading frame
PAGE	Polyacrylamide gel electrophoresis
PCR	Polymerase chain reaction
Rif	Rifampicin
RNA	Ribonucleic acid
RNAi	RNA interference
rpm	Revolutions per minute
RT	Room temperature
s	Second(s)
SD	Synthetic Dextrose
Spec	Spectinomycin

SDS	Sodium dodecyl sulfate
T-DNA	Transfer-DNA
TEM	Transmission electron microscopy
TGN	<i>Trans</i> -Golgi network
UBQ	Ubiquitin
V-ATPase	Vacuolar H ⁺ -ATPase
VHA	Vacuolar H ⁺ -ATPase
vma	vacuolar membrane acidification
Wt	Wild-type
YFP	Yellow fluorescent protein

Symbols for amino acids (one- and three-letter code)

Alanine	A	Ala	Methionine	M	Met
Cysteine	C	Cys	Asparagine	N	Asn
Aspartic acid	D	Asp	Proline	P	Pro
Glutamic acid	E	Glu	Glutamine	Q	Gln
Phenylalanine	F	Phe	Arginine	R	Arg
Glycine	G	Gly	Serine	S	Ser
Histidine	H	His	Threonine	T	Thr
Isoleucine	I	Ile	Valine	V	Val
Lysine	K	Lys	Tryptophan	W	Trp
Leucine	L	Leu	Tyrosine	Y	Tyr

Acknowledgement

“I rather believe that time is a companion who goes with us on the journey — reminds us to cherish every moment because they'll never come again. What we leave behind is not as important as how we've lived.” – *Cpt. Jean-Luc Picard*

An dieser Stelle möchte ich mich bei all jenen bedanken, die mich während meiner Doktorarbeit begleitet, unterstützt und gefördert haben. Mein besonderer Dank gilt hier Prof. Dr. Karin Schumacher, die in zahlreichen Gesprächen und Diskussionen meine wissenschaftliche Entwicklung begleitet und gefördert hat. Dafür und für die Möglichkeit in ihrem Labor zu arbeiten danke ich.

Ich bin dankbar für die Unterstützung, die ich durch meine Familie, insbesondere meine Eltern und meiner Großeltern, erfahren haben. Ihr Zuspruch, Zuwendung und ihr Verständnis waren stets erbaulich und ermutigend.

I want to thank my friends and former colleagues at the Institute of Molecular Biology at the University of Oregon. My special thanks go to Tom Stevens and Laurie Graham, who supported me during my numerous stays in the Stevens Lab.

Mein Dank gilt ebenso all meinen Freunden. Insbesondere möchte ich mich bei Danja Monje bedanken, die mich während meiner gesamten Doktorarbeit mit wunderbaren kulinarischen Leckereien beglückt hat. Desweiteren möchte ich mich bei Herbert Warmbier bedanken, der trotz seiner hohen Termindichte immer ein offenes Ohr für meine Sorgen hatte.

Zum Schluss danke ich all meinen Kollegen, die mich während meiner Doktorarbeit mit vielfältigen praktischen Tipps und Hinweisen unterstützt haben und zu einer angenehmen Arbeitsatmosphäre beigetragen haben.